Liquefaction Resistance of Saturated Sand Reinforced With Polymer

Namdar Badiee

Submitted to the
Institute of Graduate Studies and Research
in partial fulfillment of the requirements for the Degree of

Master of Science
in
Civil Engineering

Eastern Mediterranean University
February 2014
Gazima usa, North Cyprus

Approval of the Institute of Graduate Studies and Research

Prof. Dr. Elvan Yılmaz
Director

I certify that this thesis satisfies the requirements as a thesis for the degree of Master of Science in Civil Engineering.

Prof. Dr. Özgür Eren
Chair, Department of Civil Engineering

We certify that we have read this thesis and that in our opinion it is fully adequate in scope and quality as a thesis for the degree of Master of Science in Civil Engineering.

Assoc. Prof. Dr. Abbas Ghalandarzadeh
Co-supervisor

Assoc. Prof. Dr. Zalihe Sezai
Supervisor

Examining Committee

1. Prof. Dr. Özgür Eren

2. Assoc. Prof. Dr. Huriye Bilsel

3. Assoc. Prof. Dr. Zalihe Sezai

4. Asst. Prof. Dr. Giray Özay

5. Asst. Prof. Dr. Alireza Rezaei

ABSTRACT

Earthquake has sufficient strength to increase the pore-water pressure of sands while decreasing the soil strength. This phenomenon in geotechnical engineering termed as soil liquefaction which can have profound effects in structures. In most cases, the damages caused by liquefaction can be hindered by physical and chemical methods of soil stabilization which are executable either in initial state of ground before construction or even in constructed structures condition. Among the chemical reclamation materials, polymer manifested its unique nature as a stabilizer agent. This is because of flexibility characters of polymer in which resulted in soil particles stiffness. This feature improved the stress-strain behavior and failure characteristics of cohesionless soil. In the study, Polyfam 707 type polymer was used as a binding agent for sticking the particles together and preventing the liquefaction problem. Three percentages: 2.0%, 4.1% and 8.2% of polymer to dry unit weight of the soil were used. This study evaluated the typical behaviour of sand in initial and reinforced state, in order to compare the confining pressure effects with different percentages of polymer. Thus, a series of samples with varying percentages of polymer inclusion were prepared by Undercompaction method and cured for 7 days prior to testing. The samples were confined under 100, 200 and 300 kPa pressure and sheared in isotropic consolidated state by undrained compression monotonic and cyclic triaxial apparatus. Based on the results of monotonic tests, the shear strength of soil proportional to higher percentages of polymer and confining pressure increased. Unlike the contractive behaviour of the natural sand, the polymer stabilized specimens except those with 2% polymer showed dilative behaviour.

On the other hand, the result of cyclic loading tests notified that 8.2% polymer added samples did not have any risk of liquefaction problem. That was because of the strong cementation of sand particles treated with polymer. . Furthermore, the modified tested samples with Cyclic Stress Ratio, CSR of 0.4 showed different deformation responses. In 8.2% polymer mixed with the soil, the double amplitude strain was almost 1% whereas in 4.1% polymer mixed soil, the double amplitude strain was 5.5% that was almost twice the value of 2% polymer.

 The Scanning Electron Microscope, SEM images of the polymer treated sands indicated that polymer added into the sand covered almost all the surfaces of the sand particles and filled the pore spaces between the sand grains especially at higher percentages of polymer. That increased the binding forces between the grains and prevented the liquefaction problem. At 8.2% polymer to sand mixture, the CSR value was obtained to be much higher than the CSR values for the natural sand.

Keywords: Cyclic stress ratio, cyclic triaxial, liquefaction; monotonic triaxial, polymer reinforced sand; soil stabilization.

ÖZ

Deprem topra ın gücünü dü ürürken, kumların bo luk suyu basıncını artırmak için yeterli güce sahiptir. Yapılarda derin etkileri olabilen bu fenomen, geoteknik mühendisli inde zemin sıvıla ması olarak adlandırılır.

Genelde sıvıla ma nedeniyle meydana gelen hasar fiziksel ve kimyasal zemin stabilizasyonu yöntemleri ile ya zeminin ba langıç durumu yani yapım öncesi veya in aat sonrası durumlarında yürütülerek engel olunabilinir. Kimyasal zemin ıslah materyalleri arasında, polimer zemin stabilasyon malzemesi olarak e siz do asını göstermektedir. Bu polimerin flexibilite karakterinden dolayı, zemin daneciklerinin sertli i ile sonuçlanmı olması nedeniyledir. Bu özellik, gerilme- ekil de i tirme davranı ını ve kohezyonsuz zeminin göçme özelliklerini geli tirmi tir.

Bu çalı mada, Polyfam 707 tipi polimer, kum parçacıklarının birbirine yapı masını ve sıvıla tırma problemini gidermek için bir ba layıcı madde olarak kullanılmı tır. Üç polimer yüzdelik de eri: % 2.0, % 4.1 ve % 8.2 polimerin topra ın kuru birim hacim a ırlı ına oranı olarak kullanılmı tır. Bu çalı ma, kumun ilk ve takviyeli durumunda, çevre basıncı ve de i ik polimer yüzdeliklerinde tipik kum davranı ını de erlendirmek amaçlı gerçekle tirilmi tir. Bu nedenle, de i ik polimer yüzdeliklerinde, "kompaksiyon altında" metodu ve 7 günlük kür de erleri kullanılarak bir seri deneyler yapılmı tır. Numuneler, 100, 200 ve 300 kPa çevre basıncı altında, izotropik konsolidasyon durumunda, monotonik ve tekrarlı yükler altında drenajsız üç eksenli basınç cihazı kullanılarak kesmeye tabi tutulmu lardır.

Monotonik testler, daha yüksek polimer yüzdelikleri ve çevre basınç de erlerinde gerilme mukavemetinin artmı oldu unu göstermi tir. Do al kum büzülme davranı ından farklı olarak, ,% 2 polimer katkılı numune hariç, di er polimer katkılı numuneler dilative davranı gösterdi.

Öte yandan, tekrarlı yükleme test sonuçları, % 8.2 polimer katkılı numunelerin herhangi bir sıvıla tırma riski olmadı ını göstermi tir. Bunun nedeni, polimer ile muamele edilmi kum parçacıklarının güçlü çimentola ma durumunda olmasından kaynaklanmaktadır. Ayrıca, modifiye edilmi numuneler 0.4 tekrarlı basınç oranı de erinde farklı deformasyon davranı ları sergilemi lerdir. % 8.2 polimer katkılı numunelerde, çift amplitüd deformasyonu yakla ık % 1 iken, % 4.1 polimer katkılı numunelerde, çift amplitude deformasyonu % 5.5, neredeyse % 2 polimer katkılı numunelerde elde edilen çift amplitude deformasyon de erinin iki katı de erindedir.

Polimer katkılı numunelerin Taramalı Elektron Mikroskop, görüntüleri, kum parçacıklarının hemen hemen tüm yüzeylerinin polimer ile kaplandı ını ve özellikle polimer yüzdeli inin daha yüksek oldu u de erlerde kum taneleri arasındaki gözenek bo luklarının polimer ile doldurulmu oldu unu göstermektedir. Bu özellik taneler arasındaki ba lanma kuvvetlerini arttırmı ve sıvıla ma problemini önlemi tir. % 8.2 polimer katkılı numenelerde cyclic stress ratio de erinin, do al kum için elde edilen cyclic stress ratio de erlerinden çok daha yüksek oldu u tesbit edilmi tir.

Anahtar kelimeler: Tekrarlı basınç oranı, tekrarlı üç eksenli, sıvıla ma, monotonik üç eksenli, polimer katkılı kum, zemin stabilizasyonu.

IN THE NAME OF ALMIGHTY

Dedicated to my beloved family

ACKNOWLEDGEMENT

I would like to express my special appreciation and thanks to my supervisor Assoc. Prof. Dr. Zalihe Sezai, who first interested me in this topic, for her supervision and guidance throughout this research.

Dr. Abbas Ghalandarzadeh, as my co-supervisor, provided crucial guidance and assistance while I was involved in experimental work on two triaxial testing systems. I would like to thank you for being so supportive in my research and for allowing me to grow as a research scientist.

A special thanks to my family. Words cannot truly express how grateful I am to my mother. Her prayer for me was what sustained me thus far.

It is always impossible to mention all, but I would also like to thank all of my friends who supported me in writing, and incented me to strive towards my goal.

TABLE OF CONTENT

LIST OF FIGURES

LIST OF TABLES

LIST OF SYMBOLS

Roman Symbols

A	Area
B	Skempton's coefficient
C_C	Coefficient of curvature
C_U	Coefficient of uniformity
D	Diameter of specimen
D_{10}	Diameter of soil particles for which 10% of particles is finer
D_{30}	Diameter of soil particles for which 30% of particles is finer
D_{50}	Diameter of soil particles for which 50% of particles is finer
D_{60}	Diameter of soil particles for which 60% of particles is finer
D_r	$(e_{max}-e)/(e_{max}-e_{min})$
e_{max}, e_{min}	Maximum & minimum void ratios
e	Void ratio
f	Frequency
G_s	Specific Gravity
L_0	Initial height
N	Number of cycles
N_{60}	Energy Corrected SPT Blow Count
P and p′	Mean total and effective stress in triaxial conditions
q	Deviatory stress in triaxial conditions
q_{cyc}	Cyclic deviatory stress
R^2	Coefficient of correlation
U	Pore water pressure
V_0	Initial volume of sample

Greek Symbols

σ_1	Major principal stress

σ'_3	Effective confining pressure
L	Displacement changes
u	Excess pore water pressure
Δv	Volume change
	Axial strain
ε_q	Deviatory strain
ε_v	Volumetric strain
	Friction angle mobilized at critical state
γ	Dry unit weight
γ	Shear strain
γ_w	Volumetric weight of water
τ	Shear stress

LIST OF ABBREVIATIONS

BP	Back Pressure
CPT	Cone Penetration Testing
CRR	Cyclic Resistance Ratio
CSR	Cyclic Stress Ratio
CSS	Critical Steady State
ICU	Isotropically Consolidated Undrained
LVDT	Linear Variable Differential Transformer
PTL	Phase Transformation Line
PP	Pore Pressure
PVC	Poly Vinyl Chloride
QSS	Quasi Steady State
SEM	Scan Electron Microscope
SPT	Standard Penetration Test
SSL	Steady State Line
USS	Ultimate Steady State

Chapter 1

INTRODUCTION

1.1 Scope and Objective of Research

This dissertation reveals the experimental responses of fined sand before and after use of polymer. The responses were obtained from monotonic and cyclic triaxial loadings. The purpose of this work is to estimate how modified soil serves to resist liquefaction in laboratory scale. The detailed objectives are:

1. To determine the changes of stress, strain and pore-water pressure of the soil in loose and treated condition by monotonic and cyclic triaxial loadings.

2. To investigate the effect of confining pressures on the natural and polymer reinforced samples.

3. To compare the efficiency of different percentages of polymer in order to apply the best efficient and economical percent of polymer to dry unit weight of the soil.

1.2 Outline

The thesis has been structured as below:

In Chapter 2, a concise review of relevant literature was introduced. Also the typical concept of soil behaviour under monotonic and cyclic triaxial loading is described. Furthermore, the application methods of adding additives to the soil were explained briefly.

Chapter 3 discusses the material and testing method(s): a description of Silver Beach sand used in natural and polymer-added state in this study and details of experimental procedures are presented. Also the preparation processes used for the constitution of disturbed sand are given.

Chapter 4 deals with analysis of the results of natural and treated soil after adding different percentages of polymers under monotonic and cyclic undrained triaxial loading. Also the interaction of polymer with sand was shown by scanning electron microscope images with different magnifications.

Chapter 5 concludes the principal behaviour of the non-treated and treated samples under monotonic and cyclic loading and presents recommendations for future work.

Chapter 2

LITERATURE REVIEW

2.1 Introduction

In cohesionless soils, when sand particles are subjected to huge sudden forces like earthquakes, the sand particles tend to lose their strength because of rapid increases in pore pressure without giving any chance of drainage to sand. Consequently, that causes the soil particles to lose their strength and act just like a viscous fluid which termed as liquefaction. The high potential of liquefaction to damaging structures has made this phenomenon one of the most important topics in earthquake engineering studies, which is divided into flow liquefaction and cyclic mobility.

To begin with flow liquefaction, the shear stress application always followed by changes in the volume of sample as termed as dilatancy. The volume change induced of shear stress leads to displacement of soil particles either up or downward as called slip-down and roll-over movement respectively. The slip-down movement of grains tends to decrease the voids between particles in a way to make the soil denser. On the contrary, roll-over displacements of particles enlarge the volume of the soil as to be the character of dense sands (Kramer, 1996). The two ways of particles displacement work more or less simultaneously as manifested in the stress-strain behavior observed in the laboratory test (Ishihara, 1996). Thus loose sand in such a form is called strain-softening type and referred to as contractive or flow liquefaction, whereas sand in dense state referred as strain-hardening or non-flow type (Kramer, 1996). In triaxial

tests, flow and non-flow liquefaction phenomena can be simulated. Cyclic mobility is an incident where there is a remarkable reduction in the toughness of the soil mass linked with a rising in the pore water pressure induced by cyclic loading. Although this phenomenon does not exhibit any considerable loss in soil mass strength, large deformation can be produced because of degradation of hardness. During seismic loading, some structures cannot sustain the large deformation in soil mass initiated from cyclic mobility. Hence the level of deformation can be unacceptable for some structures that impose large scale damages to structures.

This literature review focuses on the behavior evaluation of sand under monotonic loading in consolidated undrained condition that contains steady, quasi-steady state and other characteristics of sand. Cyclic behaviour of sand contains liquefaction criteria and interpretations for cyclic loading, reviewing variety of physical and chemical materials tested under triaxial loadings and finally various applying techniques of materials to the cohesionless soil.

2.2 Behavior of Undrained Sand under Monotonic Triaxial Loading

Triaxial loading term is driven from three types of stresses that are in position of right angle to each other. When the sample is placed under compression loading, one of the stresses increases until the sample fails in shear (Smith, 1998).

The undrained behavior of sand under isotropically consolidated loading in monotonic test is accompanied by a change in the excess pore water pressure. The pore pressure can lead to different behaviour of soil (Figure 1).
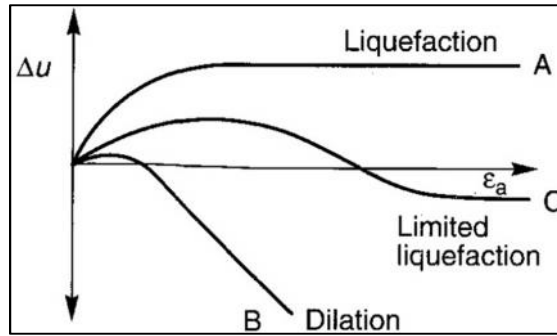
Figure 1: Pore-water pressures to axial strain in monotonic test (Kramer, 1996)

As inferred from the Figure 1, the pore-water pressure at beginning of testing gradually increased from zero pressure (path A) in which correspond to initial strain in sample followed by a constant value till the end of test. This means that the water percolated in porous spaces between particles and caused segregation of grains. In path B, because of cohesion or tiny voids between sand grains the pore pressure cannot reach to 100%. Hence this resulted in smooth curve in positive zone followed by negative pore-water pressure represented as dilation for rest of testing. The pore-water pressure condition between liquefaction and dilation path is limited liquefaction represented as path C in Figure 1.

2.2.1 Steady State

The Japanese standard sand called Toyoura for investigation of steady state was considered by Ishihara (1996). Behaviors of Toyoura sand in both contractive or strain softening and dilative or strain hardening with varying densities from 16% to 64% relative density were considered. The stress–strain and stress-mean effective stress curves for a series of undrained triaxial compression test on Toyoura sand were illustrated in Figure 2 where sand exhibits noticeable softening behaviour. For example, noticeable large peak appeared in q- in 1% strain correspond to high confining pressure in q-p'. Conversely perceptible declination from climax counted to low confining pressure in which continued till 25% strain. Despite the huge difference

in the q- (%) curve at early stage of loading, the samples show an almost monotonous behavior at a later stage of loading where the developed axial strain becomes as large as 25%, regardless of the limit of shear strain. This is termed as "flow deformation" and the mobilized shear stress of sand is called "steady state strength." or as residual strength. Similar pattern observed in 38 % and 64% in Figure 2.
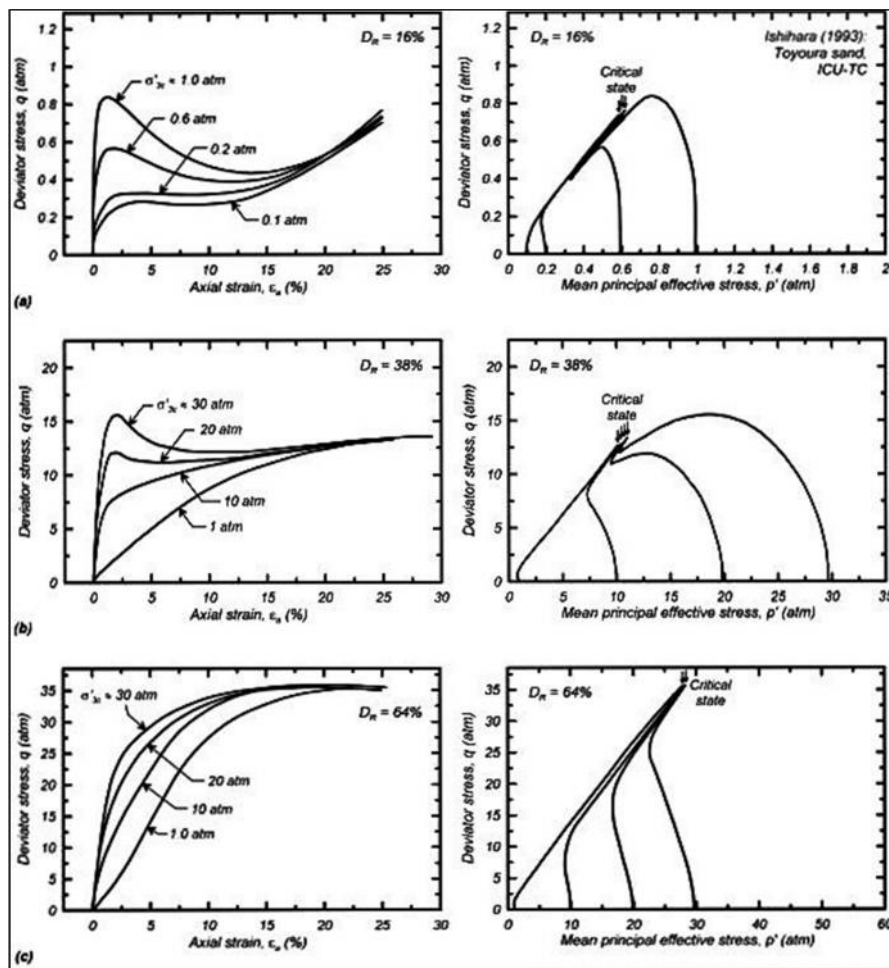

Figure 2: Stress-strain & stress-effective stress (Ishihara, 1996)

In fact, the stress paths of Toyoura sand in Figure 2 moved slightly toward left and upward simultaneously (contractive behaviour) till reaching their peaks in initial

strain of around 5% that corresponds to q- (%) graph. The point that curves enter to

dilative behaviour is called the state of phase transformation (Ishihara, 1996).

2.2.2 Quasi-Steady State

Transition state of soil from contractive to dilative behaviour in a broader sense,

regardless of whether it involves a temporary reduction in shear stress or not over a

restricted range of shear strain is termed as Quasi-steady state (QSS) as drawn by a

line in Figure 3. It has been detected from a numerous laboratory tests that QSS only

happens in loose sand and governed by void ratio and large primary confining

pressure at consolidation time.
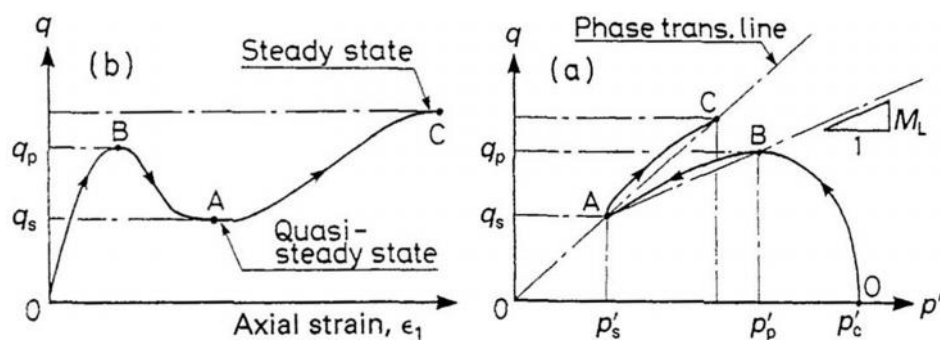
Figure 3: QSS of Toyoura sand in (a) q-p' & (b) q- curves (Ishihara, 1996)

Undrained response of loose and silty sand brought in Figure 3 point A defined as

deviator stress at QSS. This strength, called the residual strength.

2.3 Behavior of Undrained Sand under Cyclic Triaxial Loading

Typical response of soil when exposed to repetitive loading introduced by hysteresis

loop or stress-strain curve that the amplitude of strain was illustrated as γ_a in Figure 4

(a) where soil shows exhausted response due to advancement in cycles in strain-

controlled condition. When strain transformed from γ_a to γ_b in Figure 4 (b), similar

changes in cycle path was observed. Therefore, combination of curves in the both

figures resulted in Figure 5.
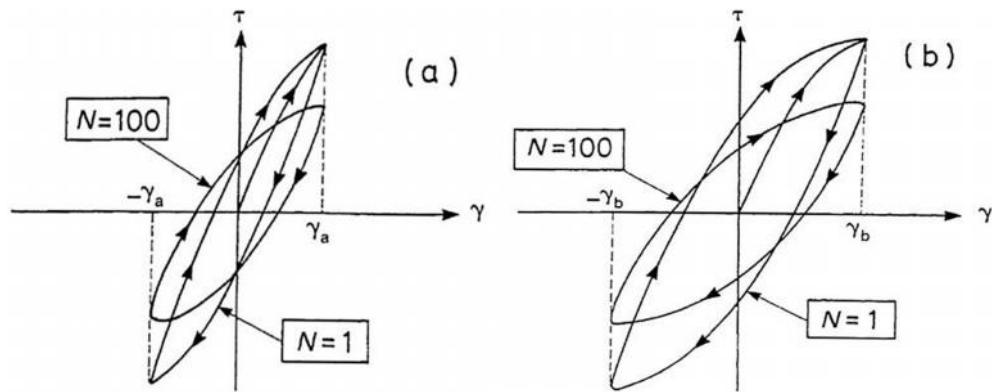
Figure 4: (a) Cyclic loading, short cyclic loading, (b) long loading (Ishihara, 1996).
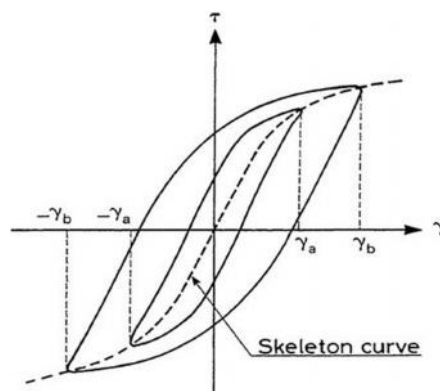
Figure 5: Combination of initial & final state of cyclic loading (Ishihara, 1996)

The two major consequences of the effect of the number of cycles, even at very low frequencies, are (i) the generation of resilient deformation under stress controlled cycles, and (ii) excess pore water pressure increase in undrained conditions.

In cyclic loading, pore water pressure continually builds up to 100% in loose sand while the cyclic axial loading applied and in the long run the pore pressure value becomes equivalent to initial confining pressure. Also for medium and dense sand the pore pressure reaches to 100% accompanied by 5% double-amplitude axial strain shown in Figure 6 (Ishihara, 1996). Nevertheless, total loss of strength does not experienced even after the very beginning of liquefaction.

The Figure 6 presents the data of hollow cylindrical test on Fuji River sand (Ishihara, 1996). The samples with medium density (Dr = 47%) and effective confining pressure of 98 kPa in undrained state were sheared torsionally.
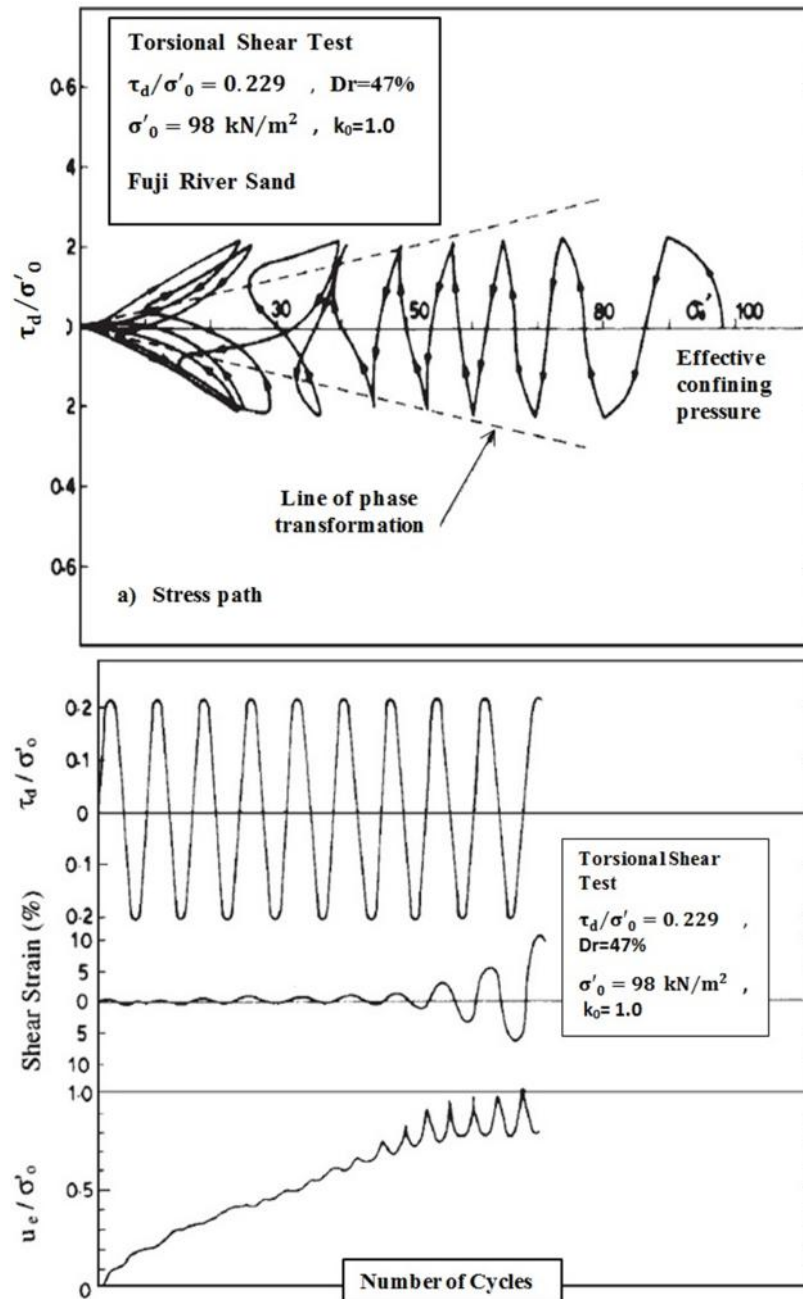
Figure 6: Behaviour of sand under cyclic loading (Ishihara, 1996)

Different plots are depicted in Figure 6 as follow:

1. Effective stress path:

The uppermost graph shows the stress path while the cyclic shear stress with constant amplitude is running. As the stress path moves toward the left permanently lose its shear strength by each individual cycle. For soil with high relative density the loss in shear strength is not permanent as the path moves to the left.

2. Cyclic shear stress graph (τ / σ'_0):

The Figure 6 illustrated that the cyclic stress follows constant amplitude showed by sinusoidal pattern. The amplitude (τ) was normalized by dividing it into the effective confining pressure (Day, 2002).

3. Shear strain in percent to the number of cycle's graph:

What induced from the Figure 6 is that the strain amplitude is constant for about 2%, but in the vicinity of liquefaction the strain rapidly increased to 20 percent that is initial liquefaction state.

4. Excess pore pressure to the number of cycles:

In the last graph, the pore-water pressure also was normalized (u $/ \sigma'_0$). In undrained shearing state the excess pore pressure developed gradually to become equal to confining pressure while the cyclic stress maintained constant. In this regard, the effective stress will become less and less to finally reach zero value and this occurred when the ratio (u $/ \sigma'_0$) reached to 1.0 (Figure 6).

2.4 Review of Applied Materials Behaviour under Triaxial Loading

Structure damages as a consequence of liquefaction proposed necessity of applying stabilizers into soil to minimizing the chance of liquefaction in sand. These stabilizers typically assorted as physical and chemical types that some of them are multipurpose materials. Most common mechanical stabilizers in cohesionless soil are geotextile, geogrid, geomembranes, geosynthetic etc. Nevertheless, chemical treatment of sand particles by (sticking them together) such as natural resins, fibers, agar, artificial stabilizers like, lime, fly ash, cement-fiber polymers etc. are possible. Polymer as a modifier can be used to prevent the slippage of sand particles by binding them together firmly so that liquefaction will not be a problem during earthquake periods. Generally polymers varied as biodegradable polymers and synthetic polymers. Synthetic polymers in most cases are more preferable than the natural polymers because of its availability and non-decomposability.

2.4.1 Chemical Reinforcement

2.4.1.1 Cement Reinforcement

Cement is one of the oldest binding agents since the advent of soil stabilization technology in 1960's (Makusa, 2012). Cement as a hydrophilic modifier agent can satisfies the required stabilizing level of soil due to the presence of water in almost every soil. This can be the reason why cement has been the first choice material in soil modification researches. Depending on the condition of soil, different types of cement can be used (Asghari et al., 2002).

Cemented soils can be found naturally, or induced artificially for the purpose of improving the bearing capacity of weak soils. Cementation plays a major role in the engineering behaviour of soils, and has been investigated extensively around the

11

world. The beneficial effects of cement treatment on the performance of a broad range of soils have been widely documented.

Kiousis & Abdulla (1997) Illustrated that addition of cement in soil mass leads to a more rigid and brittle material whereas increase of confining pressure reduces the softening tendencies, and generally results in a more ductile inflection with large initial volumetric compression. However, there is no general agreement regarding to the influences of cement inclusion of soil on the peak friction angle. The post-peak behaviour of cemented sand is in general characterized by some softening which is diminished as the confinement pressure increases. The cohesive shear strength decreased around 1% strain and at the same time the frictional strength becomes dominant. They reported that a very high confining stress could break the cementation bonds as well.

2.4.1.2 Lime Reinforcement

Asghari et al. (2002) conducted series of consolidated drained and undrained triaxial compression test on uncemented, artificially cemented and destructured samples derived from Tehran alluvial. The lime used as an agent to cement sandy gravel and gravely sand with three percentages of 1.5% , 3% and 4.5% of the weight of dry soil.

Samples prepared by crushing the 3% lime cemented samples to compare the behavior of destructured samples rather than the uncemented samples. He concluded that shear zone is visible for those cemented samples with less than 1000Kpa confining pressure, whereas cemented samples with higher than 1000kpa confining stress showed barreling transition to ductile behaviour. Also the behaviour of uncemented samples represented contraction or barreling state in period of shearing the specimens.
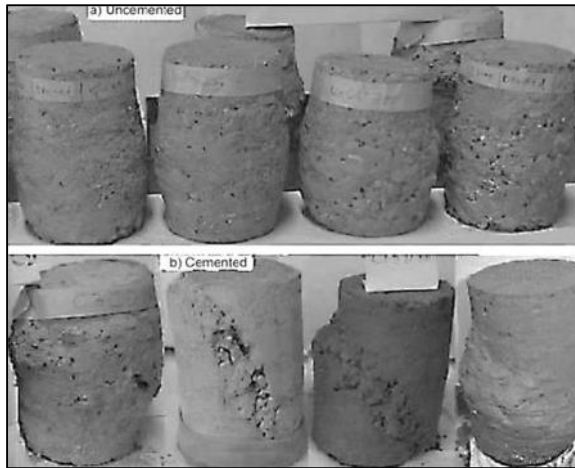
Figure 7: (a) Natural samples (b) cemented samples (Asghari et al., 2002)

He observed that as long as the amount of cement increases in the soil, the strength of samples increases but addition of cement to the soil with increase of confining pressure lose its efficiency and does not make any noticeable change in strength of the samples. Unlike barreled and linear line of failure in cemented samples, the non-treated specimens only barreled as illustrated in Figure 7.

2.4.1.3 Fiber Reinforcement

Fiber as a flexible material had a key role in construction of building in some countries like Iran. Fiber admixture within a soil mass can satisfy a reinforcement requirement by developing tensile forces which contribute to the stability of the soil-fibers composite. They are commonly deferred as natural fibers like coconut fiber, straw fiber, cotton fiber and kinds like nylon, polypropylene etc. counted as artificial fibers.

Consoli & Coop (2005) performed high confining pressure triaxial test on Osorio Sand located in southern Brazil that classified as non-plastic uniform sand. They reported changes in normal compression lines on tensile strength of the sand while Polypropylene fibers were randomly inserted into the soil as distinct and parallel

orientation into the samples. In reinforced specimens, fiber was found to be extended and broken after isotropic compression testing (Figure 8).
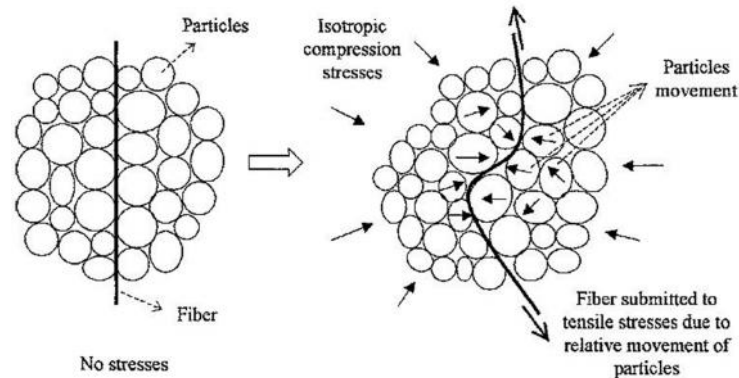

Figure 8: Fiber breakage under isotropic loading (Consoli & Coop, 2005)

Swami (2005) reported that beyond 2%-3% of fiber in dry weight of soil makes difficulties in mixing of fiber into soils.

2.4.1.4 Cement and Fiber Reinforcement

One of the difficulties in using cement is brittleness character of cement stabilized sands. This problem is resolvable by combining cement with fiber. The addition of cement increases the shear strength and stiffness of fiber reinforced sand and also amplifies the effect of fiber on residual strength. On the other hand, combining of cement with fiber increases peak and residual triaxial strength and reduced the stiffness behaviour of cement reinforced samples. It means the behaviour of soil transformed from brittle character into a more ductile form (Consoli, 1998) (Figure 9).
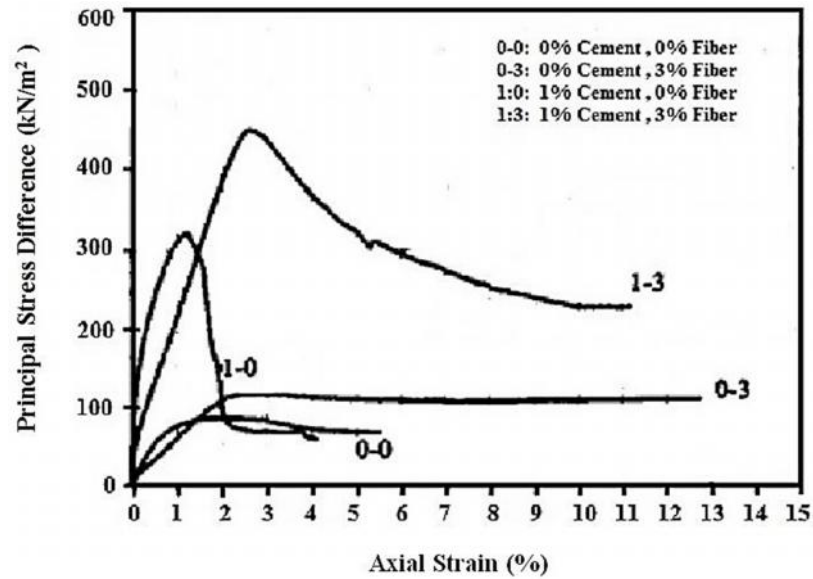
Figure 9: Stress-strain behaviour of cement-fiber reinforced sand (Consoli, 1998)

The measured friction angle of the untreated soil is increased from 35° to 46° because of soil fiber content. The fiber could slightly change the cohesion of the soil. Also The 1% cemented soil sample with 3% fiber inclusion reduced the brittleness index from on the soil samples containing 1% of cement reduced the brittleness index from 2.6 to 0.6.

2.4.1.5 Polymer Reinforcement

The term polymer is derived from Greek root that describes infinite number of compounds that can be synthesized from a relatively limited number of monomer units (small molecular units) (Lehman et al., 2004).

A large variety of polymers, with a wide range of properties, have been developed commercially since 1955 (Domone, 2010). Many of these materials have been used in construction industry; however polymers stiffness is very low for structural applications, unless combined with tough material. This section illustrates the processing, properties and applications of those that have been applied as adhesives, sealant, geosynthetic and elastomers (Domone, 2010).

15

In general, polymers varied as thermoplastic and thermoset types. Thermoplastic polymers consist of polymerized long chain molecules that are separable with ability of sliding over one another. Strong structure of this kind of polymer made it non degradable material by repetition of heating and cooling process. In contrast with thermoplastic polymers, thermosets cannot be easily softened or reshaped by heating. Thermoset molecular chains cross-linked, in which solid produced polymer cannot be softened or flowed (Figure 10). Plasticity and forming features of this type of polymer resulted in a non-softening rigid solid. This kind of polymer is used for composite as combined with a fibrous material or adhesive.
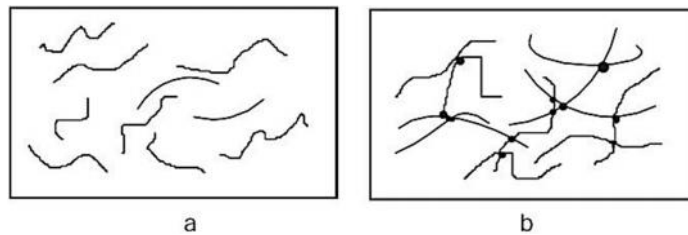

Figure 10: (a) Polymer molecules in disperse and (b) link molecules condition

Synthetic polymers can be classified as thermoset, thermoplastic and rubber polymers. Thermoset polymers are generally preferred than the other because of their rigidity in low temperature. They have high tensile strength and also have high melting point.

Khatami & O'Kelly (2013) have carried out many unconfined compression and unconsolidated undrained triaxial test on Fontainebleau sand. They used agar gel and starch as biopolymers with the soil in a way that agar with 1, 2 and 4 percent of the weight of soil and six different starches were selected. Different percentages of alone agar was mixed with the sand and subjected to unconfined compression. The result illustrates noticeable increase in the strength of the soil. Because, both the soil and agar have negative charges, 1% of agar was also mixed with 0.5% of six different

types of starches. In general, compressive strength and firmness came from the most starches considerably increased specially for Strapol 600 & Strapol 136.

2.4.2 Mechanical Reinforcement

2.4.2.1 Fabric Reinforcement

Use of polymers in the geotechnical engineering industry has been increasing for 35 years. Most common types of fabric reinforcements used in geotechnical engineering are geotextile, geogrid, geomembrane, geosynthetic. In the early 1970s, these materials were referred to as civil engineering fabrics or filter fabrics, and their primary use being as filters in soil. Geosynthetics have proven to be among the most versatile cost-effective materials compared to all other alternatives of ground improvement, besides being more resistant to corrosion and other chemical reactions (Murthy, 2006).

Murthy (2006) presented the result of an overall of 36 undrained triaxial compression tests on poorly graded sand with relative density of 70 %. The woven geotextile, geogrid and polyester film as stabilizers. These reinforcements were inserted in 2, 3, 4 and 8 layers in the soil shown in Figure 11. Then samples were sheared under different confining pressures of 100, 150 and 200 kPa in order to evaluate of the stabilized behavior of the sand from their shear stress and tensile strength point of view.
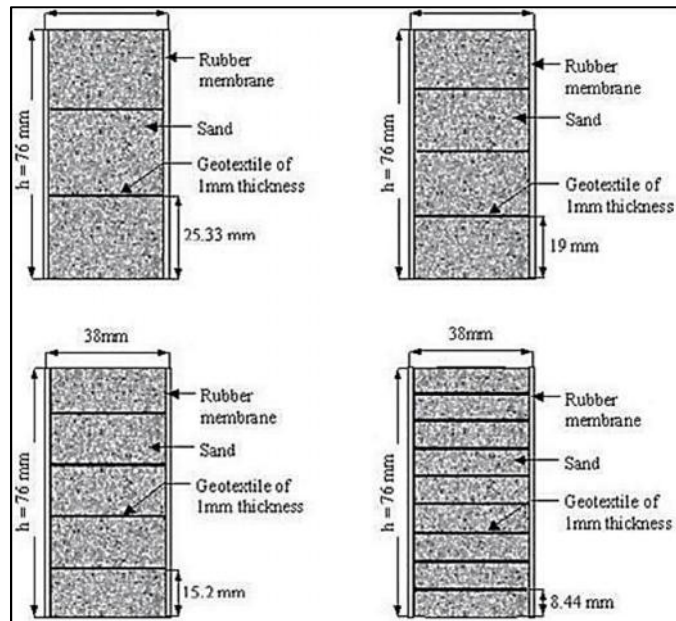
Figure 11: Reinforcements used for soil stabilization (Murthy, 2006)

Murthy (2006) found that geogrid has the lowest tensile strength, compared with geotextile and polyester film due to its inferior load durability features. Polyester film depicted ascending shear strength, but descending tensile strength trend in contrast with the highest value of deviator stress in geotextile reinforcement in comparison with unreinforced sand.

2.5 Methods of Applying Stabilizer to the Ground

2.5.1 Grouting

The grouting term defined as a process of injecting the low viscosity tiny particles or chemical fluids are penetrated into the soil mass. The suitability of different types of grouts for different soil conditions is most strongly influenced by the grain size of the soil (Kramer, 1996).

2.5.2 Permeation Grouting

In permeation grouting (Figure 12), materials like silica gel, lignin gels and acrylic resins injected to the soil mass with minimum physical change in the structure of soil. The aim of this method is to strengthen the soil resistance in case of liquefaction.
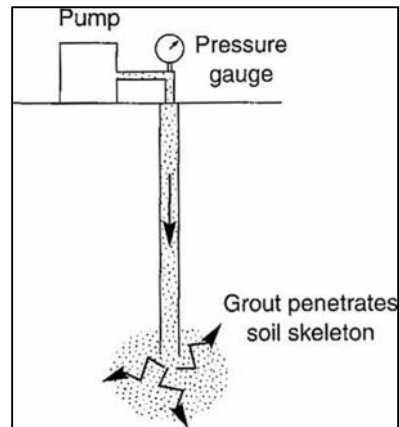
Figure 12: Permeation grouting (Hausmann, 1990)

2.5.3 Jet Grouting

In this method, a small nozzle, jets the grout with high pressure into the soil while the drill rod rotationally excavating the required depth of ground. This technique was widely was used for liquefiable soils for strengthening them (Figure 13).
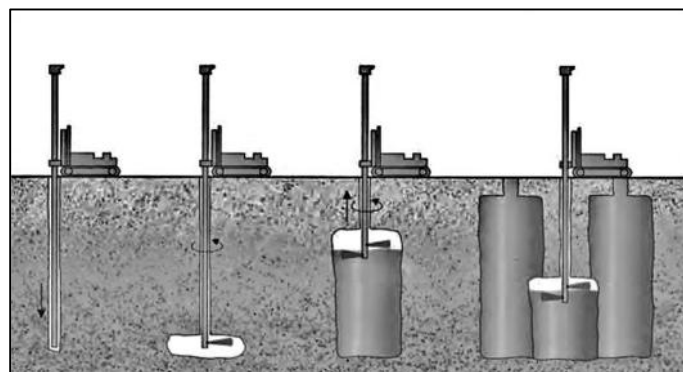

Figure 13: Jet grouting (Chung, 1995)

2.5.4 Intrusion Grouting

In this method, fluid with relative to high viscosity can be intruded into the ground. Intrusion grouting, is applicable in the soils where voids between particles were substituted by fractures (Figure 14).
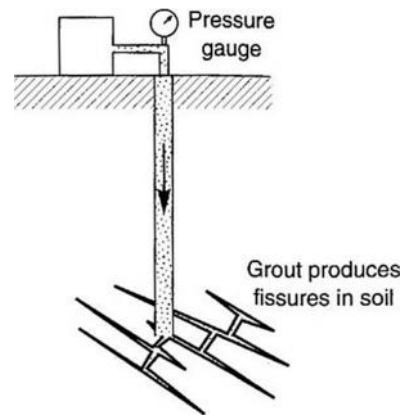
Figure 14: Intrusion grouting (Kramer, 1996)

2.5.5 Soil Mixing

The term of soil mixing refers to the mechanical improvement of soil and stabilizing materials via special mixing bar and rotating auger. As the mixing bar rotated into the ground, grout injected through tips of auger. Then create a uniform cemented column after reaching to desired depth of ground as shown in Figure 15. This type of mixing is called deep mixing method that is appropriate for ground level of 35 meter and has minimal effect on surrounding area (Port and Harbour Research Institute, 1997).
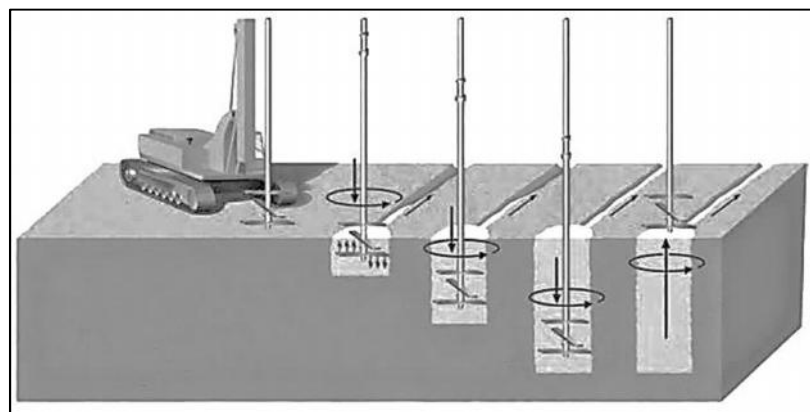

Figure 15: Soil mixing instrument (Chung, 1995)

Premix method is another way that has been successfully used to stabilize embankment, slopes, increase bearing capacity of foundations and prevent liquefaction-induced ground displacement (Chung, 1995).

In this method, since the mixed sand with stabilizer may fall into water the quality of water must be controlled (Port and Harbour Research Institute, 1997).

Chapter 3

MATERIALS AND METHODOLOGY

3.1 Introduction

Triaxial test apparatus simulates the real field condition of soil. Unlike horizontal shearing of soil in direct shear test apparatus, forces are applied vertically in all directions in the triaxial test. Therefore the failure plane is no longer conditioned by the apparatus itself but develops along the plane of less resistance within the sample. Also control of drainage of pore pressure in the triaxial test makes the test more realistic and advantageous over the direct shear test in which the drainage is hardly controllable. The triaxial test also allows measurement of radial strain of the sample under load; this feature is not present in the consolidation tests performed with odometers. Different types of loading conditions can be selected and tested and the soil properties such as cohesion and internal friction angle can be found.

The basic requirements for reliable triaxial testing are controlled specimen preparation to ensure reproducible initial state, complete saturation of the specimen, well centered axial load, negligible friction on the loading ram, well-controlled cell and pore pressures, and accurate measurements of axial load, axial deformation, and volumetric change.

3.2 Materials

The soil tested in this research is located along Mediterranean coast in Silver Beach area of Famagusta in North Cyprus (Figure 16). The representative soil sample was taken from the surface.

Figure 16: Silver Beach sand located in Famagusta in North Cyprus

3.2.1 Minimum & Maximum Void Ratios of Silver Beach Sand

The minimum and maximum void ratio of Silver Beach sand were determined in accordance with ASTM standard D4254-00 (2006) & ASTM D4253-00 (2006) .In determination of the maximum density, the test on sands was carried out by filling ASTM standard mold with Silver Beach sand through a funnel, then standard cylindrical weight placed and fixed over trimmed sand controlled by a retained plate. For 8 minutes, mold was vibrated and amount of soil settlement or decreased height of soil during compaction was measured (Figure 17) in determination of minimum dry density, mold was merely filled with sand and dry density calculated via division of weight of soil by volume of the mold.

Figure 17: Relative density tests

3.2.2 Particle Size Analysis of Silver Beach Sand

The sieve analysis test conducted is based on standard of ASTM D6913-04 (2009). The test is for determination of the particle size distribution of sand by shaking dry soil through a set of sieves and recording the mass of soil retained on each of them. The particle size distribution of Silver Beach sand is depicted in Figure 18.
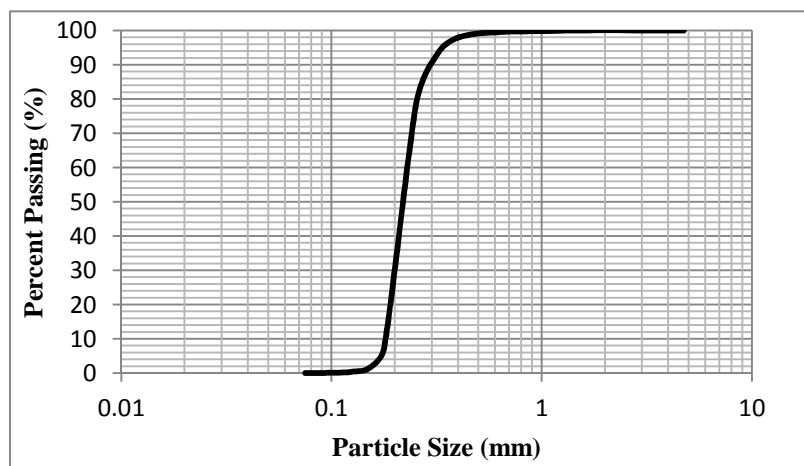

Figure 18: Particle size distribution of Silver Beach sand

Index parameters of the sand extracted from particle distribution graph in Figure 18 with other parameters from water-pycnometer and void ratios test were tabulated in Table 1.

Table 1: Index properties of Silver Beach sand

SILVER BEACH SAND			
$D10$	0.174	Gs (gr/cm3)	2.68
$\dfrac{D10}{D30}$	0.206	(gr/cm3) $emax$	0.935
$\dfrac{D30}{D50}$	0.232	$\dfrac{emax}{emin}$	0.67
$\dfrac{D50}{D60}$	0.247	$\dfrac{emin}{dmax}$ (g/cm3)	1.605
Cu	1.41	$\dfrac{dmax}{dmin}$ (g/cm3)	1.39
$\dfrac{C}{Cc}$	0.98	**Particle shape**	Sub-angular to rounded

The mean particle size of Silver Beach sand (D_{50}) is 0.23 that categorized the sand as fine sand and poorly-graded sand in accordance with Unified Soil Classification System (ASTM D2487-11, 2011).

In accordance with Scan Electron Microscopy image of Portaway sand (Wang, 2005), the sand particles categorized into sub-angular to rounded shapes.
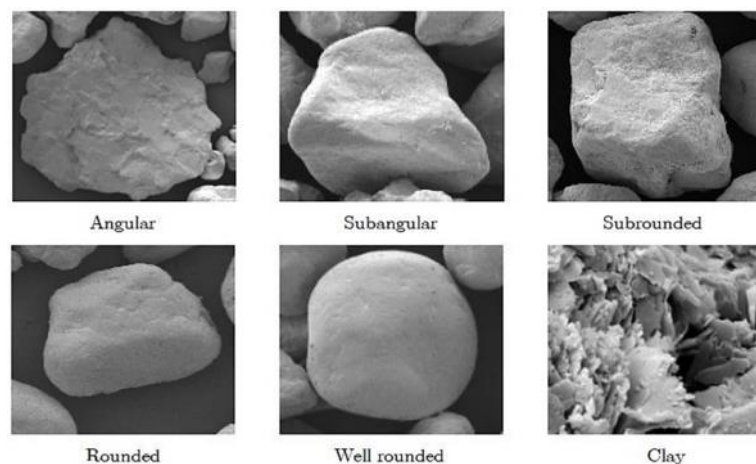
Figure 19: Characterization of particle shapes of Portaway sand (Wang, 2005)
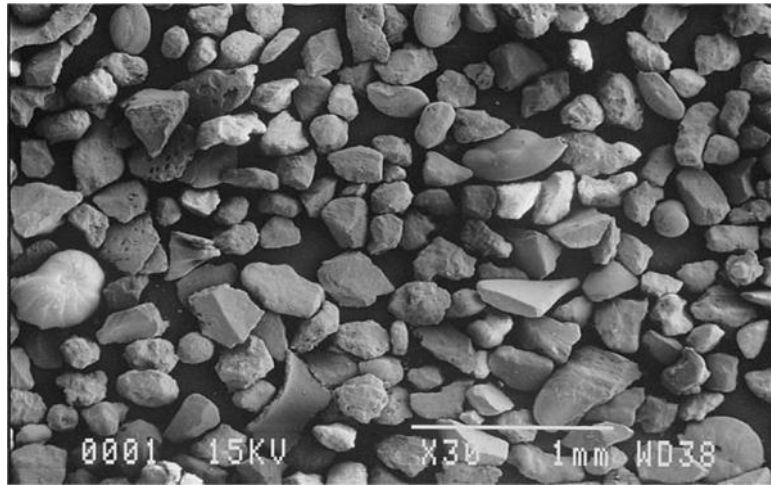
Figure 20: Silver Beach sand SEM image with magnification of x30

3.2.3 Compaction

Compaction is the application of mechanical energy to a soil to rearrange the particles and reduce the void ratio (Kousik Deb, 2010). Compaction of existing soils or fills is required for the construction of earth dams, canal embankments, highways, runways and in many other engineering applications. In general, the impact method of compaction (ASTM D698-7, 1942) is useful for evaluating soils with a percent fines ranging from 5 to 95 % (Terry, 2011). The impact compaction testing is typically used as a criteria method on fine-grained soils including silty sand, sandy silt, silty clay, clay silt and clay soils. Compaction is easy way to enhancing the bearing capacity and stability of loose soils. In this study standard protector compaction method were used.

3.2.4 Test Procedure

Test procedure based on ASTM D698-12 (2012) was followed. Silver Beach sand mixed with desired water content was kept interacted for 12 hours in plastic packs. In due time, an ASTM mold of 101.6 mm and 116 mm height filled with three layers. A 24.5 N weighted rammer dropped from 30cm height with pounding energy of 600kN-

m/m^3 and compact every layer by 25 blows then the mold afore soil extraction weighted. Amount of water content determined by sampling from top, middle and bottom of molded sand (Figure 21).

Figure 21: (Left to right) Weighting, extracting and sampling of the sand

By this method of soil compaction, maximum dry unit weight of the soil and the optimum water content were obtained for 14.7kN/m^3 and 16.5% respectively. The results are shown in Figure 22.
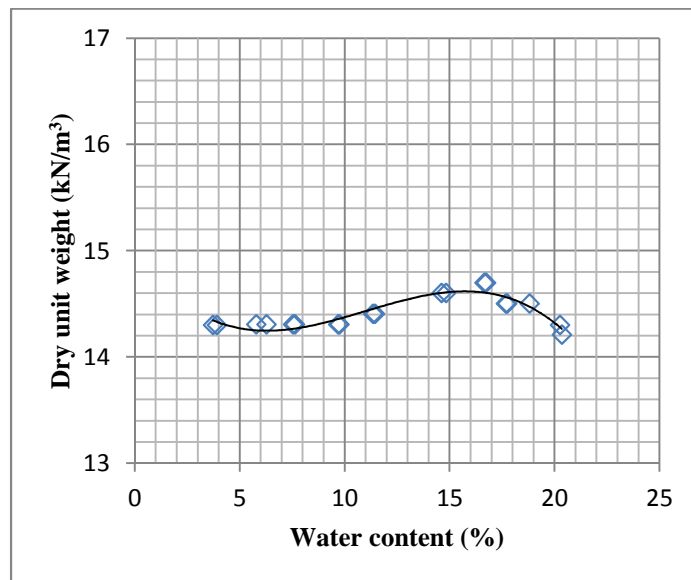

Figure 22: Dry unit weight to water content for Silver Beach sand

Generally, the dry density of soils is increased as the moisture content is increased. At the optimum moisture content, the dry density reaches the maximum, and then is reduced with an increase of water beyond the optimum moisture content.

3.2.5 Polymer (Polyfam 707)

The type of polymer used in this study was anionic dispersed polymer contained ultrafine particles and medium viscosity as shown in Figure 23. The material was Styrene and Acrylate Butyl polymer prepared by Resinfam Company (Iran) that counted as a member of thermoplastic polymers family. The material mainly was used as a host ingredient in paint industry that binds pigments and fillers.

Figure 23: Polyfam 707 polymer

This type of material was non-toxic, hydrophilic and water-soluble polymer with perfect tensile solidity.

3.3 Sample Preparation

Soils which possess little or no cohesion are difficult if not impossible to trim into a specimen. If undisturbed samples of such materials are available in sampling tubes, satisfactory specimens can be obtained by freezing the sample to permit cutting out suitable specimens. Samples should be drained before freezing. The frozen specimens

are placed in the triaxial chamber, allowed to thaw after application of the chamber pressure, and then tested as desired. Some slight disturbance probably occurs as a result of the freezing, but the natural stratification and structure of the material are retained. In most cases, however, it is permissible to test cohesionless soils in the remolded state by forming the specimen at the desired density or at a series of densities which will permit interpolation to the desired density.

Although liquefaction effect on in situ soil for earth fill dam mostly considered by undisturbed samples, basic laboratory studying on reconstitute methods is feasible. There are a number of methods for reconstituting samples, which greatly influence on the result of tests. Based on ASTM, these methods are water sediment, dry or moist vibration, dry funnel deposition and tamping method. The last two methods were applied in this study and these were presented below:

3.3.1 Dry Funnel Deposition Method

In this method, the de-aired and oven dried sand was poured into the mold through a flask. The gap between flask and top of pouring layer was maintained constant (Figure 24), because increasing in the height of the flask nozzles from surface of the pouring soil or also reducing the rate of fall (less grain-to-grain collision and energy loss) leads to constitution of dense sand (Kolbuszewski, 1948).
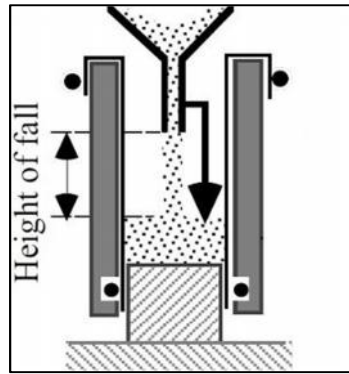
Figure 24: Dry Funnel Technique (Towhata, 2008)

This method was applied in this study for purpose of achieving low density samples, but the result proved otherwise (Figure 25).
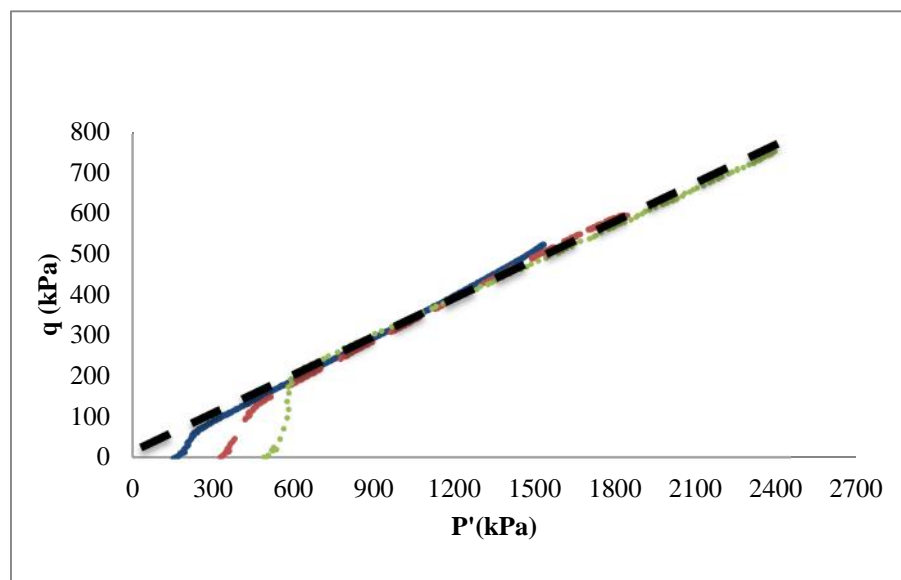
Figure 25: Deviator stress to effective stress of dense sand

Figure 25, illustrated that the effective stress paths initiated from different amount of consolidation. The data curves of the samples at the beginning of shearing tend to move towards the right of the graph which is representing the strain hardening state or dilative behaviour of soil.

3.3.2 Tamping Method

This method was followed in this study. Silver Beach sand was mixed with deaired water and poured in five layers by following Undercompaction technique proposed by Ladd (1974). By this method, the lower layers were given light blows in compare with successive upper layers in order to obtain a uniform density throughout the samples. The recommended moisture by Ishihara (1996) was 5% water content of soil, but in this study moisture based on obtained data from Figure 22 in section 3.2.4. was taken as 8.2% of soil water content. Each portion of the slightly moist sand is strewed with fingers to a predetermined height (Ishihara, 1996). Then Tamping was gently applied with a small flat-bottomed rod for five lifts (Figure 26).
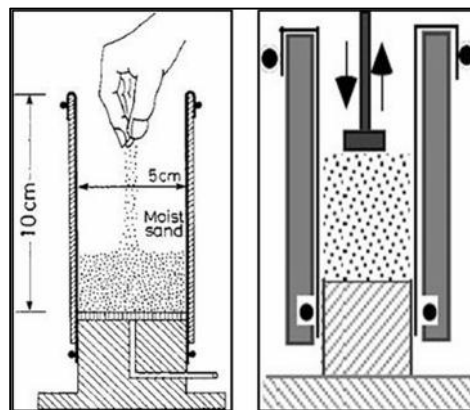
Figure 26: (Left) Sand infusion and (right) compation of layers (Towhata, 2008)

One of the advantages of this method is the versatility in permitting sample to be prepared within a wide range of void ratios. Also prepared samples by this method reduce the chance of particle segregation and functional for most types of sand.
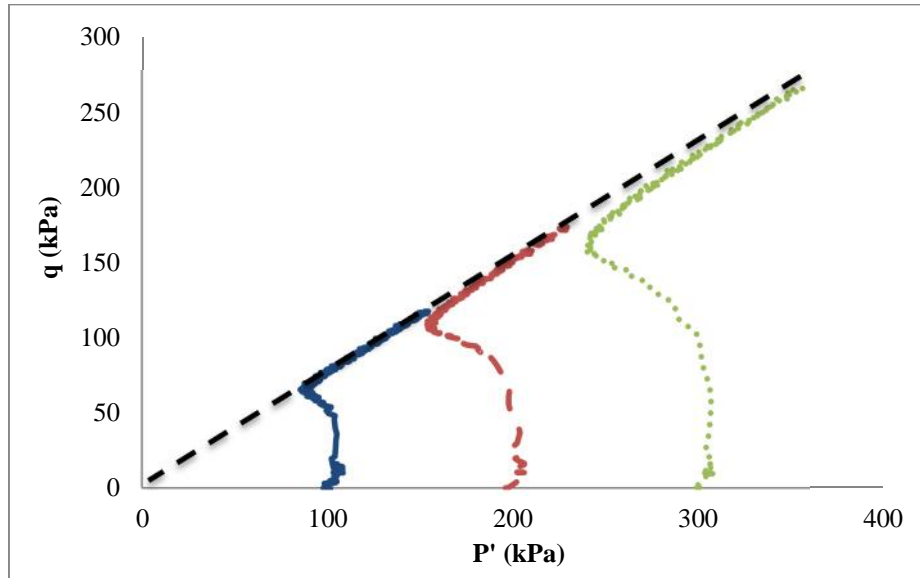
Figure 27: Deviator stress vs effective stress, loose sand

In Figure above, the result obtained by tamping method which shows the effective stress paths for different confining pressures tend to be contracted then dilated by moving toward the right.

3.3.3 Preparation Procedure of Natural Sand

The samples with 50mm diameter and 100mm of height were shaped and prepared by fastening two semi-cylindrical shells around them. The shells simply can be held together with a metal girth at their bottom part. Then the mold was connected to vacuum burette in order to stick the inside placed membrane tightly to its walls. The vacuumed pressure was taken as low as possible for almost 10kPa to not disturb the pre-determined density of the samples. The density was calculated from the given relative density formula:

$$D_r = \frac{e_{max} - e}{max - e_{min}} \hspace{2cm} [1]$$

Before and after pouring the Silver Beach sand into the mold, two porous stones were placed on the pedestal of the apparatus and also top of the constituted samples in order to prevent any blockage that may cause by the sand grains. Then the soil was tamped in layers by following Undercompaction method proposed by Ladd (1974) as shown in Figure 28.
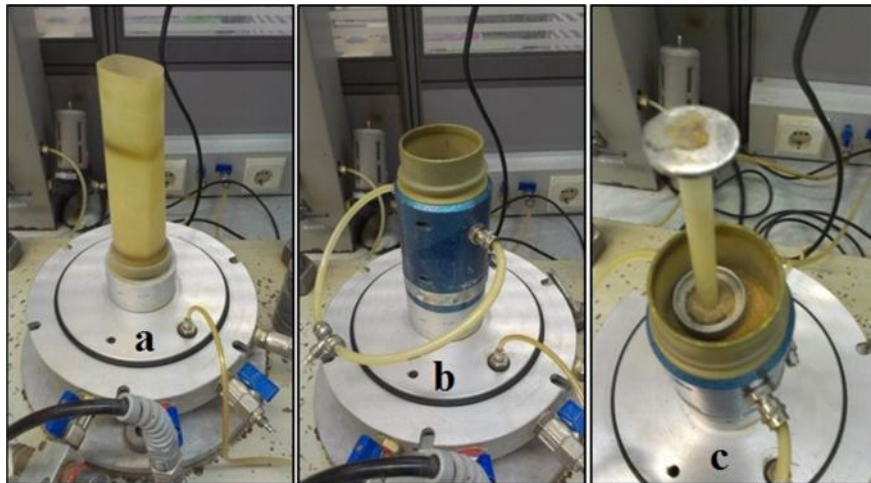
Figure 28: (a) Membrane erection, (b) vacuum application & (c) compaction

Then the mold was detached from the samples and cell case installed on the triaxial pedestal. The vacuumed was connected to the bottom of the samples until the moment that cell filled with water then pressurized (Figure 29).
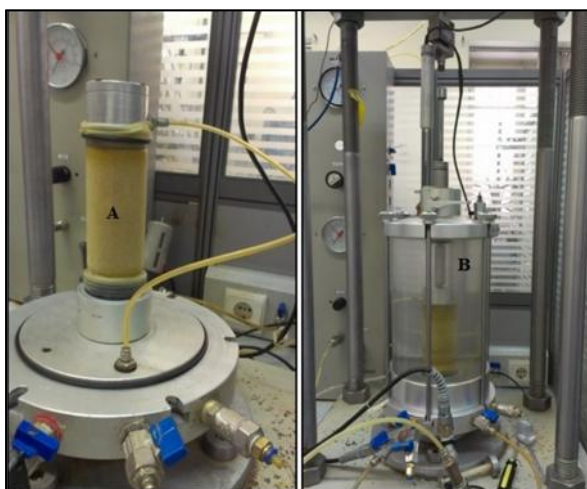
Figure 29: (A) Mold detachment, (B) confining pressure application

3.4 Reinforced Sample Preparation

3.4.1 Method

The intermediate viscosity of polymer (Polyfam 707) caused some difficulties in sand combination with the polymer and some restrictions in depth of percolation of polymer into the sand. Hence, the Polyfam 707 was diluted in order to lower its viscosity, by means of adding different amount of distilled water following the calculations given in Table 2 (Yasrobi, 2011).

Table 2: Calculation of synthesized polymer

(P/F)	(F/S)	(P/S)
12.5%	16.5%	2%
25%	16.5%	4.1%
50%	16.5%	8.2%
P/F = weight ratio of polymer to solution **F/S** = weight ratio of solution to sand **P/S** = weight ratio of polymer to sand		

As a result, three different percentages of diluted polymers from viscosity point of view were selected and were added in optimum water of the sand. The viscosity values of three sand-

polymer mixtures used in both monotonic and cyclic triaxial tests were determined by using Rockwell rheometer device (Figure 30).
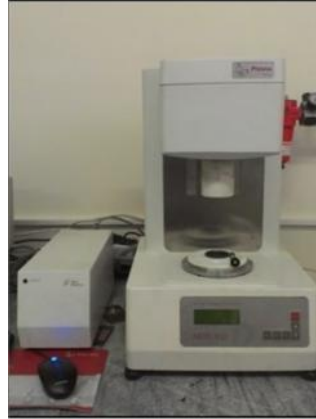
Figure 30: Rockwell rheometer

Some index properties of the polymer such as viscosity, pH, density and minimum filming formation temperature (MFFT), with its different percentages are given in Table 3.

Table 3: Index properties of Polyfam 707

Polyfam 707 (%)	Viscosity (Mpa.s)	PH	Density (G/Cm^3)	MFFT ($^{\circ}$c)	Color	Reinforcement Mechanism
Polyfam 707	3500±1500	8±1	1.02	18	White	adherence
2% (P/S)	1.54	8.44	1	18	White	adherence
4.1% (P/S)	1.91	8.43	1.01	18	White	adherence
8.2% (P/S)	2.41	8.36	1.02	18	White	adherence

As it can be inferred from the data of viscosities of different percentages of polymer in Table 3, the values approached to water viscosity.

The taken values of polymer to dry weight of sand mixed and poured in prefabricated mold by using wet tamping method as proposed by Ladd (1974).

3.4.2 Preparation Procedure of Treated Sand

Series of Poly Vinyl Chloride (PVC) pipes were cut according to the dimension of the both triaxial devices for 5cm in diameter and 10cm in height with negligible deviation. Due to some probable distortion of the trimmed pipes, internal space of the molds was covered with talc as illustrated in Figure 31. The polymer contented sand was poured in the molds with Undercompaction technique.
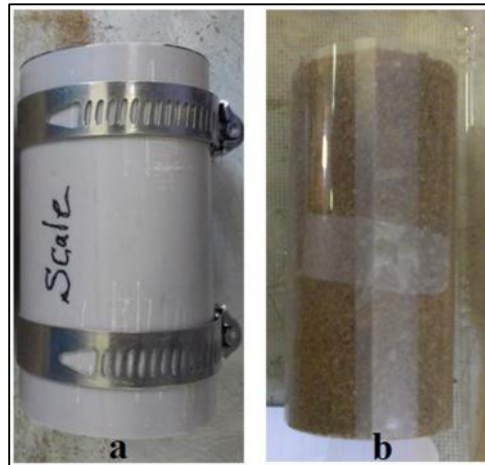
Figure 31: (a) PVC mold and (b) talc covered sample

Talc placed in the mold is for two reasons: Firstly to control internal diameter of cut mold, secondly to avoid sample failure due to stickiness of mixed material to the wall of pipes in time of extraction (Figure 32). In latter case, talc lubricated the mold before pouring the soil.
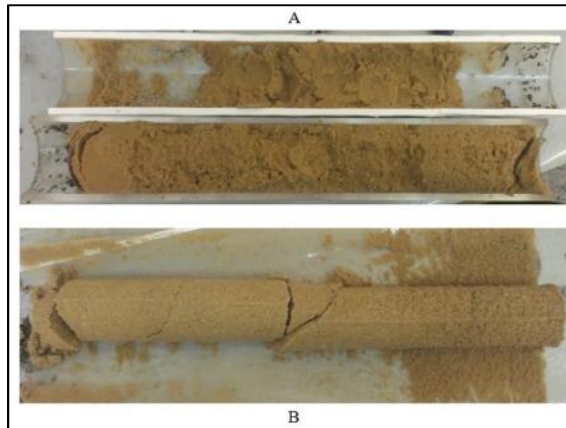
Figure 32: (A) Disturbed and (B) non-disturbed sample

In this study, a total number of 23 natural and added-material samples with density of 20% were prepared. For evaluation of stickiness effect of the polymer on non-treated samples, all the reconstituted samples were given 7 days curing time in a way that they were kept in the PVC pipes for 2 days then removed and exposed to room temperature of 21 degree (Figure 33).
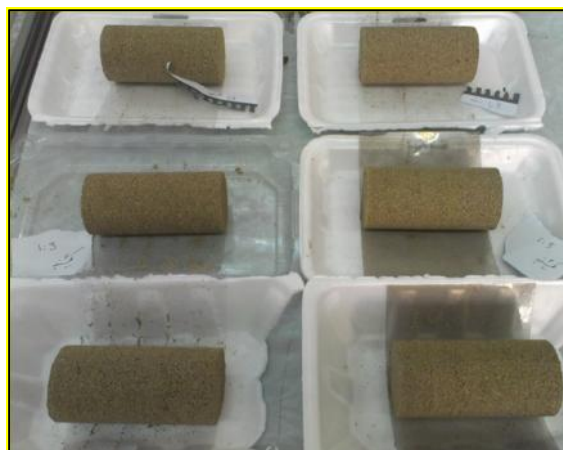
Figure 33: Exposed samples at room temperature

In cohesionless soils, particles tend to slide over each other; by this reason vacuuming of soil is a way to stand them still. Vacuum is kept connected to specimen until generation of confining pressure in the system; however polymerized soil due to the stickiness character of polymer is rigid enough to hold them without usage of vacuum

37

as shown in Figure 34. The rest of the test stages are just like of non-polymerized clean sand.
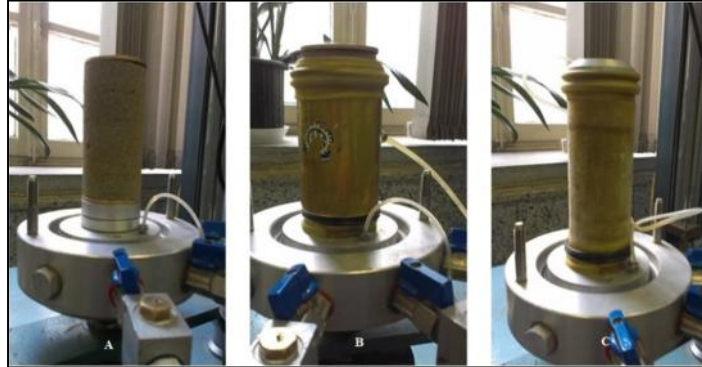
Figure 34: Stages of polymeric sand testing

3.5 Test Procedure for Natural and Reinforced Sand

3.5.1 Saturation of Sample

The main objective of this phase of experiment was to fill the pore spaces with water. Prior to saturation of the sample, Carbon-dioxide (CO_2) gas was circulated into the sample for 20-40 minutes, in order to expedite the process of reaching to 95% Skempton's B-value given in equation 2. Carbon-dioxide (CO_2) gas slowly circulated into the specimen bottom up so the grain packing of sand was not disturbed by the flow (Towhata, 2008).

$$\text{Skempton's B-value} = \frac{u}{3} \qquad [2]$$

where,

u = Excess pore water pressure

$_3$ = Cell Pressure changes

38

Next step was the entry of de-aired water into the sample from bottom to top of sample and finally exiting from back pressure channel. De-aired water passed through the sand twice the volume of the pores (Figure 35). Usually this value was achieved in five coincide increment of cell pressure and pore pressure. Above procedure was applied to all samples.
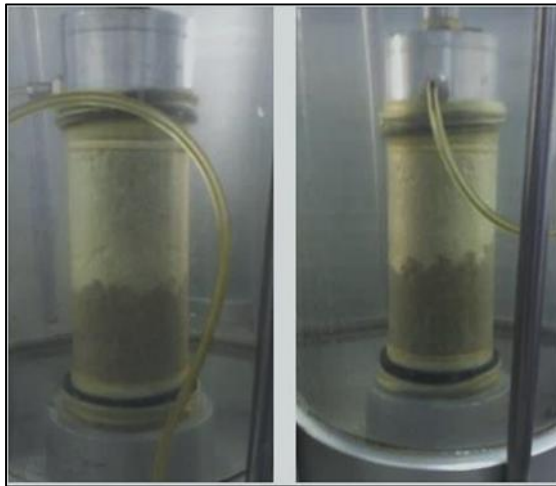
Figure 35: Saturation level

3.5.2 Isotropic Consolidation of Samples

The objective of the consolidation stage is to bring the specimen to the state of effective stress required for carrying out the monotonic and cyclic test. For this purpose the applied pore and back pressure maintained constant and the chamber pressure (σ_3) increased as the differences between the confining pressure and average of pore and back pressure equals the prescribed consolidation pressure. Specimens were isotropically consolidated with the confining pressures of 100, 200 and 300 kPa.

Following consolidation, the samples were allowed to be drained for a period of 10 minutes. Then the changes in volume of samples were recorded via a hinged water burette on the control panel (Figure 36). This recorded data induced the final and

reliable relative density of the samples which was a little higher than the desired

density at the beginning of testing.
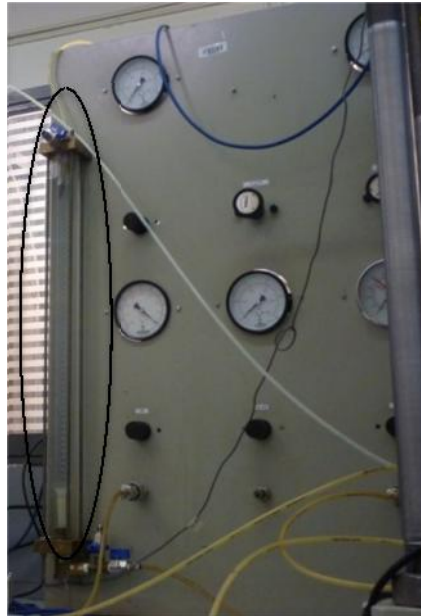
Figure 36: Water graduated tube

3.6 Test Setup

3.6.1 Static Triaxial Loading Device

In this section, the working mechanism, samples parameters and the test setup of the

static triaxial loading device are described in detail.

Figure 37: Monotonic triaxial device

The static triaxial loading device shown in Figure 37 is a strain controlled device. Monotonic triaxial test comprises of five main parts of shearing device, cell, pressure panel, data logger and a computer that are connected to two instruments. Before shearing the samples a hydraulic jack in the bottom part of the device moves the cell upward to involve the axial force with the sample inside the cell then the sample was sheared with 1.5 mm per minute rate of shearing. Real field conditions of soil element simulated through creation of confining pore and back pressures by 25 kN standard triaxial cell. The pressures can be set-out through the connected sensors to pressure panel (Figure 38) described as follow:

1) One for measuring the axial loading amount with 24 kN capacities.

2) One for axial displacement with 55 mm range.

3) One for cell pressure control of 500 kPa.

4) One for setting pore pressure and measuring volume change.

5) One for measuring back pressure.

Figure 38: Triaxial device sensors

The task of sensors was to transfer the changes in value of pressures or samples displacements to the data acquisition system (Figure 39).

Figure 39: Data acquisition system

3.6.2 Cyclic Triaxial Loading Device

The device is mostly popular for analyzing cohesionless soil behavior under cyclic loading just like how it happens in reality with capability of adjusting diverse frequency and amplitude proportional to density and type of soil. The device shown in Figure 40 comprises of a data logger, pressure panel, cell and driving force or pneumatic jack. All the sections are similar to monotonic device except some parts which will be defined in the following paragraphs.
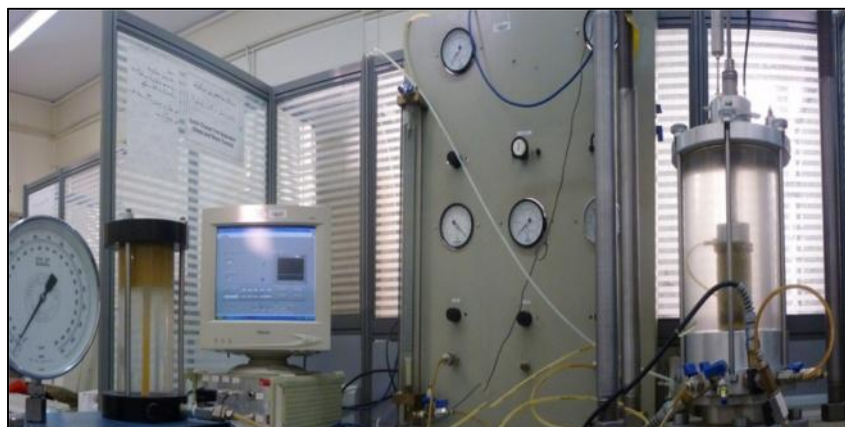
Figure 40: Cyclic triaxial device

Unlike monotonic test in which a hydraulic jack sheared the samples slowly with a constant rate while tests are running, in cyclic testing the pneumatic jack provided quick reciprocate loading. This jack derived its forces from pressurized air that was connected to air compressor with capacity of maximum 500 kPa pressure as shown in Figure 40.

Figure 41: Pneumatic load generator

3.7 Data Interpretation

The obtained data from monotonic and cyclic triaxial loading were analyzed by using the following equations given below:

Strain,

- Axial strain,

$$= \frac{\Delta L}{L_0} \qquad [3]$$

- Volumetric strain

$$v = \frac{\Delta v}{v_0} \qquad [4]$$

where,

$\dot{L}$ = Displacement changes

L_0 = Initial height of sample

$\dot{v}$ = Volume changes

v_0 = Initial volume

Stress,

- Axial stress**,**

$$= \frac{N}{A} \qquad [5]$$

- Deviatory stress,

$$q = (\sigma_1 - \sigma_3)/2 \qquad [6]$$

- Mean stress

$$p' = \sigma'_1 + 2 \times \sigma_3 \qquad [7]$$

- Major principle stress,

$$\sigma_1 = (\sigma_3 + q) \qquad [8]$$

- Effective Major Principle stress,

$$\sigma_1 = \sigma_1 - u \qquad [9]$$

- Effective confining stress,

$$\sigma_3 = \sigma_3 - u \qquad [10]$$

- Cyclic stress ratio

$$CSR = q_{cyc}/2\sigma'_{3c} \qquad [11]$$

where,

N = normal force

A = cross section of the sample

σ_1 = major principle stress

σ'_1 = effective major principle

σ_3 = confining stress

σ'_3 = effective confining pressure

$'_{3c}$ = isotropic consolidation stress

q_{cyc} = cyclic loading

Chapter 4

RESULTS AND DISCUSSIONS
MONOTONIC AND CYCLIC TRIAXIAL TEST

4.1 Introduction

The main purpose of this study is to consider the sand response in natural and treated condition while liquefaction is occurring in laboratory scale by triaxial devices. The triaxial monotonic and cyclic loading simulates flow and cyclic mobility liquefaction on an element of soil beneath the surface. In the first type of response, the sand may lose its large resistance portion and deform continuously and in latter case, large deformations may result from progressive stiffness degradation of the soil.

Although both flow liquefaction and cyclic mobility result in large deformations which are generally unacceptable for engineering purposes, the mechanisms of strain development as a consequence of flow liquefaction and cyclic mobility are quite different. It is generally believed that relative density is the most important initial state parameter of sand controlling the development of strain under cyclic loading. Flow liquefaction only occurs in very loose sand; while cyclic mobility can be caused by wide range of densities.

In the first part of this chapter the results of monotonic triaxial test will be presented and discussed. In undrained test no drainage was allowed and pore pressure for loose sand increased.

The soils as natural and polymer reinforced state were reconstituted with relative density of 20% by employing wet tamping method described in Chapter 2. In order to investigate the influence of polymer on the natural soil, samples with 7 days curing time were subjected to monotonic and cyclic triaxial loading. Regarding the evaluation of reinforced sand behaviour at different depths of ground, samples were confined under different imposed pressure.

In cyclic mobility section of this chapter, all the tests, the effective stress paths moved toward the failure envelopes during cyclic loading and finally they traced the steady loops which were tangent to failure envelopes.

4.2 Monotonic Test Results of Silver Beach Sand

A total of 12 undrained monotonic triaxial compression tests on natural and treated sand were conducted. The reinforced samples with 2 to 8.2% polymers to the dry unit weight of the sand were tested with variety of confining pressures as depicted in Table 4.1. The natural and treated specimens were isotropically consolidated in undrained state and sheared with a strain rate of 1.5 mm/min. the outcome data were depicted as effective stress paths; stress-strain and pore water pressure to strain (Figures 41-44).

Table 4: Properties of monotonic triaxial loadings

Test No.	Confining stress (kPa)	Treated sand by polymer (%)	Dr (%)
1	100	2	
2	200	2	
3	300	2	
4	100	4.1	
5	200	4.1	20
6	300	4.1	
7	100	8.2	
8	200	8.2	
9	300	8.2	

As can be seen in Figures 43 and 44, the phase transformation in q-p' graphs of the treated samples do not show any peak in initial strains. The stress paths for those samples tend to move to the right from very beginning of samples shearing which is opposite to movement of effective stress for Figure 42. In this figure phase transformation is easily detectable just like the natural sand samples. This shows similar behaviour of 2% polymer with natural sand that inferred its inefficiency for 7 days curing time. When the samples maintained for 3 days more than 10 days it showed same behaviour of higher percentages of polymer depicted in Figure 43 and 44. As far as the polymer type applied in this study was air-drying thermoplastic polymer it had opportunity to become more rigid in 3 more curing days.

In Figure 44, the confining pressures of 200 and 300 kPa were similar to that of the natural sand pattern illustrated in Figure 41. On the other hand, the stress-strain curves of reinforced samples in all graphs raised abruptly in initial stages of loading followed by gradual increase in deviator stress until 12% strain. For this reason, no Quasi-steady state was observed in the samples whereas, in confining pressure of 100 & 200 kPa for natural sand the Quasi-state occurred in strain range of below 3%. As inferred from the figures of q- of reinforced sand those added samples with polymer and confined with 300 kPa pressures showed 262 kPa of deviator stress in 8.2% polymer to dry weight of sand that is 100 kPa more than the natural sand. Also for 4.1% and 2% polymer to the sand, the deviator stress is 238 and 179 kPa respectively. The deviator stress curves in confining pressure of 100 & 200 kPa in Figure 42 overlapped which each other and also in Figure 44 these curves were close to each other in strain of 3% that shows equal deviator stress of 8.2% and 2% polymerized sand in large strain.

In the reinforced samples with different confining pressures, the pore water pressure began with the imposed back pressure in samples graphs. After sharp movement of pore-water pressure curves towards the positive value in the graph that state the contractive behaviour of the soil, the path moved downward with a tedious slope until reached a plateau in negative portion of graph with further strain that showed dilative character of samples. In reverse, pore-water pressure paths in the loose samples in Figure 41 passed the positive peak with almost smooth line till 5% strain then gently moved downward with a steady slope toward the end of test.
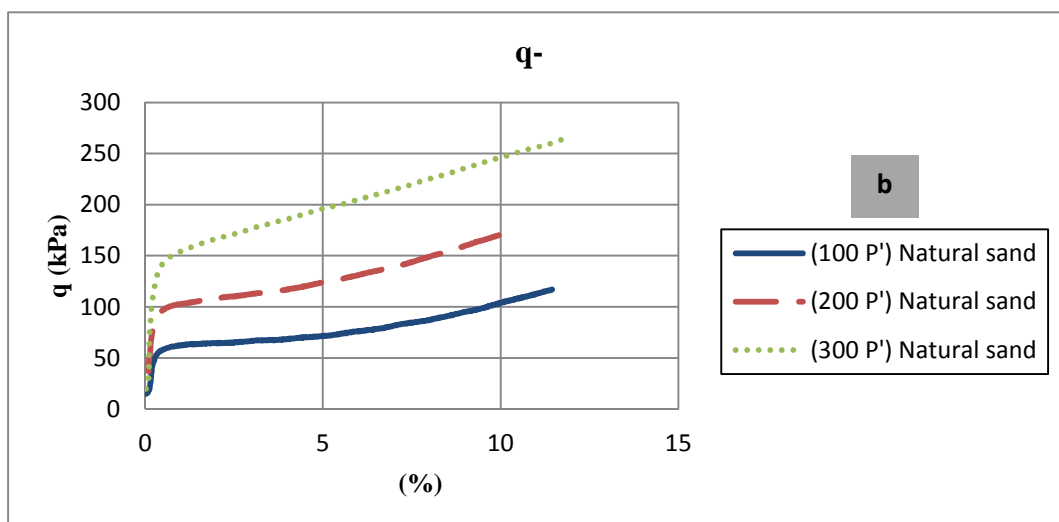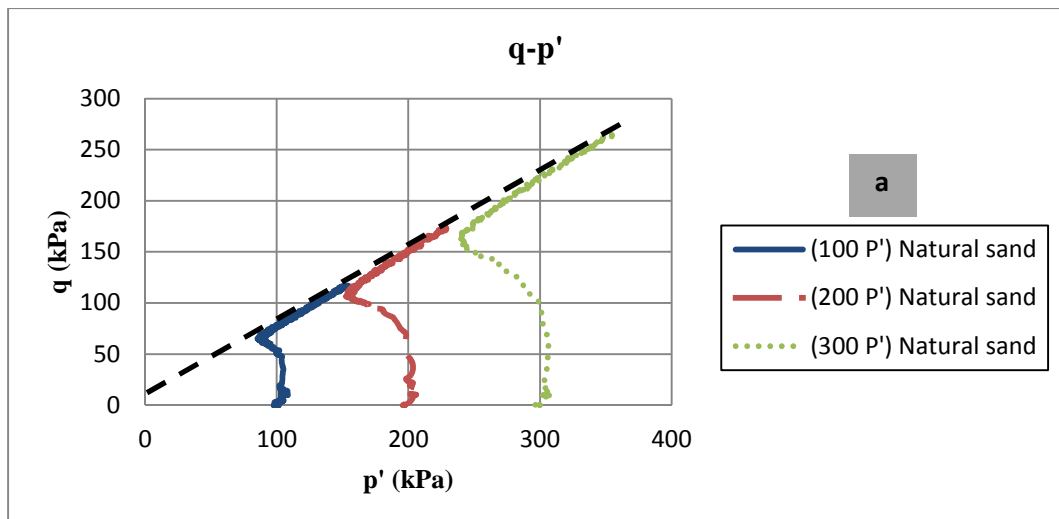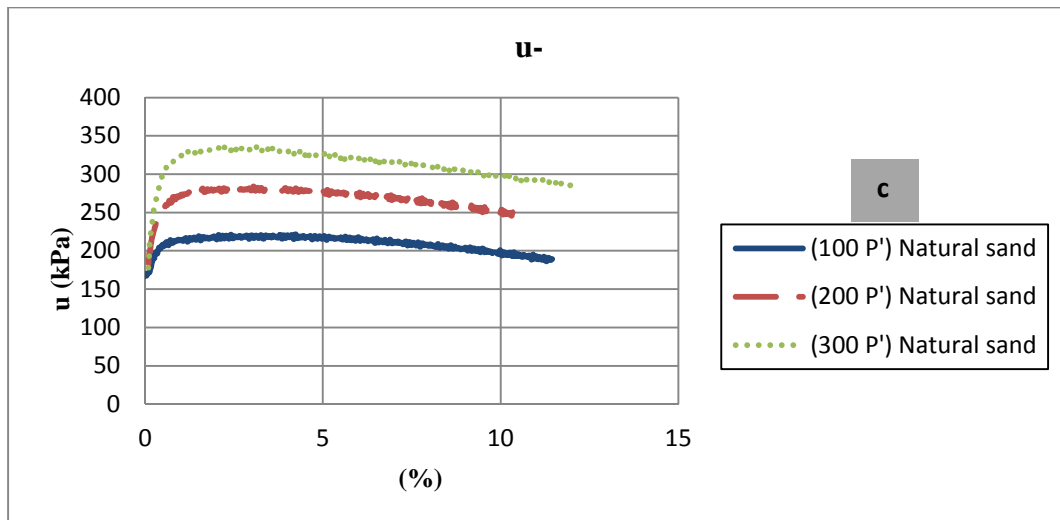
Figure 42: (a) Effective stress, (b) stress-strain and (c) pore water pressure vs. strain

curves of natural soil in undrained monotonic compression loading condition.
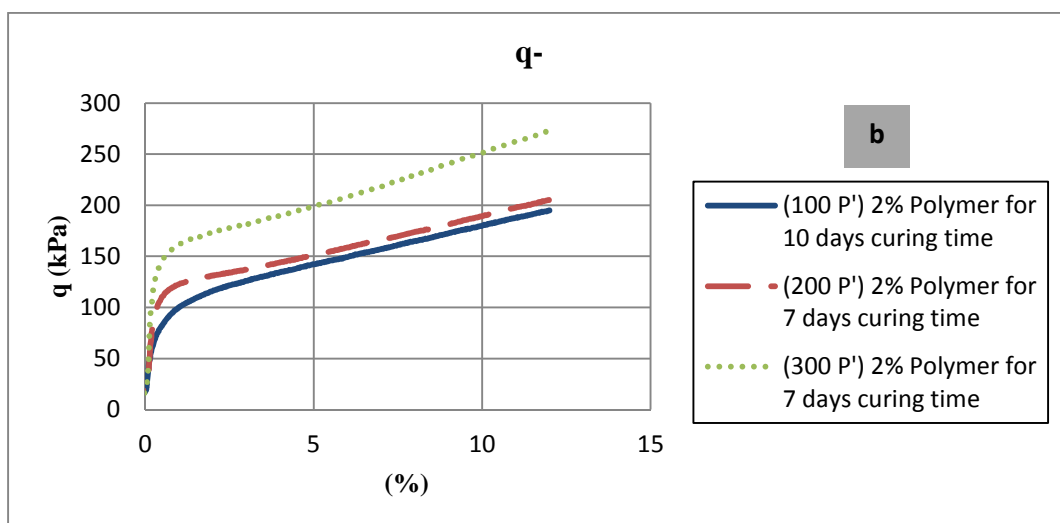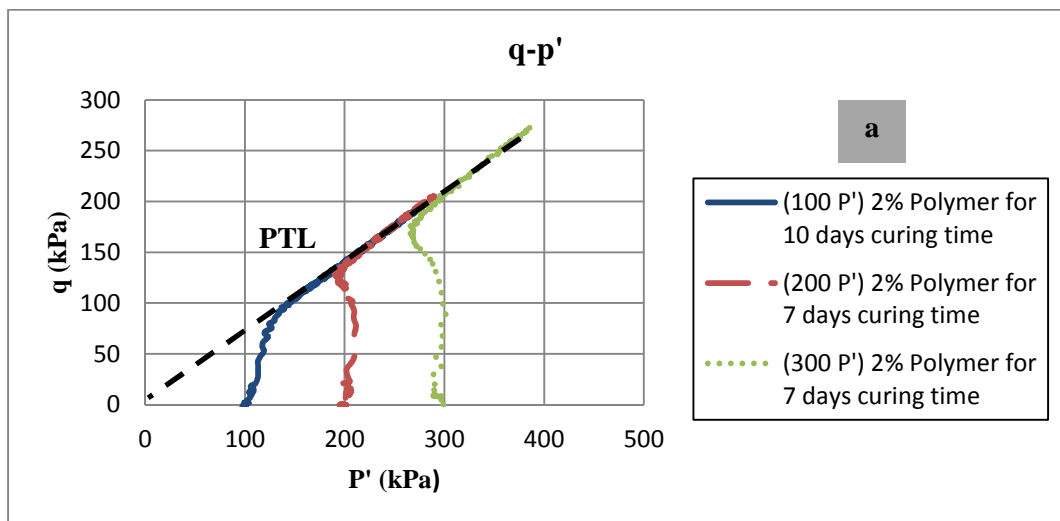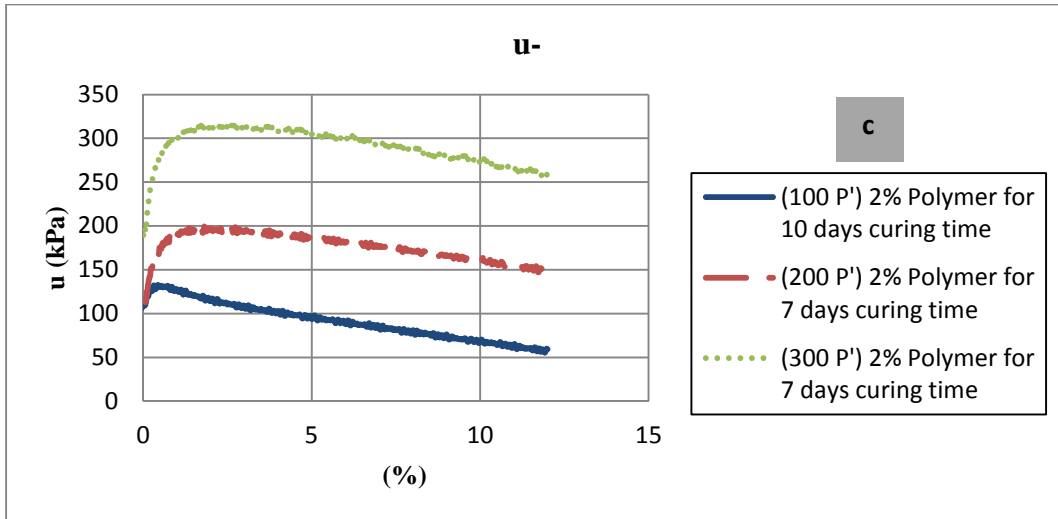
Figure 43: (a) Effective stress, (b) stress-strain and (c) pore water pressure vs. strain curves of 2% polymer to the natural soil in undrained monotonic compression loading condition.
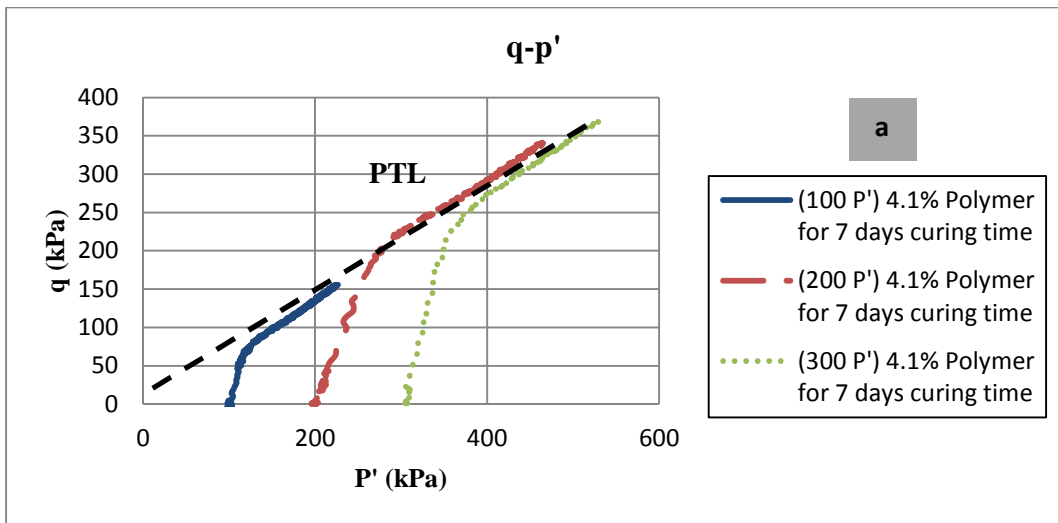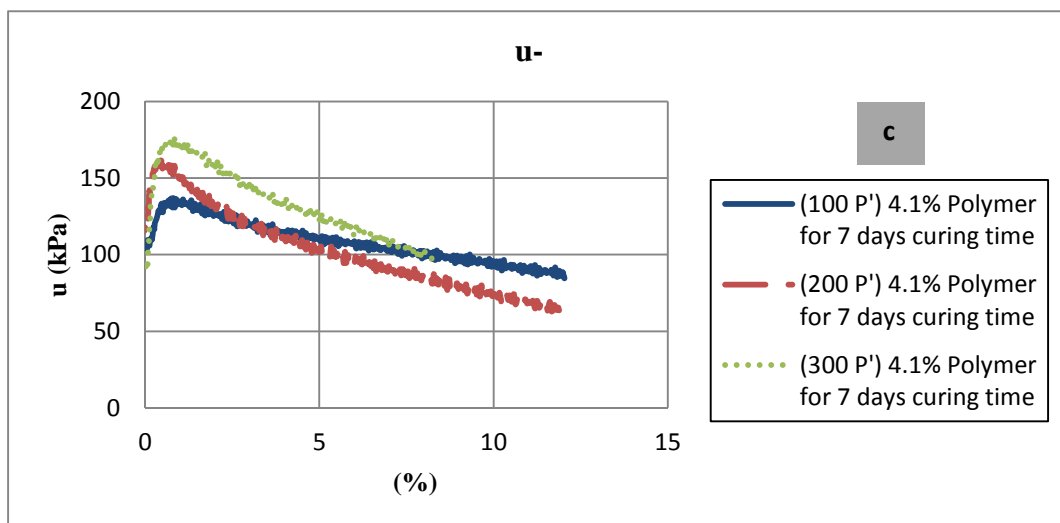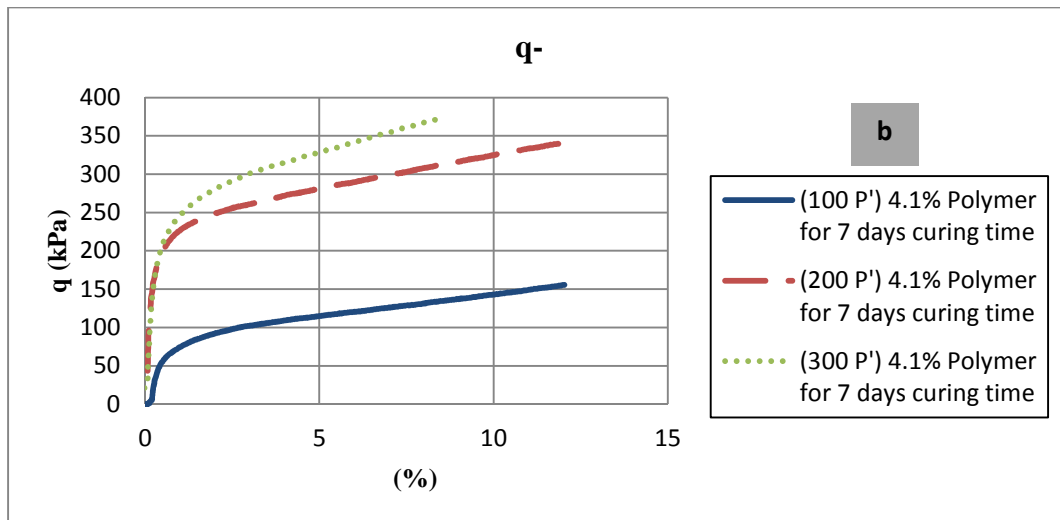
Figure 44: (a) Effective stress, (b) stress-strain and (c) pore water pressure vs. strain curves of 4.1% polymer to the natural soil in undrained monotonic compression loading condition.
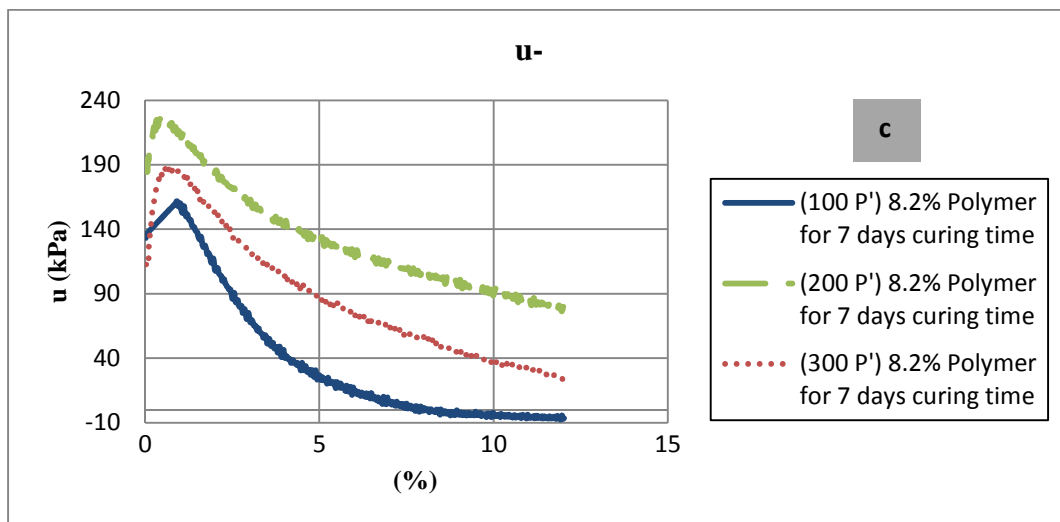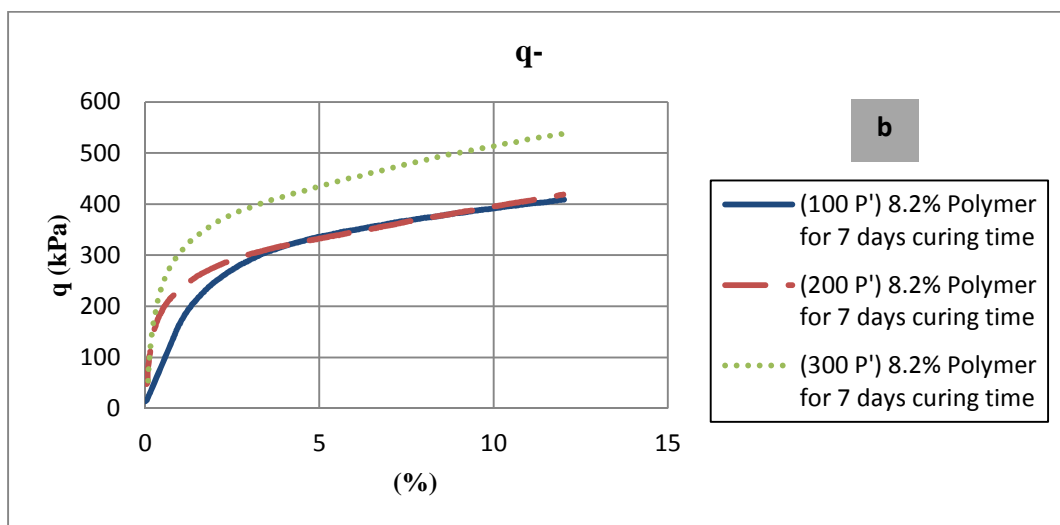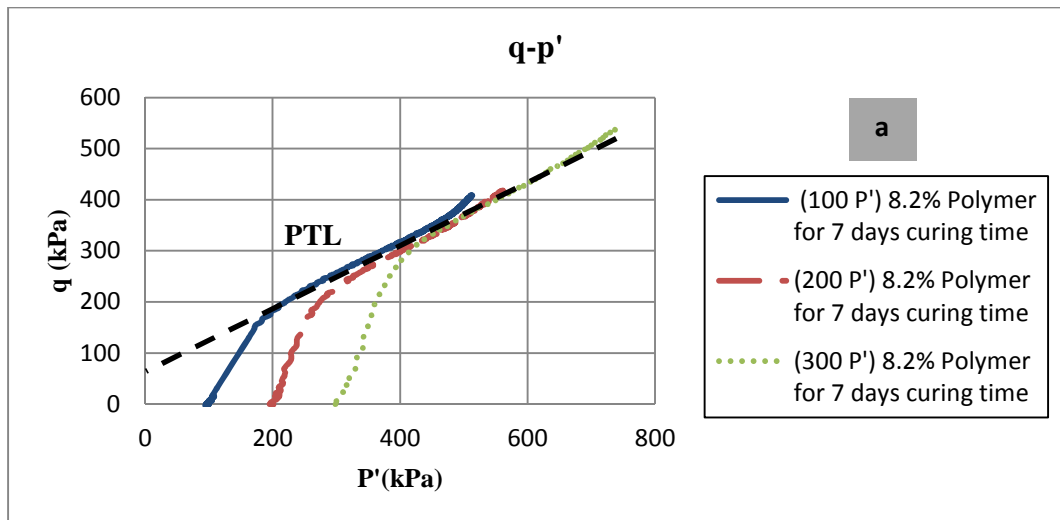
Figure 45: (a) Effective stress, (b) stress-strain and (c) pore water pressure vs. strain curves of 8.2% polymer to the natural soil in undrained monotonic compression loading condition.

4.3 Cyclic Triaxial Test Results

4.3.1 Presentation of Data

The presented results in the main body of this thesis are individual tests of natural, 2%, 4.1% and 8.2% polymerized sand (Figures 46-49). Other data were brought in appendix section (Figures 56-63). Finally the results summarized in Figure 50.

Several frequent used parameters should be defined before proceeding into the analysis of presented results.

Initial liquefaction: is first cycle of appreciable strain occurs. Usually it means 0.2% to 0.4% of axial strain.

CSR: the term stands form of cyclic stress ratio of applied deviator stress to mean principal stress while cyclic loading is running.

Double amplitude (peak to peak) strain: is the difference between maximum and minimum of axial strain in compression and extension respectively (ASTM, 2013).

Necking: In extension, samples enlarged and the cross section of sample in one area of the specimens became less than the total average of sample which was termed as necking phenomenon as shown in Figure 45.
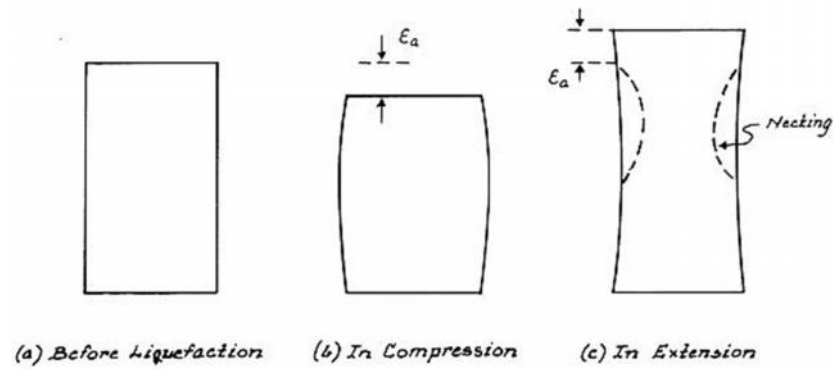
Figure 46: Deformation of soil sample in compression & extension (Rocker, 1968)

This chapter investigates the typical behavior of Silver Beach sand in its primary and treated states when subjected to diverse cyclic stress ratio. A total of 13 cyclic tests with different CSR but with uniform frequency of 0.02 and void ratio were conducted.

The effective confining stress ($´_3$) considered as 200 kPa in which represent the condition of soil in depth of almost 15 meters beneath the ground surface. The tests properties detailed in Table 5.

Table 5: Index properties of cyclic triaxial loadings

Test No.	CSR	Natural sand	σ^{cyc} (kPa)	Number of cycles	Confining stress (kPa)	Dr (%)
1	0.3		60	17		
2	0.22		44	42		
3	0.15		30	118		
Test No.	CSR	Treated sand By polymer (%)	σ^{cyc} (kPa)	Number of cycles		
1	0.4	2	80	12		
2	0.3	2	60	25		
3	0.2	2	40	132	200 kPa	20
4	0.45	4.1	90	46		
5	0.4	4.1	80	51		
6	0.37	4.1	74	17		
7	0.3	4.1	60	162		
8	0.2	4.1	40	201		
9 & 10	0.2 &0.4	8.2	40 & 80	168		

A comparison in data of liquefied, non-liquefiable with natural sand will then made.

4.3.1.1 Investigation on effective stress in liquefaction

In cyclic test, the deviator stress applied alternately in compression and extension. As far as the samples were consolidated isotropically, the shear force in extension and compression was equal in the study. When pore-water pressure increases, effective stress reduces to zero during liquefaction. The higher the cyclic deviator stress, the lower the number of cycles of deviator stress required to cause initial liquefaction. In the reinforced samples with 4.1% polymer with 0.4 CSR in Figure 48, 51 cycles were required to enter into the initial liquefaction stage compared to Figures 60 & 61given in appendix (0.2 and 0.3 CSR required 201 and 162 cycles respectively). The effective stress paths in the samples moved toward the left to accomplish the steady tangent

loop to the failure envelopes at zero effective stress value. This means that when the effective stress becomes zero, the total stress will be equal to pore-water pressure.

4.3.1.2 Investigation on strain of the samples

The strain of the samples during pore pressure build up is negligible in comparison to large strain of the samples in post liquefaction. The strain deformation in some treated samples with low and high CSR in 4.1% and 8.2% polymer respectively was constant with no large strain as shown in Figure 49 (b). In this figure, the deformation of the sample remained unchanged for 1.0% double amplitude strain, whereas the same double strain amplitude caused initial liquefaction in natural sand (Figure 46).

In treated samples, large deformation mostly initiated from extension strain. Only few of the treated samples were deformed in compression. In this regard, the reinforced samples with 2% polymer in Figures 47 and Figure 58 given in the Appendix section verified this.

Necking was observed in all of the samples except those treated with 8.2% polymer. That was because of the strong cementation of the sand particles. The phenomenon took place mostly at extension phase with less than 5% strain in the treated samples and 1% for natural sand.

4.3.1.3 Investigation on pore-water pressure of samples

Pore-water pressure changes are controlled by the amount of rearrangement or collapse of soil structure. In cohesionless soils, particle to particle contact is made over any highly stressed small contacts areas. Repetitive stressing of these contact points caused particle rearrangement from sliding and from abrasive wear. Both actions tend to move particle centers closer together; cyclic loading causes little translational straining with resulting possible dilation. Through this mechanism, pore-

water pressure buildup will occur in all samples, even in polymeric samples especially those reconstituted by lower percentage. Dimensionless pore-water pressure vs. number of cycling was given in Appendix and marked as **d**.

The pore-water pressure in reinforced samples with lowest percentage of polymer increased rapidly in early stages of cyclic loading. Then the loading was continued till the initiation of liquefaction. In reinforced samples with 8.2% polymer the pore-water pressure path was linear (Figure 49). Also this linear path was observed in 4.1% polymer with low cyclic loading in Figures 60 and 61 in Appendix section.

In treated samples, with 2% polymerized sand pore-water pressure reached less than 2.5 kPa (Figure 4.7) that is almost twice the amount of 8.2% polymer reinforced samples (less than 1.2 kPa) (Figure 49). The data inferred that lower percentages of polymer-added samples liquefied in higher pore-water pressure.
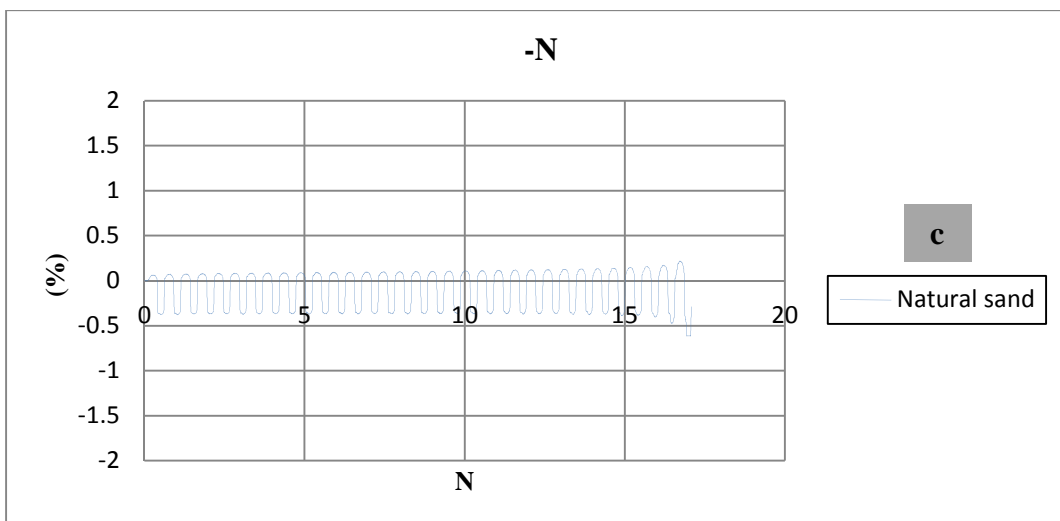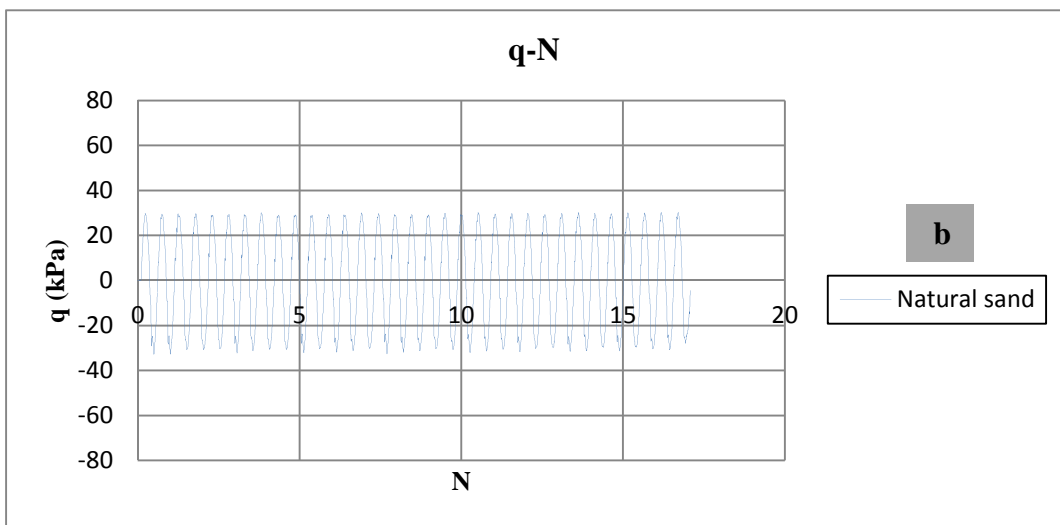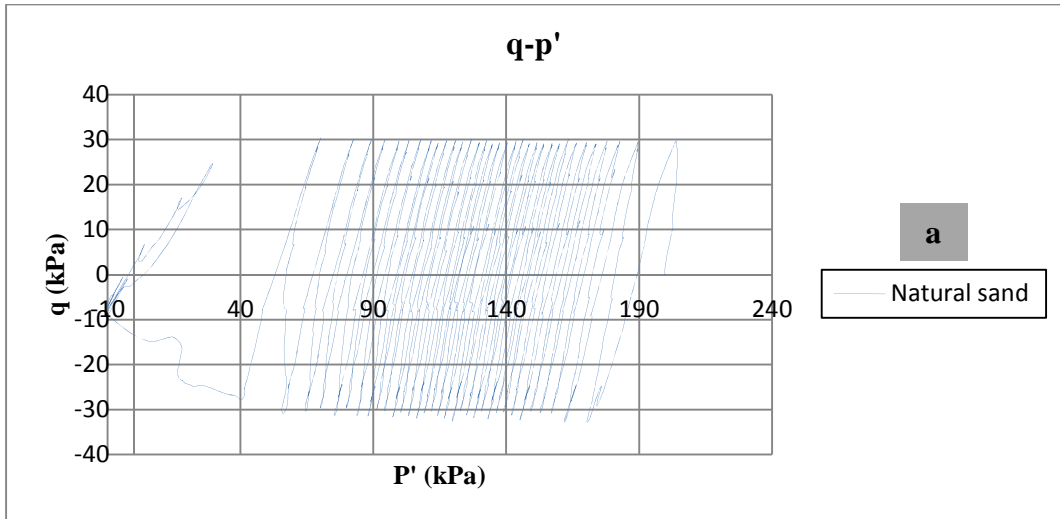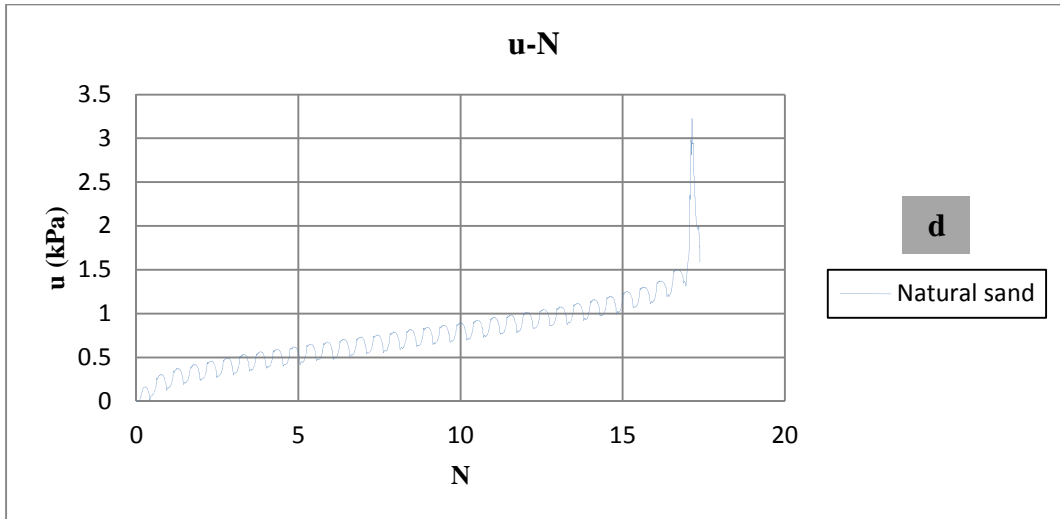
Figure 47: Natural sand with CSR of 0.3, and frequency of 0.02
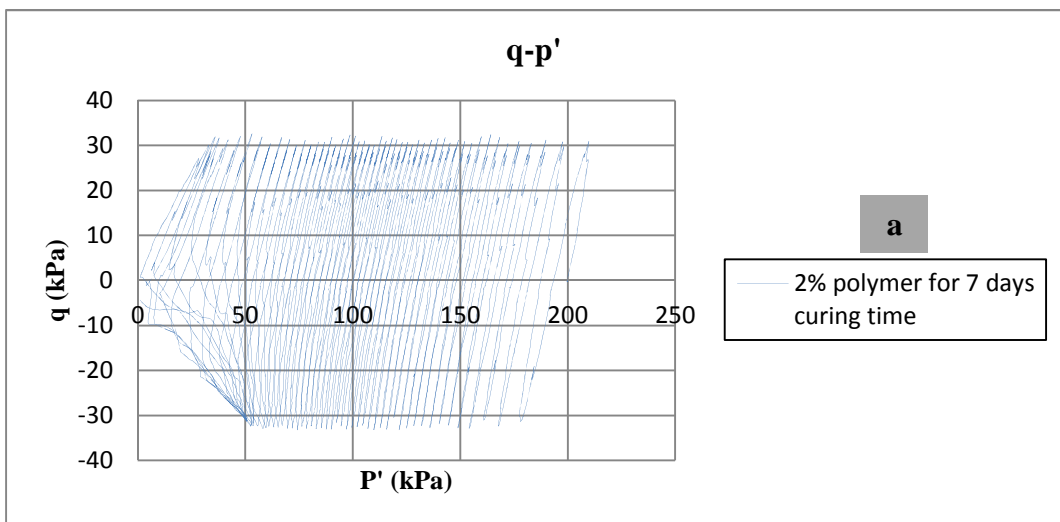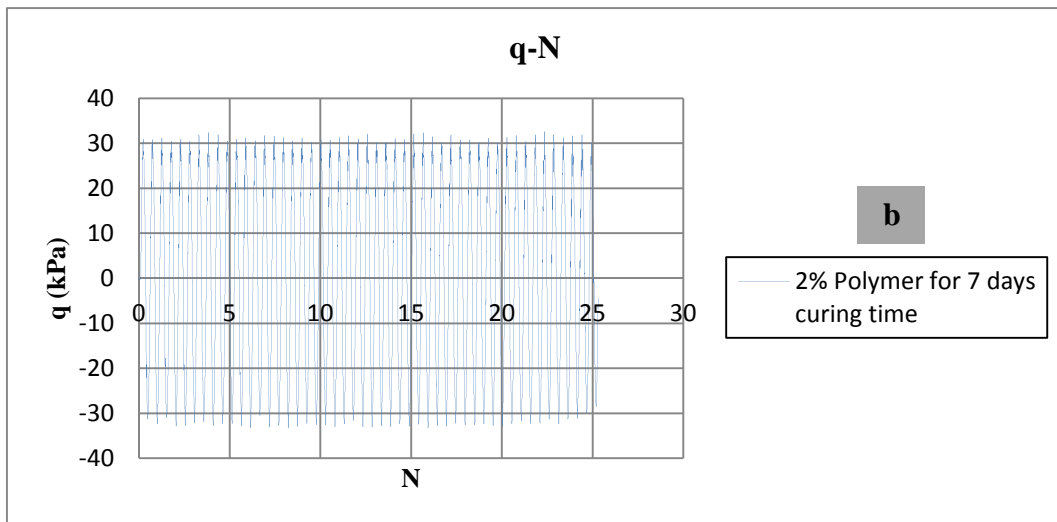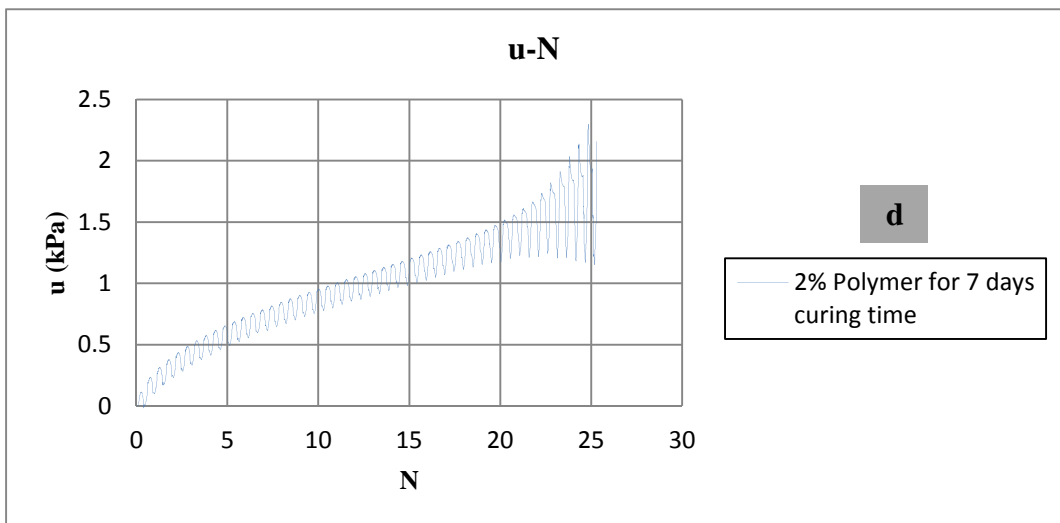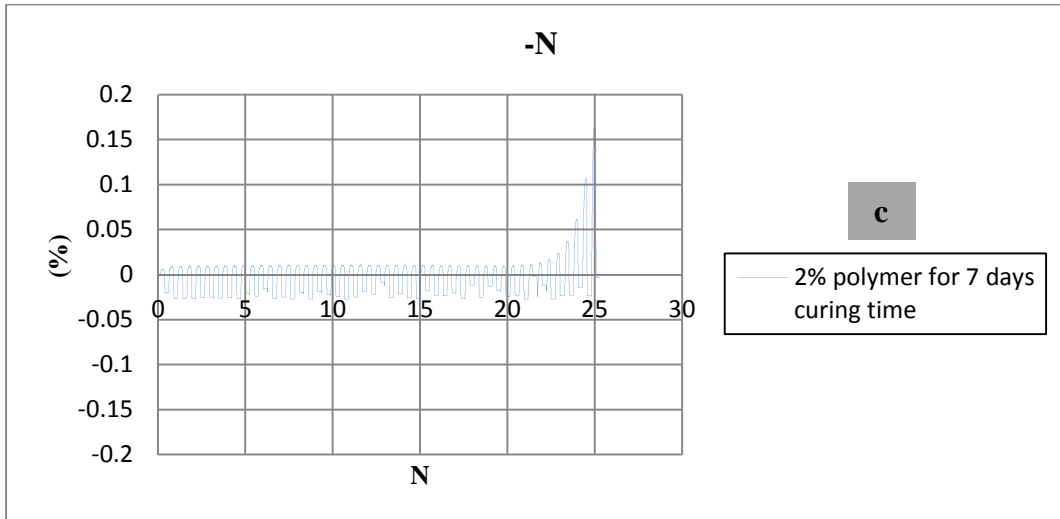
Figure 48: 2% Polymer to sand with CSR of 0.3, frequency of 0.02

q-N

b

4.1% Polymer for 7 days curing time

-N

c

4.1 % Polymer for 7 days curing time

u-N

d

4.1 % Polymer for 7 days curing time
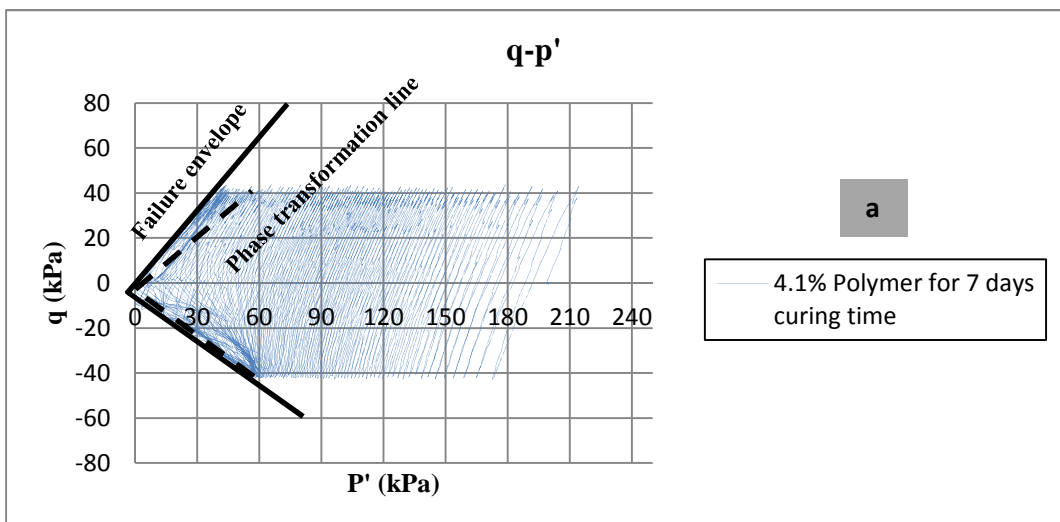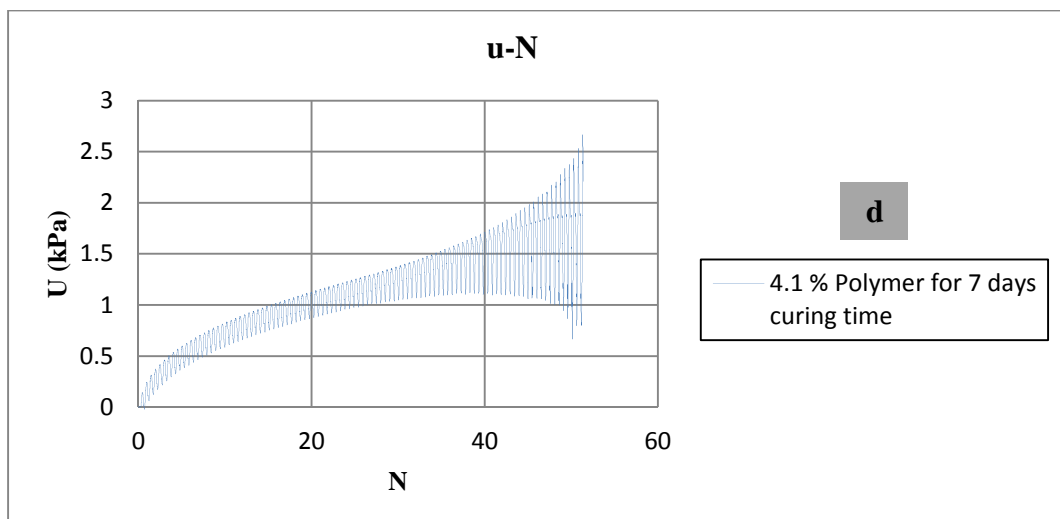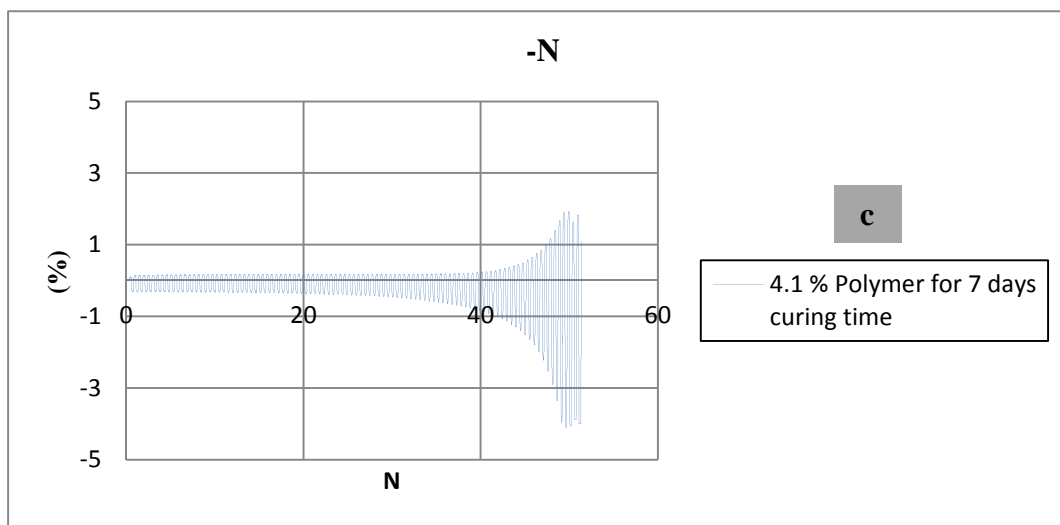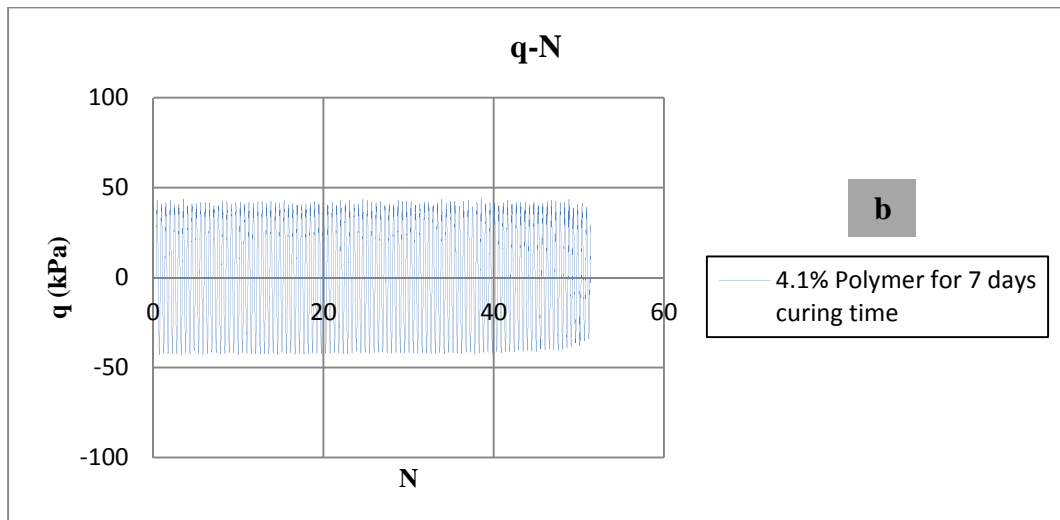
Figure 49: 4.1% Polymer to sand with CSR of 0.4, frequency of 0.02

q-p'

a

8.2% Polymer for 7 days curing time

q-N

b

8% Polymer for 7 days curing time

-N

c

8.2% Polymer for 7 days curing time
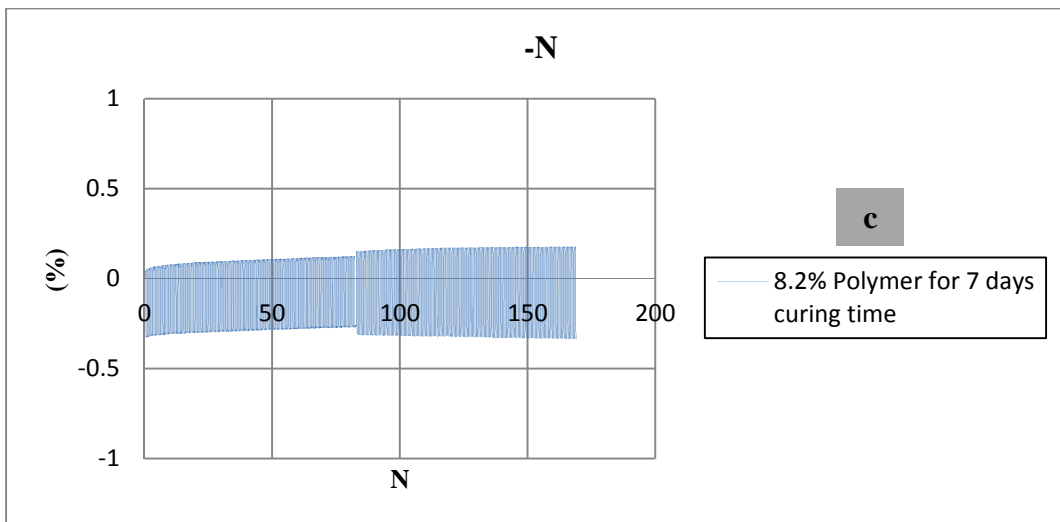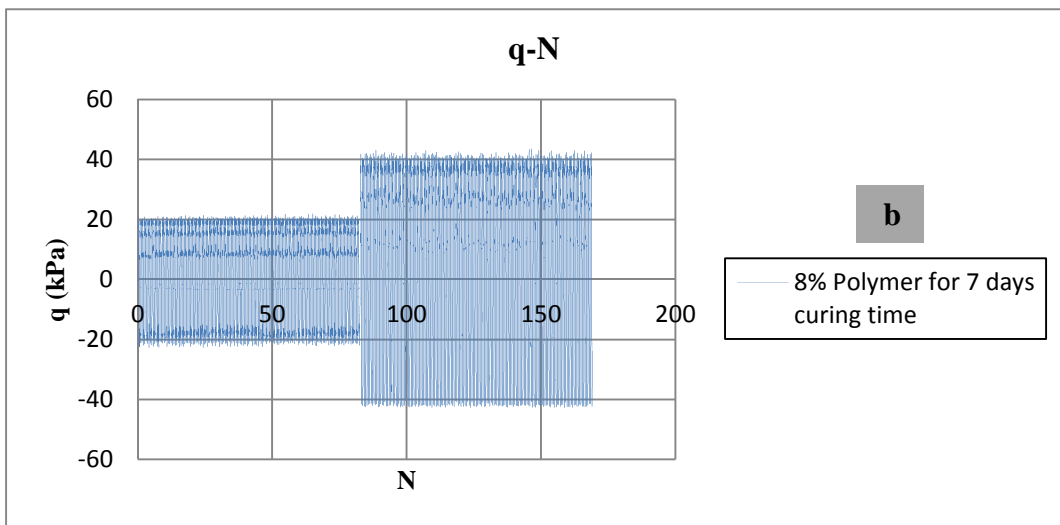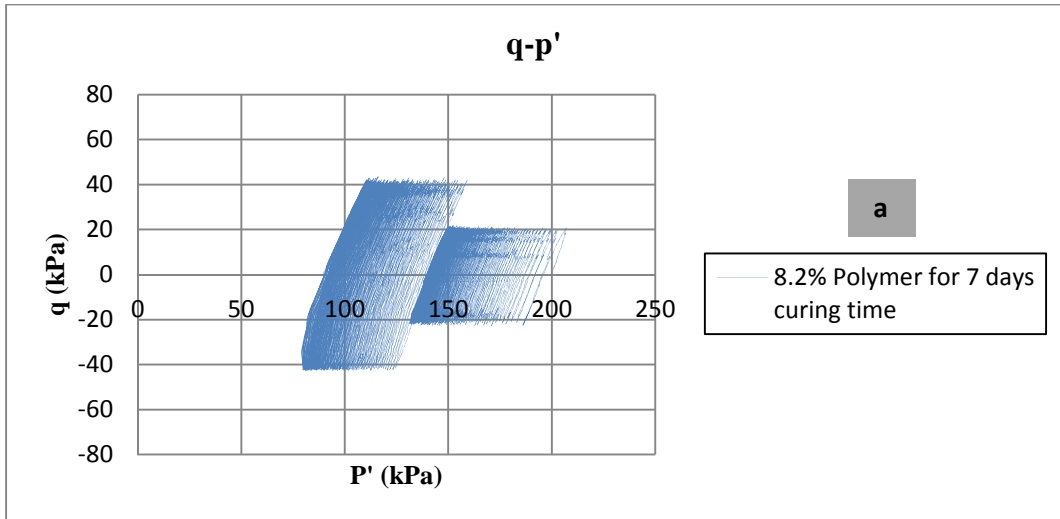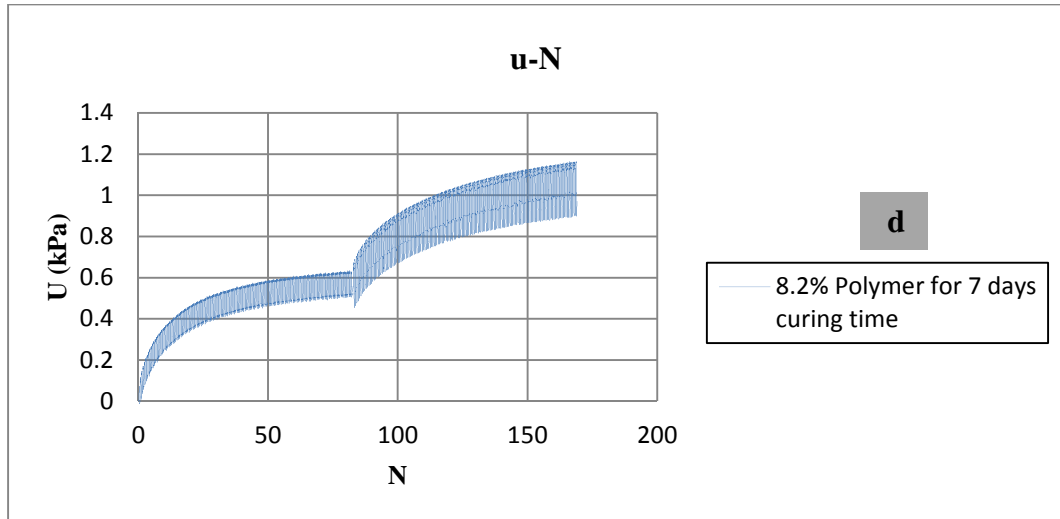
Figure 50: 8.2% Polymer to sand with CSR of 0.2 and 0.4, frequency of 0.02

Figure 50 summarizes the results of performed tests at effective stress of 200 kPa under a variety of cyclic stress ratio. The plotted data in this figure representing the cyclic stress ratio of the liquefied and non-liquefied samples to the number of cycles. The treated samples with 4.1% polymer and CSR of 0.2 and 0.3 were put in non-liquefiable category. The required number of cycles needed for 4.1% reinforced samples is almost twice as 2% polymerized soil both in high and low CSR. The data in loose natural sand and treated with 2% polymer scattered in a line, but in 4.1% polymer the data scattered which reduced the accuracy of test in half of the others.
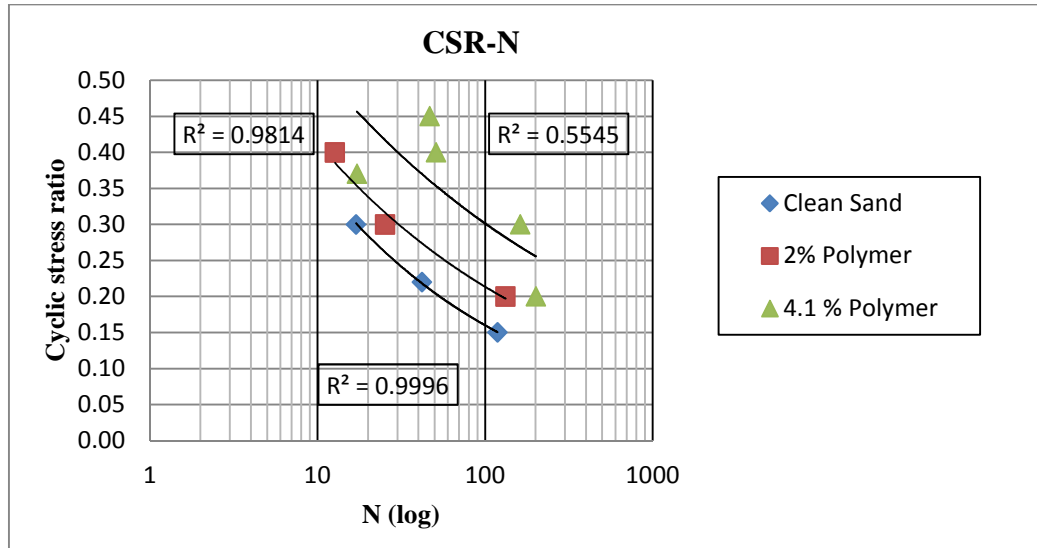
Figure 51: Cyclic stress ratio to number of cycles for the cyclic tests

4.4 Scanning Electron Microscopy (SEM)

Structure of soils in controlling the mechanical behaviour of sand is very important. The sand particle shapes as described in Chapter 3, sorted as sub-angular to rounded grains. Thus, while liquefaction phenomenon occurs during earthquake these particles have great potential to be unstable. For this reason polymer was used in this study as a cohesive agent for sticking the particles together and preventing the liquefaction problem. The distributed polymers in the soil samples act as a three dimensional halo to interlock sand particles and restrict them not to be displaced. Binding effect of different percentages of polymer on Silver Beach sand was considered via SEM images. The SEM is a microscope that uses electrons instead of light to form a virtual image of the emitted signals from the soil particles.

Scanning Electron Microscopy analysis was carried out on the natural and polymer treated samples before shearing. SEM images were taken with magnification of 30, 150 and 300. The SEM microscopic observations of the samples illustrated a reasonable homogeneous and uniform distribution of the polymer-soil composite.

Figure 51 indicates the soil structure of the Silver Beach sand with three enlarged micrograph images. The overall structure of soil exhibited to be segregated. This finding is consistent with relatively low shear strength depicted in Figure 41.

In Figures 52-53 the voids between the sand particles were gradually filled with polymer until almost full coverage of them with 8.2% polymer as visible in Figure 54.

The SEM images in Figure 51 showed lowest percent of polymer in compare with SEM images in Figures 52-54.

The SEM images of the polymer treated soils are in good harmony with the values obtained for CSR values of the natural and the treated sands. Addition of polymer into the sand increased the binding between the particles and that prevented the sudden increase in the pore water pressure and thus decreased the risk of liquefaction.
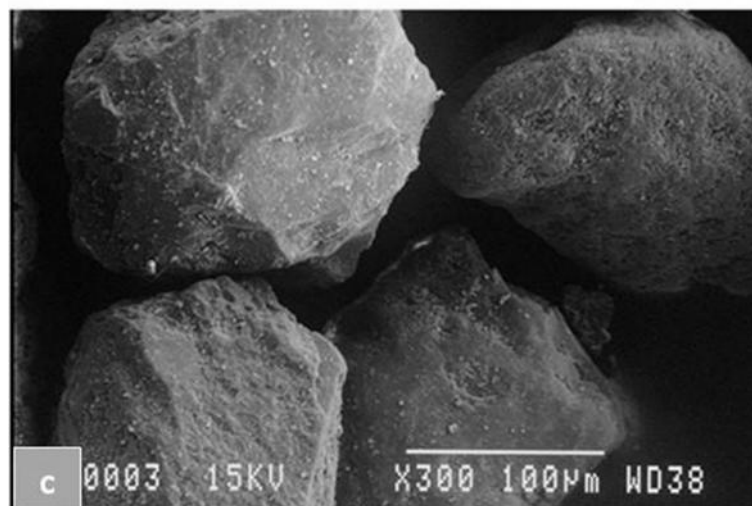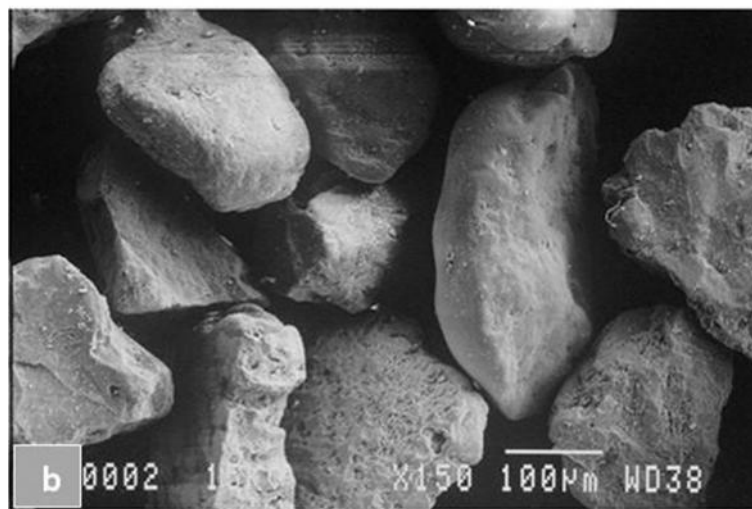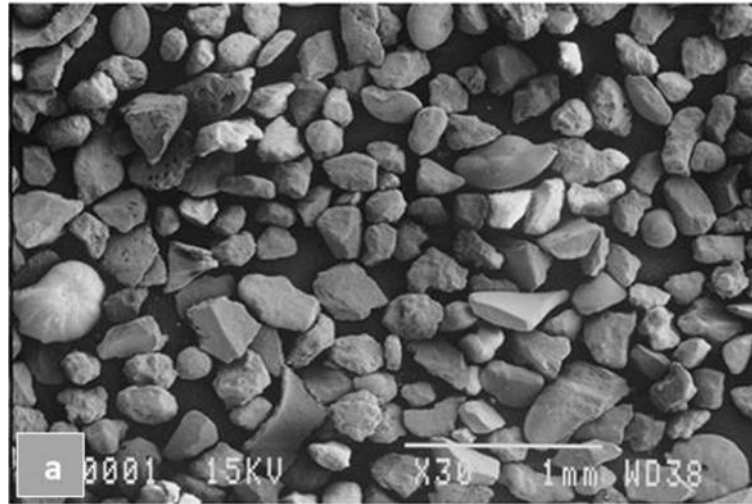
Figure 52: Natural sand with magnification of (A) X30, (B) X150 and (C) X300
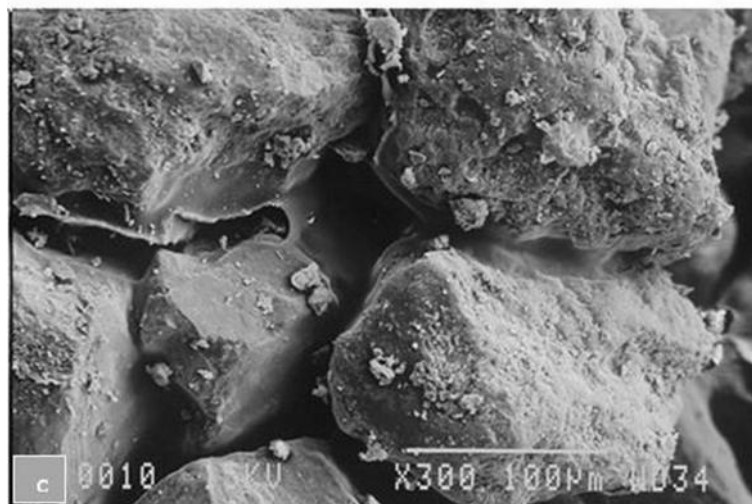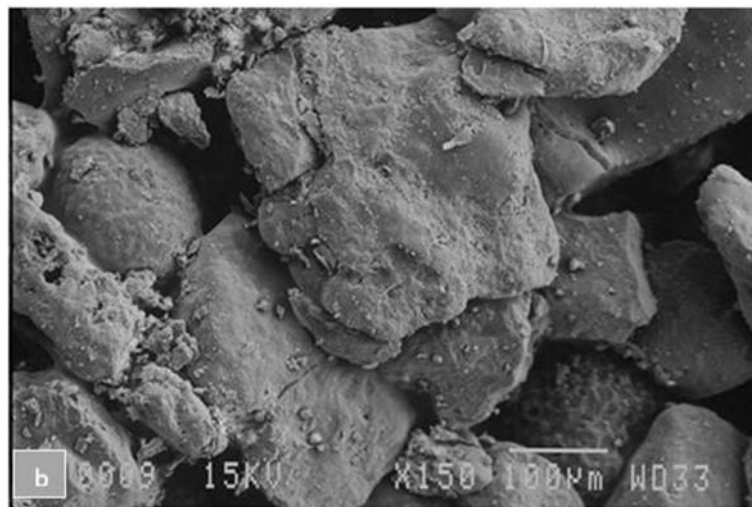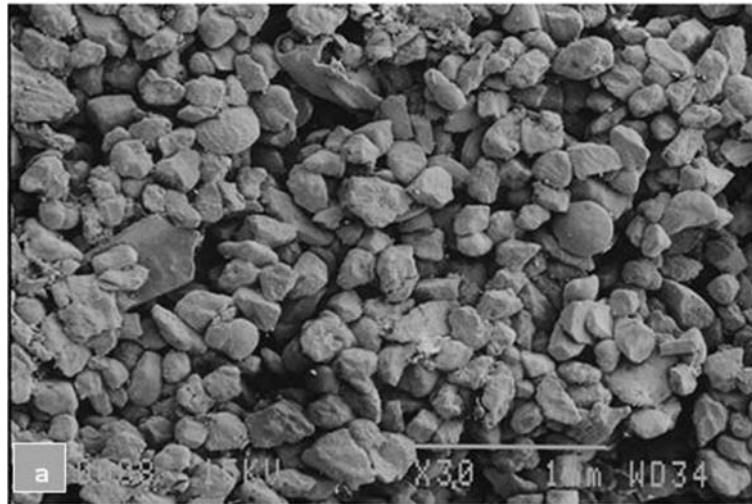
Figure 53: 2% Polymer with magnification of (A) X30, (B) X150 and (C) X300
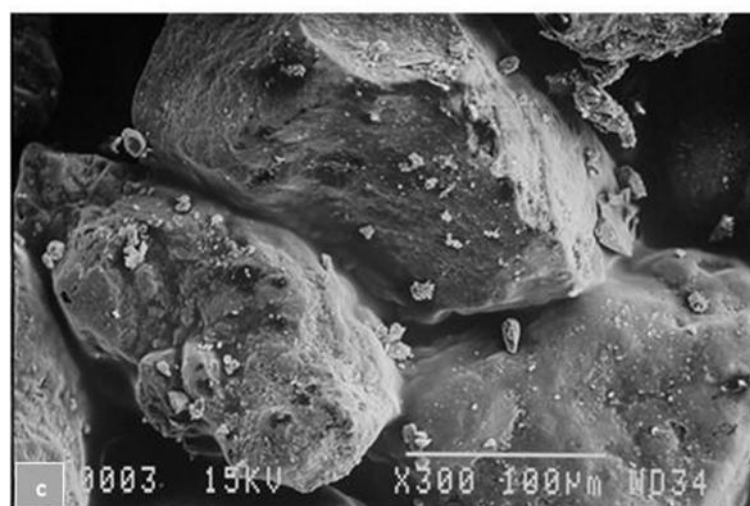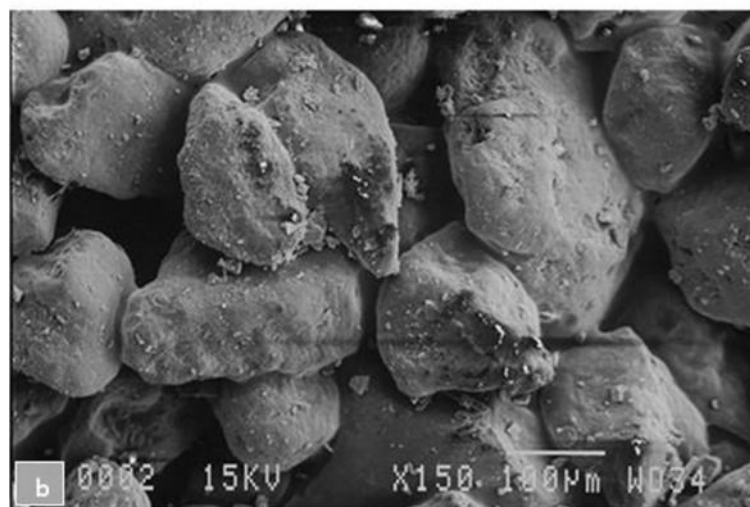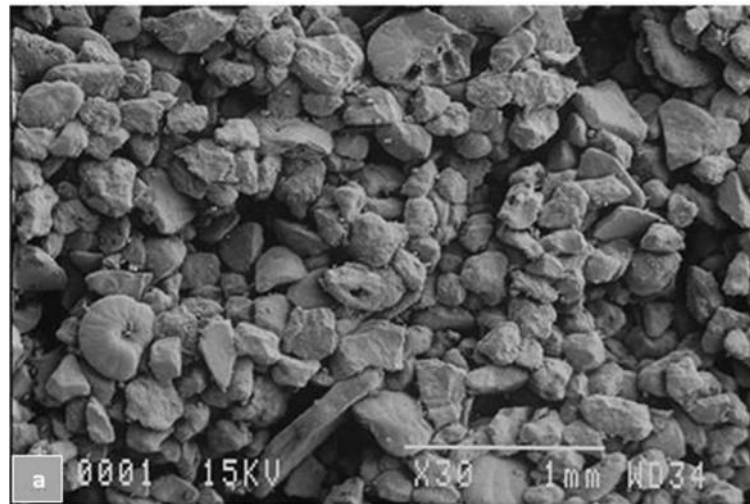
Figure 54: 4.1% Polymer with magnification of (A) X30, (B) X150 and (C) X300
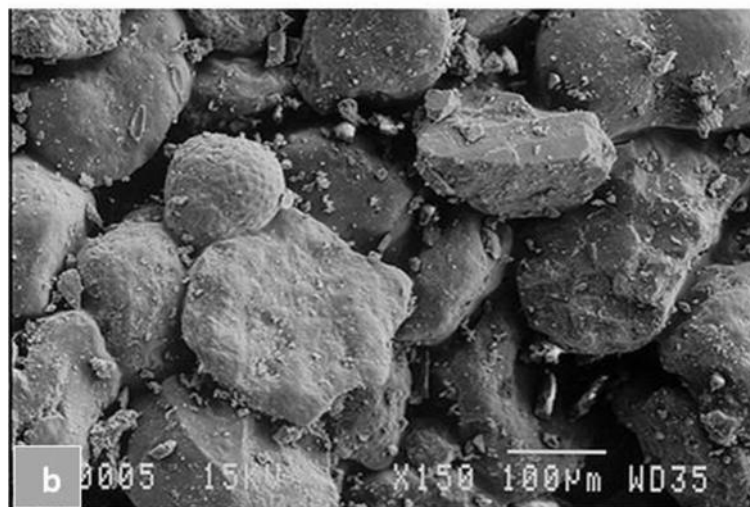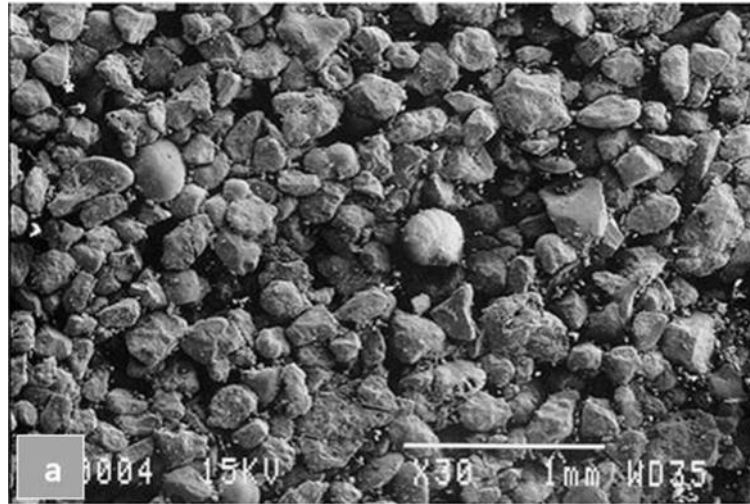
Figure 55: 8.2% with magnification of (A) X30, (B) X150 and (C) X300

Chapter 5

CONCLUSIONS AND RECOMMENDATIONS

5.1 Conclusions

The findings in undrained monotonic and cyclic shearing tests were compared and summarized as follows:

These results indicated the importance of void ratio and confining stress on behaviour of soil element. The type of polymer applied to the soil with highest percent showed higher deviator stress over 12% strain.

In monotonic triaxial test, the trend of effective stress paths for 2% added polymer to the soil showed that polymer was not very effective in changing the sand behaviour. The test results indicated that the behaviour of the reinforced sand was similar to the non-reinforced Silver Beach sand with confining pressures greater than 100 kPa.

In monotonic testing, all the treated samples showed dilative or strain-hardening behaviour from very initial shearing and that was similar to the behaviour of dense sand.

In cyclic testing, the results of treated samples with 2% and 4.1% polymer inferred that as the cyclic stress ratio increased, the number of cycles decreased.

In cyclic testing, the strain deformation in samples with 8.2% polymer and also some samples reinforced with 4.1% polymer left unchanged.

In cyclic testing, large deformation of almost all treated samples stemmed from extension phase.

In cyclic tests, treated samples with 8.2% polymer generated strong binding between the sand particles in a way that, even at high cyclic stress ratio (over 100 cycles) the polymer treated samples did not carried the risk of liquefaction problem.

In cyclic tests, the treated samples with 4.1% polymer showed non-liquefiable behaviour in low cyclic stress ratio.

As the SEM images of the natural and treated sands indicated, the polymer acted as a binding agent in the soil which locked the sand grains together. Thus, as the amount of polymer increases the chance of water percolation into the voids reduces.

5.2 Recommendation for Future Works

This laboratory research was introduced to compare the behaviour of uniform fine grained Silver Beach sand with different amounts of polymers. These soils were subjected to both monotonic and cyclic loading with seven day curing time. The recommended works for improving the obtained results are as follow:

1. The effect of polymer used in this study can be compared with the other materials like metal fiber or cement and the results can be discussed.

2. The triaxial tests can be performed at different confining pressure values and the possibility of liquefaction at different depths can also be evaluated.

3. In order to study the soil conditions similar to the real field conditions, anisotropic soil conditions can also be studied in the triaxial test.

4. Partial saturation state, especially on the vicinity of complete saturation can also be evaluated.

5. Standard Penetration Test, SPT and Cone Penetration Test, CPT data of Silver Beach area can be used to study the plot of CRR to N_{60} and determine the safety factor for liquefaction for that area.

REFERENCES

Asghari, E., Toll, D. G., & Haeri, S. M. (2002). Triaxial Behaviour of A Cemented Gravely Sand, Tehran Alluvium. *Geotechnical and Geological Engineering*, 28.

ASTM D2487-11. (2011). Standard Practice for Classification of Soils for Engineering Purposes (Unified Soil Classification System). *ASTM International Journal*, 12.

ASTM D2216-10. (1963). Standard Test Methods for Laboratory Determination of Water (Moisture) Content of Soil and Rock by Mass. *ASTM Journal*.

ASTM D4253-00. (2006). Standard Test Methods for Maximum Index Density and Unit Weight of Soils Using a Vibratory Table. *Annual book of ASTM, 04.08*.

ASTM D4254-00. (2006). Standard Test Methods for Minimum Index Density and Unit Weight of Soils and Calculation of Relative Density. *Annual book of ASTM standards, 04.08*.

ASTM D6913-04. (2009). Standard Test Methods for Particle-Size Distribution of Soils Using Sieve Analysis. *Annual book of ASTM standards, 04.08*.

ASTM D698-12. (2012). Standard Test Methods for Laboratory Compaction Characteristics of Soil Using Standard Effort. *Annual book of ASTM Standards, 04.08*.

ASTM D854. (1945). Standard Test Methods for Specific Gravity of Solids By Water Pycnometer. *Annual book of ASTM Standards, 04.08*.

ASTM, D. (2013). Standard Test Method for Load Controlled Cyclic Triaxial Strength of Soil. *Annual Book of ASTM*, 11.

Beckman Institute for Advanced Science & Technology. (n.d.). Remote Access Microscopy. Retrieved December 26, 2013, from http://www.itg.uiuc.edu/: http://virtual.itg.uiuc.edu/training/EM_tutorial/

Boulanger, R. W., & Truman, S. P. (1996). Void Redistribution in Sand under Post-earthquake Loading. *Canadian Geotechnical Journal*, 829-34.

Chung., R. D. (1995). Ground Improvement Techniques for Liquefaction Remediation Near Existing Lifelines. Maryland: U.S. Department of Commerce.

Consoli, N. C., & Coop, M. D. (2005). Effect of Fiber Reinforcement on the Isotropic Compression Behavior of a Sand. *Journal of Geotechnical and Geoenvironmental Engineering, ASCE.*, 3.

Consoli, N. P. (1998). Influence of Fiber and Cement Addition on Behavior of Sandy Soil. *Journal of Geotechnical and Geoenvironmental Engineering*, 1211-1214.

Day, R. W. (2002). Geotechnical Earthquake Engineering Handbook. Mc Graw-Hill.

Domone, P. (2010). Construction Materials Their Nature and Behaviour. London & New York: Spon Press.

Germaine, J., & Ladd, C. (1988). Triaxial Testing of Saturated Cohesive Soils . Advanced Triaxial Testing of Soil and Rock ASTM.

Hausmann, M. (1990). Engineering Principles of Ground Modification. New York: McGraw-Hill.

I.M.Idriss, & Boulanger, R. (2008). Soil Liquefaction During Earthquake. California, Davis: Earthquake Engineering Research Institute.

Ishihara, K. (1993). Liquefaction and Flow Failure During Earthquakes. *Thirty-third Rankine Lecture, Geotechnique, Vol. 43, No. 3*, 351-451.

Ishihara, K. (1996). Soil Behaviour in Earthquake Geotechnics. Tokyo: Clarendon Press Oxford.

Kaniraj, S., & Havangi, V. (2001). Behaviour of Cement-Stabilized Fiber-Reinforced Fly Ash-Soil Mixtures. *Journal of Geotechnical and Geoenvironmental Engineering*, 574-584.

Karl Rocker, J. (1968, June). The Liquefaction Behaviour of Sands Subjected to Cyclic Loading. Boston: Massachusetts Institute of Technology.

76

Khatami, H. R., & O'Kelly, B. C. (2013). Improving Mechanical Properties of Sand Using Biopolymers. *Journal of Geotechnical and Geoenvironmental Engineering*, 5.

Kiousis, P. D., & Abdulla, A. A. (1997). Behavior of Cemented Sands-Testing. *International Journal for Numerical and Analytical Methods in Geomechanics.*, 15.

Kolbuszewski, J. (1948). General Investment of The Fundamental Factors Controlling Loose Packing of Sands. *Proc.2nd Int. Conf. Soil Mech. Found Eng*, (pp. 47-49).

Kousik Deb, V. A. (2010). Effects of Fines on Compaction Characteristics of Poorly Graded Sands. *International Journal of Geotechnical Engineering*, 7.

Kramer, S. L. (1996). Geotechnical Earthquake Engineering (pp. 517-522). Washington: Prentice Hall.

Ladd, R. (1974). Specimen Preparation and Liquefaction of Sands. *Journal of the Geotechnical Engineering Division, ASCE*, 1180-1184.

Lehman, L., Idol, J., & Richard, D. (2004). The CRC Handbook of Mechanical Engineering. CRC Press.

Makusa, G. P. (2012). Soil Stabilization Methods and Materials. Sweden: Luleå University of Technology.

Moghaddas, S., & Asakereh, A. (2007). Strength Evaluation of Wet Reinforced Silty Sand by Triaxial Test. *International Journal of Civil Engineerng, Vol. 5, No. 4*, 10.

Murthy, M. G. (2006). Investigations on Sand Reinforced with Different Geosynthetics. *Geotechnical Testing Journal, Vol. 29, No. 6*, 8.

Navy, U. (2013, December 31). Google Earth. Retrieved December 31, 2013, from www.Google.com: http://www.google.com/earth/

Nilo C. Consoli, t. P. (1998). Influence of Fiber and Cement Addition on Behaviour of Sandy Soil. *Journal of Geotechnical and Geoenvironmental Engineering*, 4.

Port and Harbour Research Institute. (1997). Handbook on Liquefaction Remediation of Reclaimed Land. Rotterdam: A.A. Balkema.

Salah-ud-din. (2012). Behaviour of Fibre Reinforced Cemented Sand at High Pressure. Malaysia: The University of Nottingham.

Sariosseiri, F., & Muhunthan, B. (2008). Effect of Cement Treatment on Geotechnical Properties of Some Washington State Soils. *Engineering Geology*, 7.

Smith, G. (1998). Elements of Soil Mechanics. Blackwell Science.

Swami, S. (2005). Reinforced Soil and its Engineering Applications. *I.K International Pvt. Ltd.*

Terry, H. (2011). Quality Control of Soil Compaction. West Conhohocken, PA.: ASTM International Journal.

Towhata, I. (2008). Geotechnical Earthquake Engineering. Tokyo: Springer Journal.

Vaid, Y., & Chern. (1985). Cyclic and Monotonic Undrained Response of Saturated Sands. Advances In The Art of Testing. (V.Khosi., Ed.) *ASCE*.

Vaid, Y., Chung, E., & Kuerbis, R. (1989). Preshearing and Undrained Response of Sand. *Soils and Foundations, Vol. 29, No.4*, 49-61.

Wang, J. (2005). The Stress-Strain and Strength Characteristics of Portaway Sand. *Thesis*. London: The University of Nottingham.

Wayne Clough, G., & Kuppusamy, T. (1989). Influence of Cementation on Liquefaction of Sands. *Journal of Geotechnical Engineering, ASCE*, 16.

Yasrobi, Z. J. (2011). Stabilization of Dune Sand with Poly(Methyl Methacrylate) and Polyvinyl Acetate Using Dry and Wet Processing. *Springer Journal*, 9.

Yi Cai, B. S. (2006). Effect of Polypropylene Fibre and Lime Admixture on Engineering Properties of Clayey Soil. *Elsevier*, 11.

APPENDICES

Appendix A

In this section, further data that were shown in CSR-N diagram in Figure 50 in chapter 4 were presented. These figures include the series of the natural and polymerized sand with different cyclic stress ratio but uniform effective stress of 200kPa that categorized as follow:

1. Deviator stress to effective stress shown as "**a**"

2. Deviator stress to number of cycles shown as "**b**"

3. Strain in percent to number of cycles shown as "**c**"

4. Pore-water pressure to number of cycles shown as "**d**"
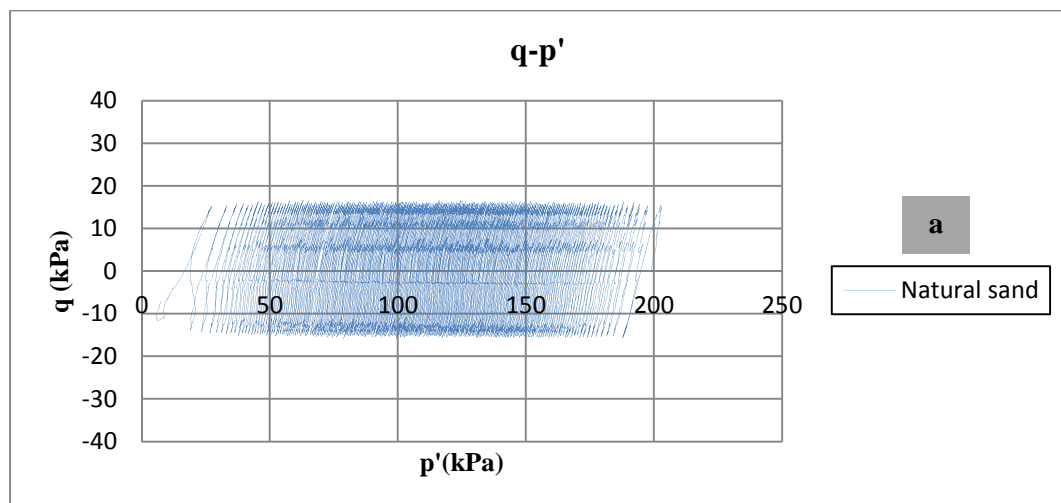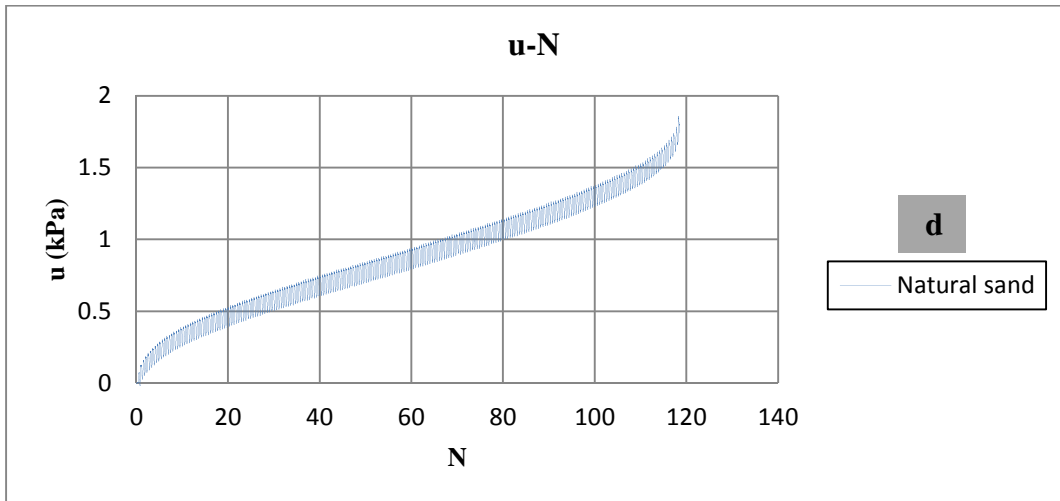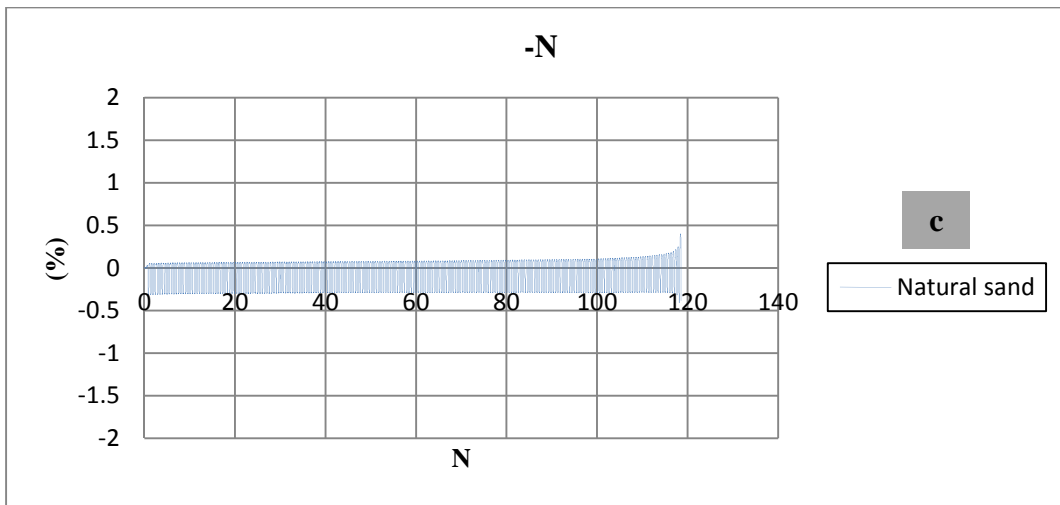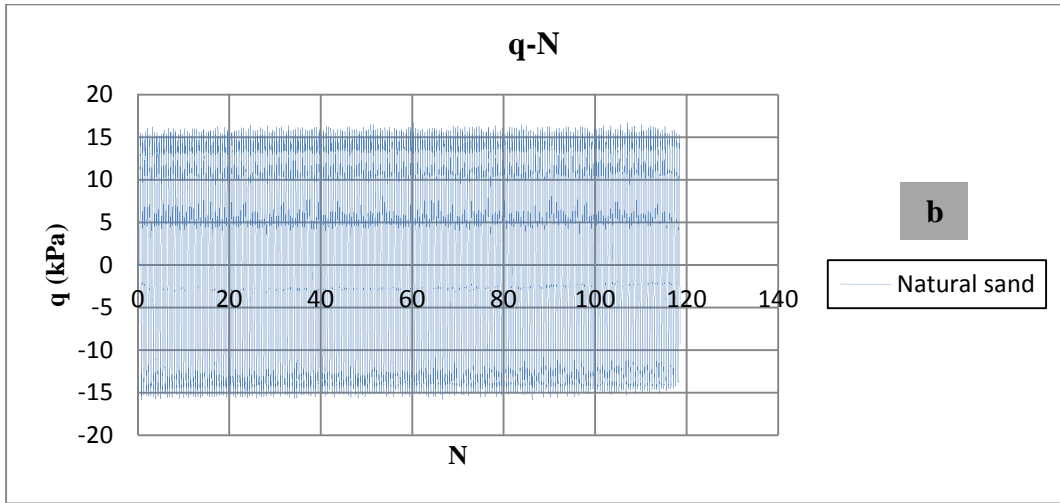
Figure 56: Natural sand with 0.15 CSR & 0.02 Frequency
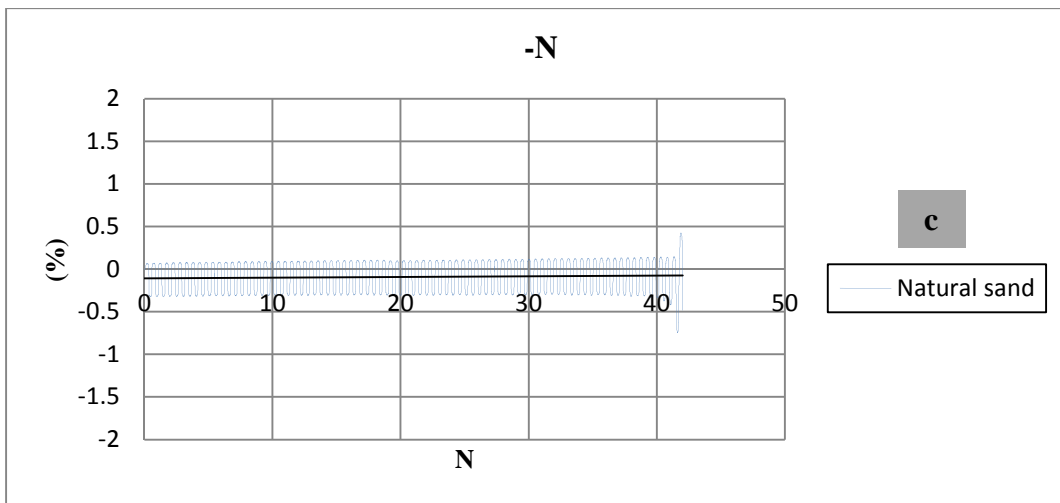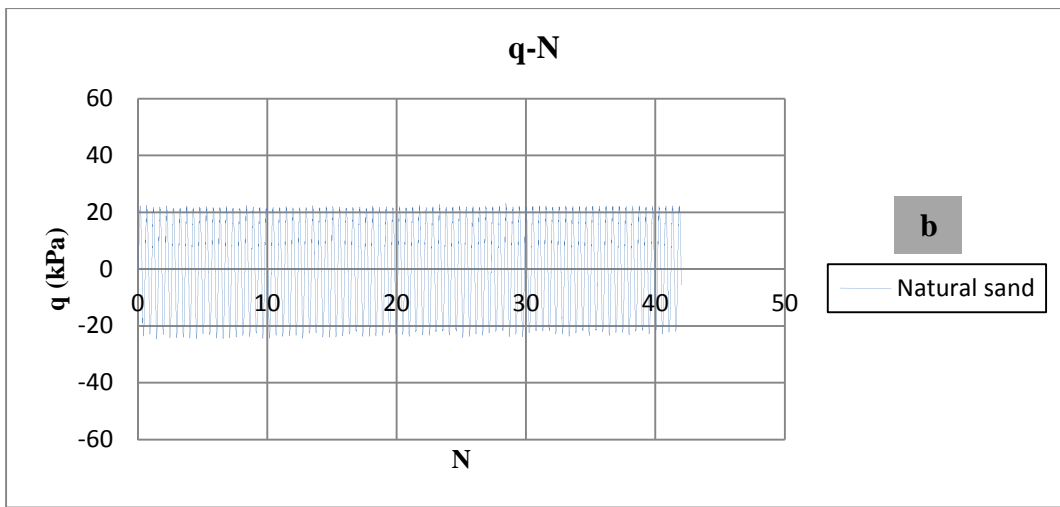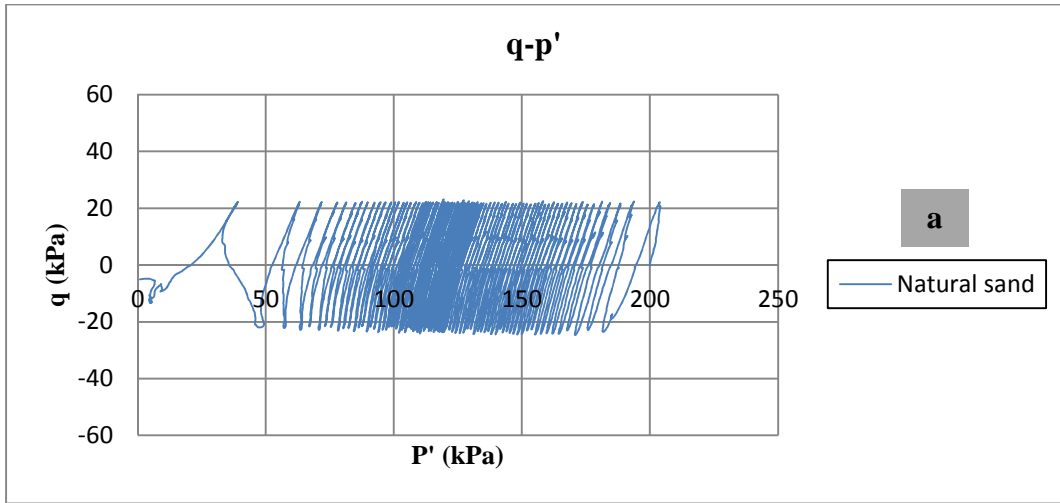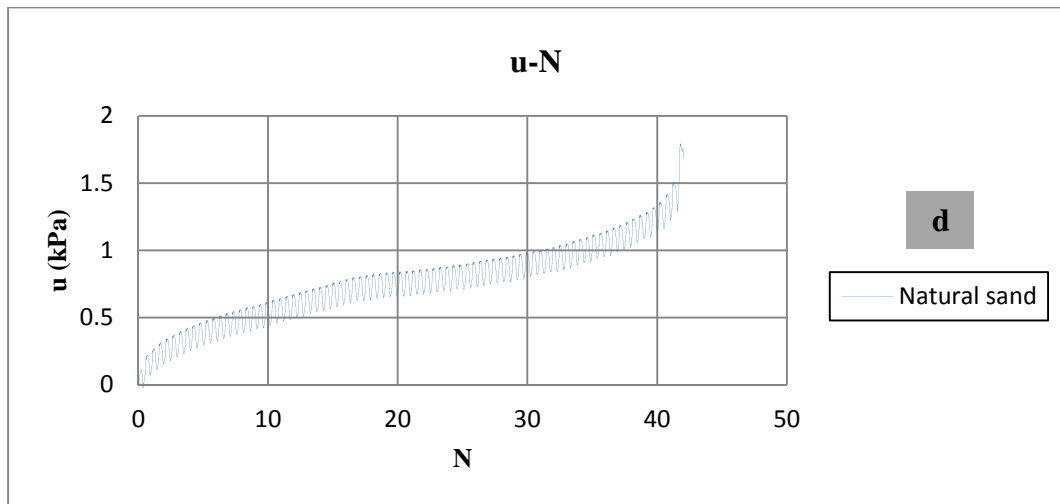
Figure 57: Natural sand with 0.22 CSR & 0.02 Frequency
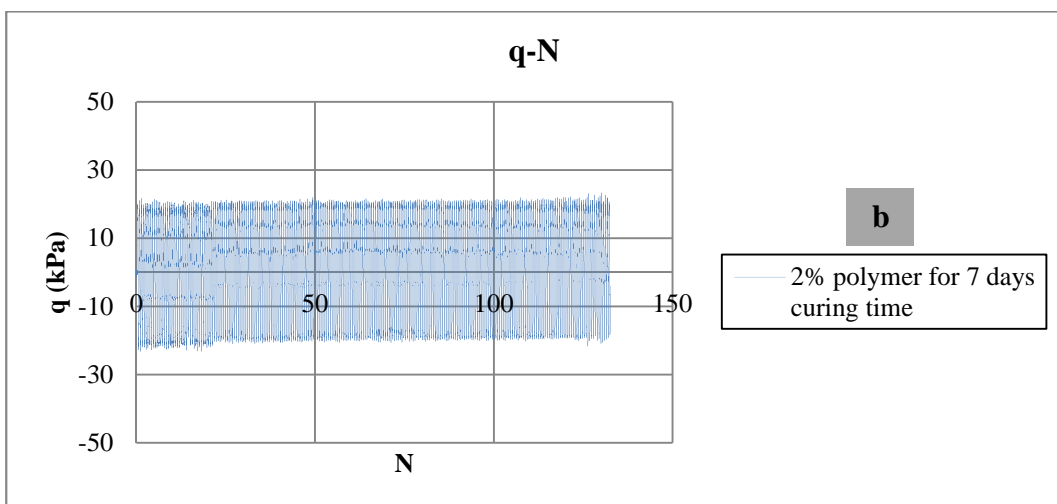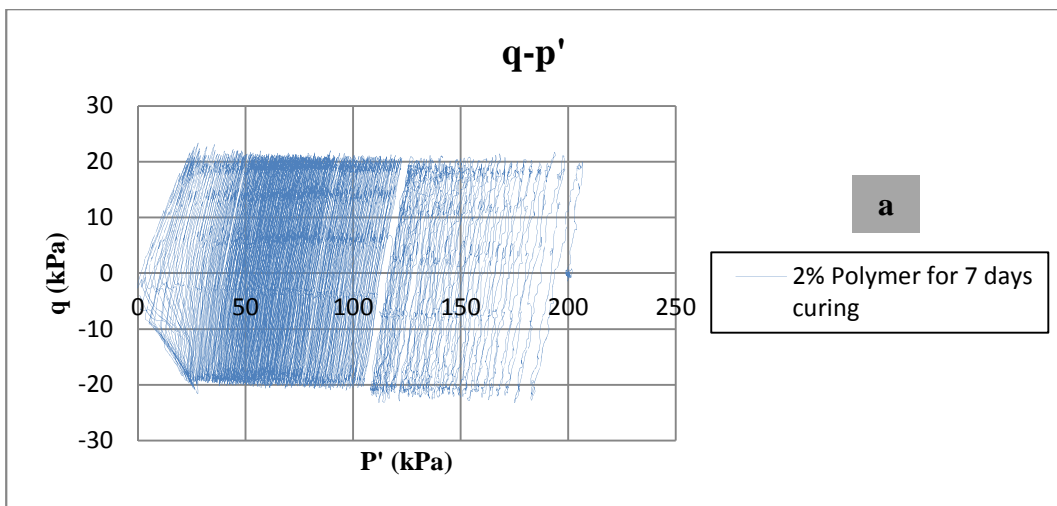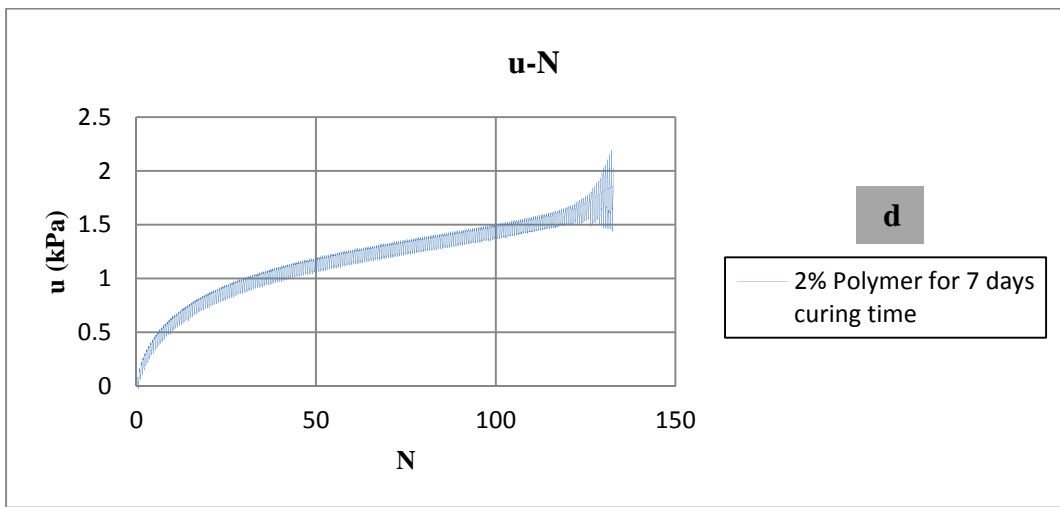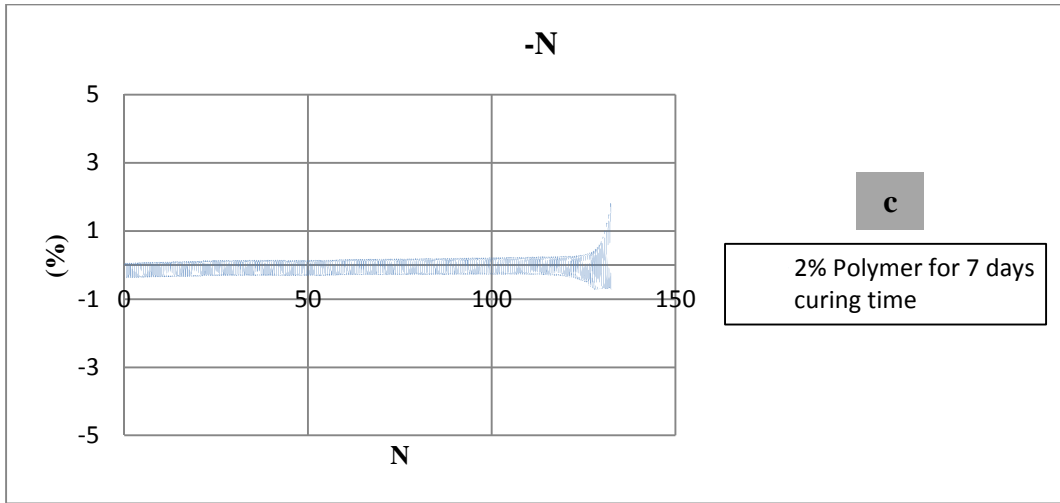
Figure 58: 2% Polymer to sand with 0.2 CSR & 0.02 frequency
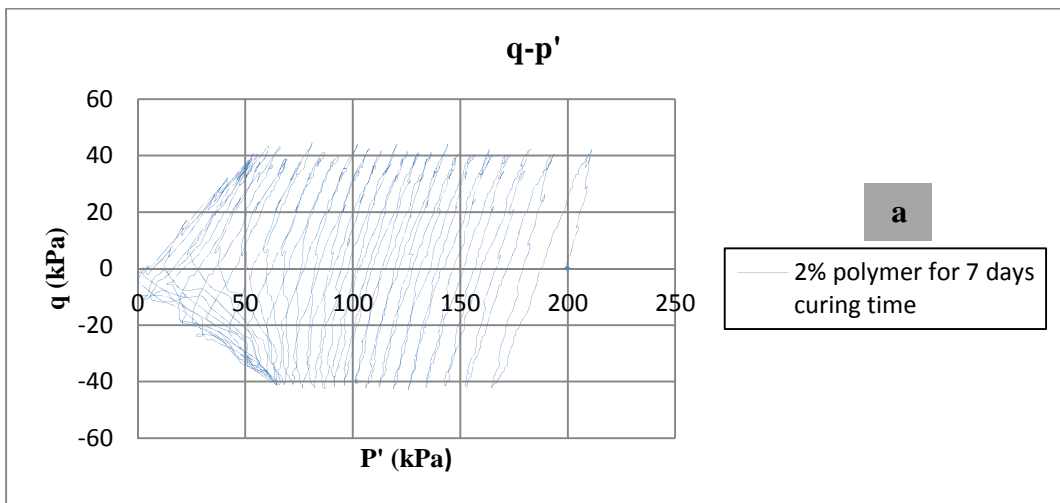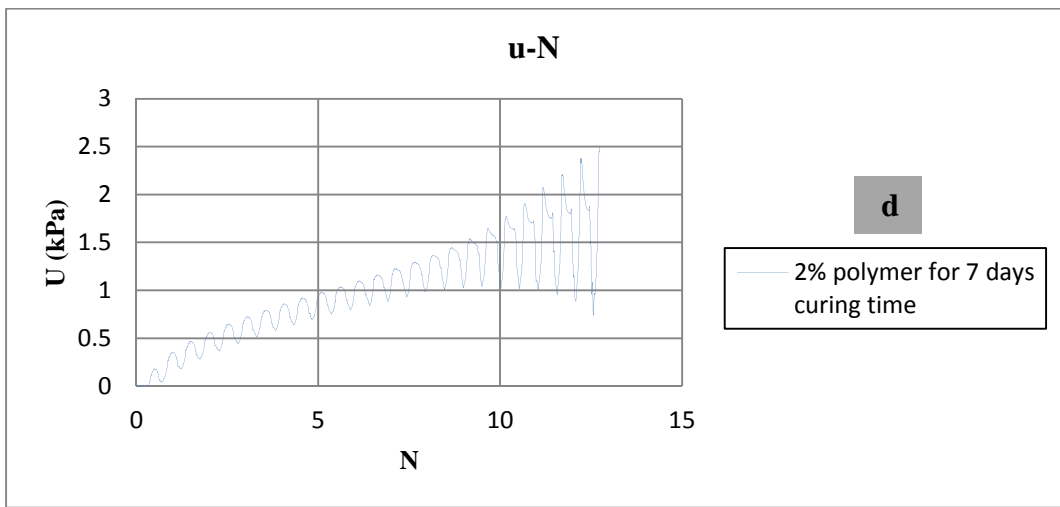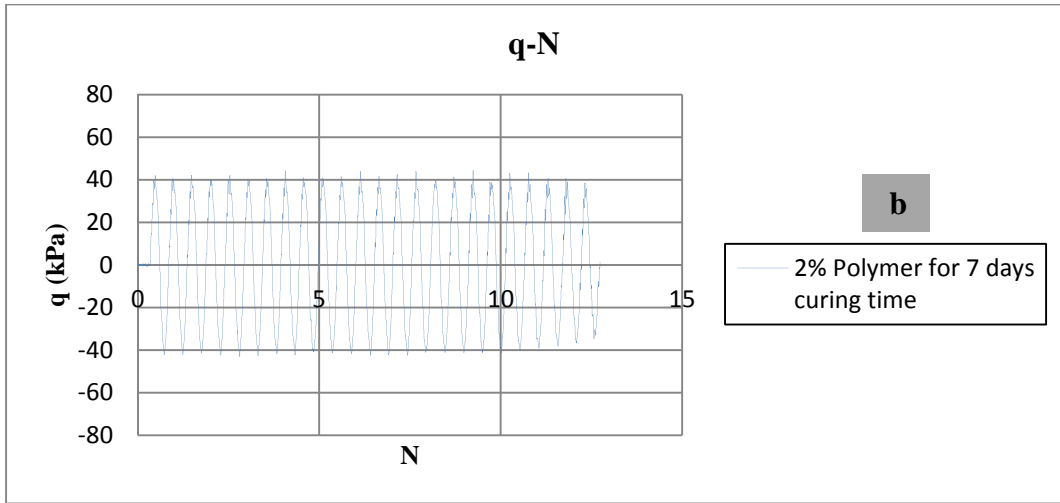
Figure 59: 2% Polymer to sand with 0.4 CSR & 0.02 frequency
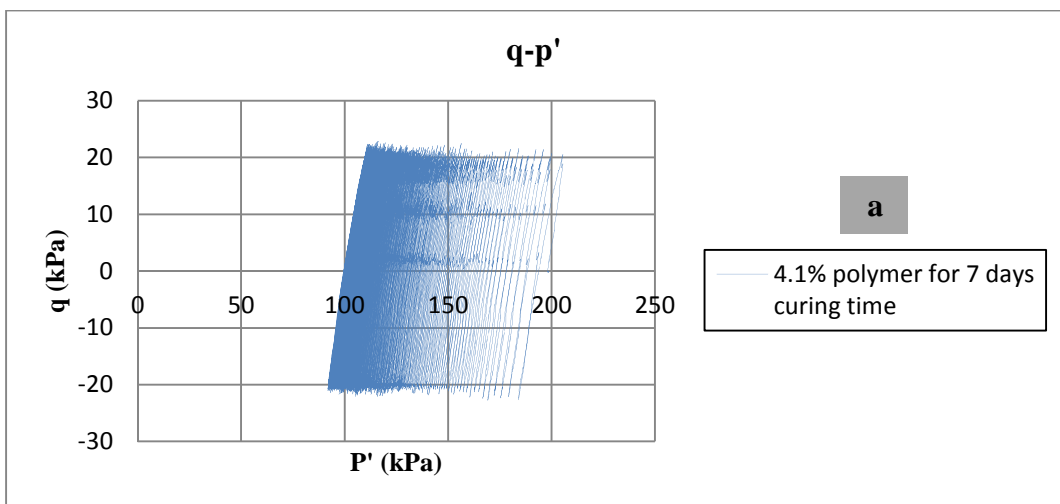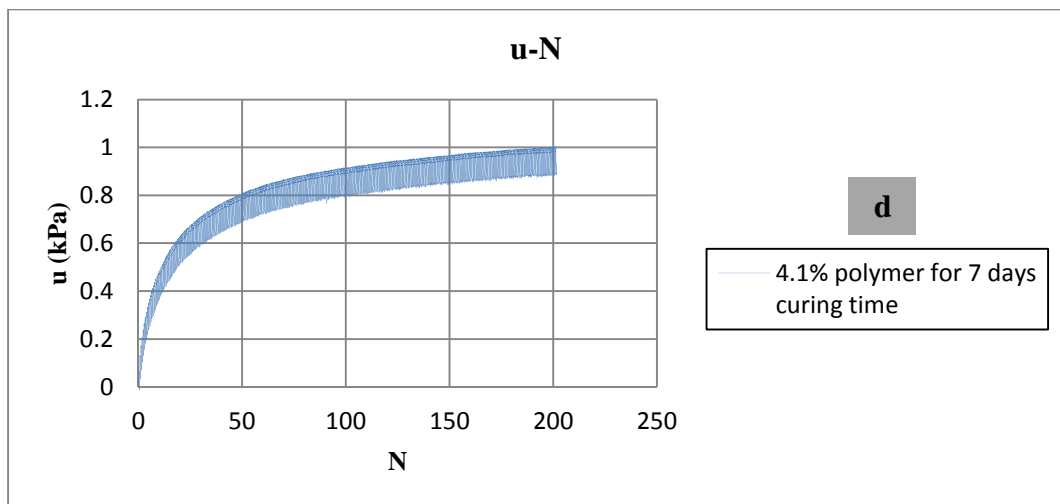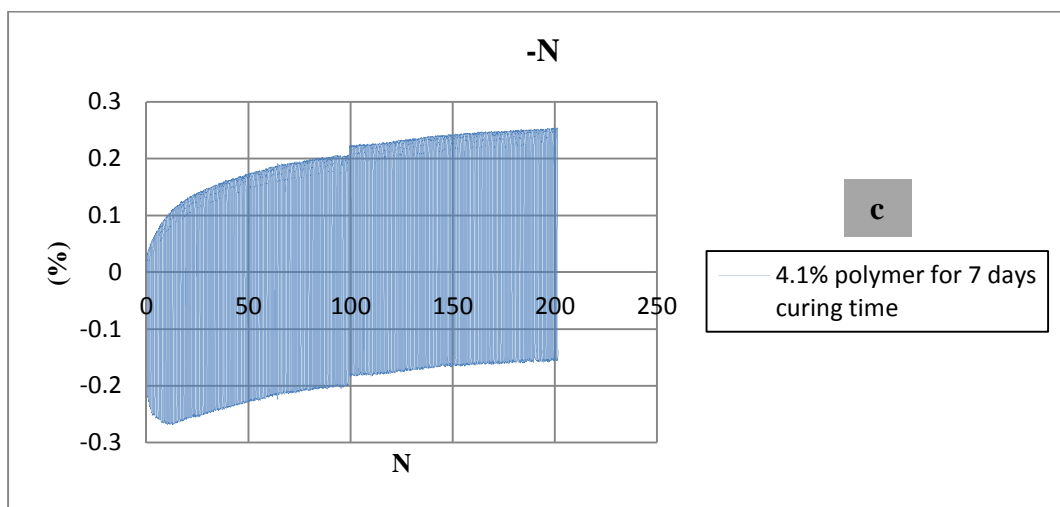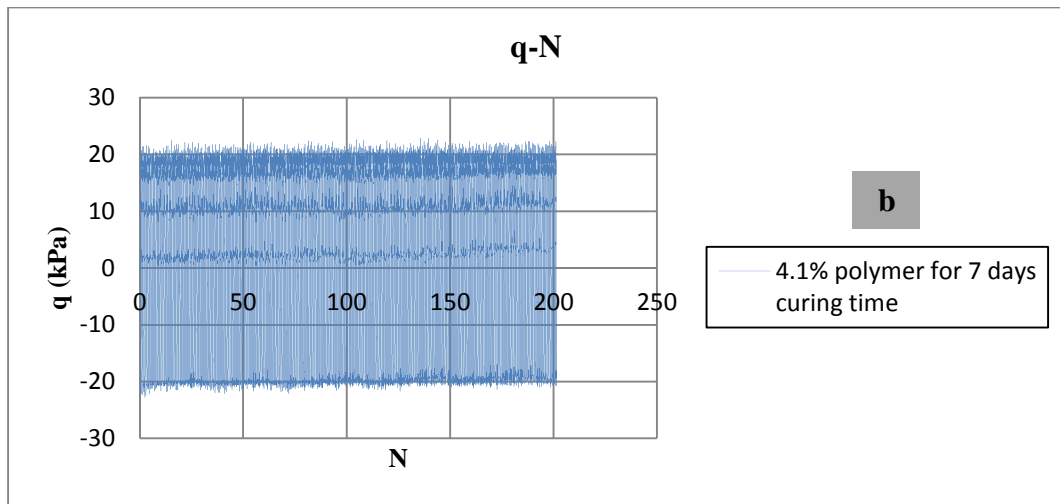
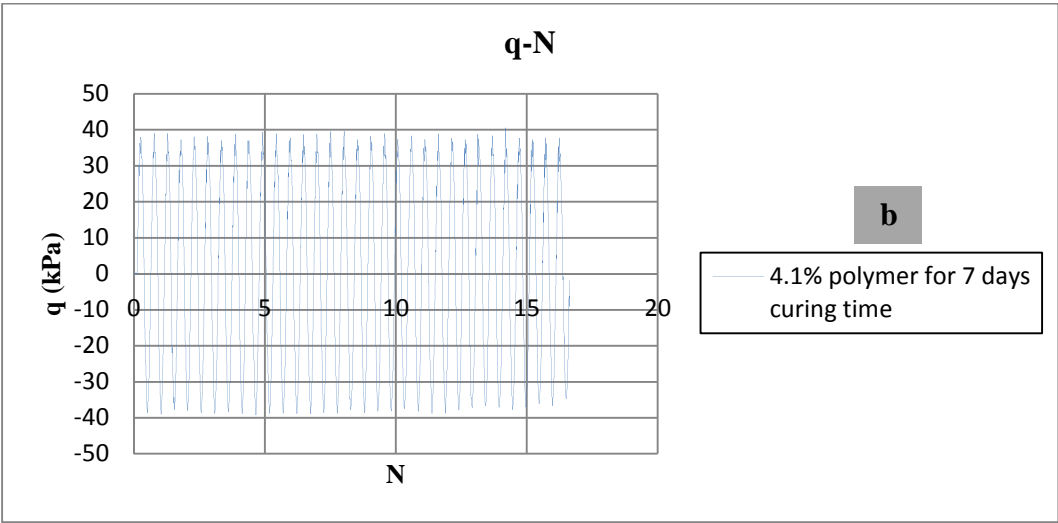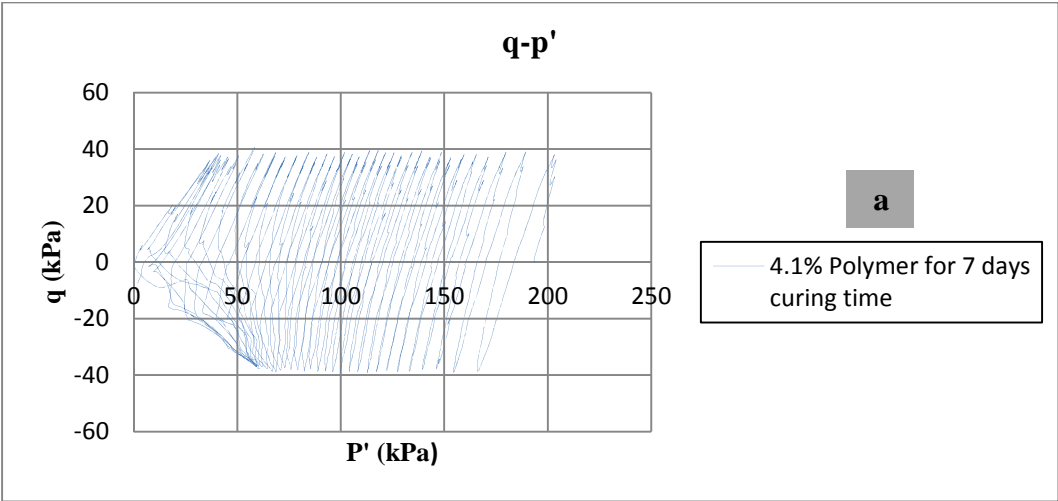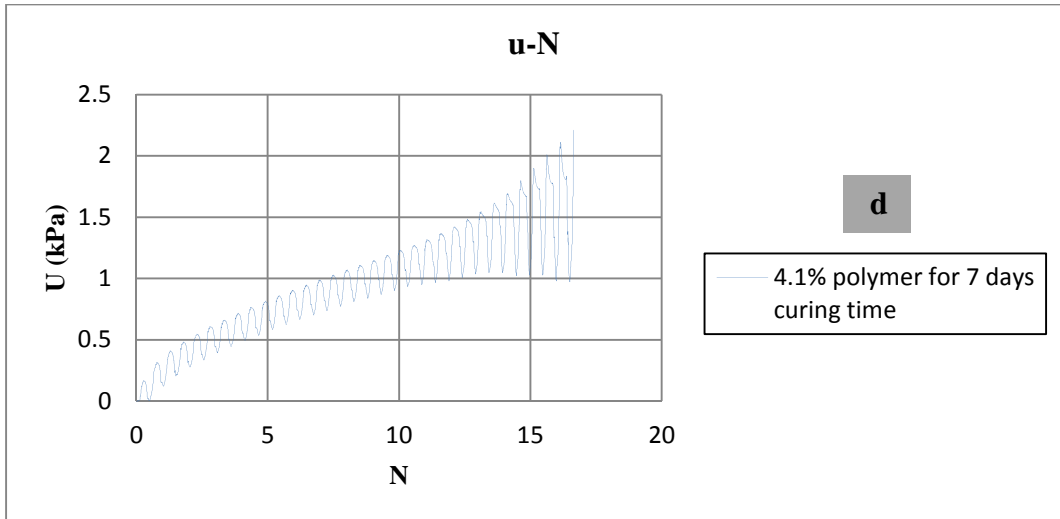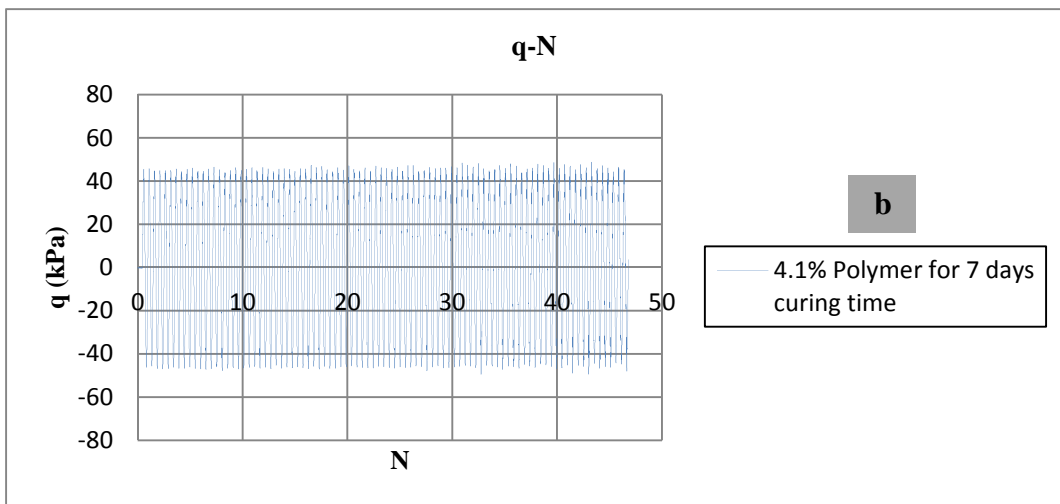Figure 60: 4.1% Polymer to sand with 0.2 CSR & 0.02 frequency
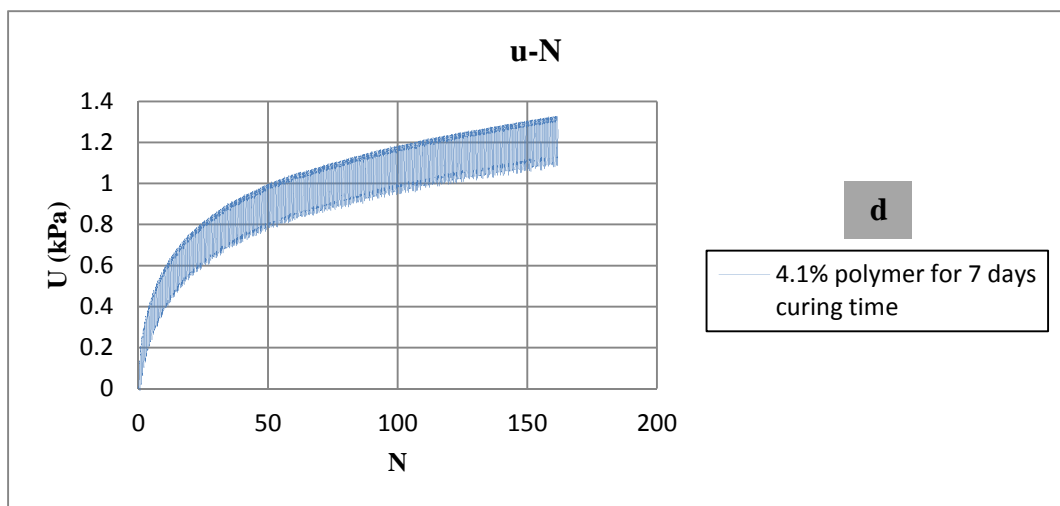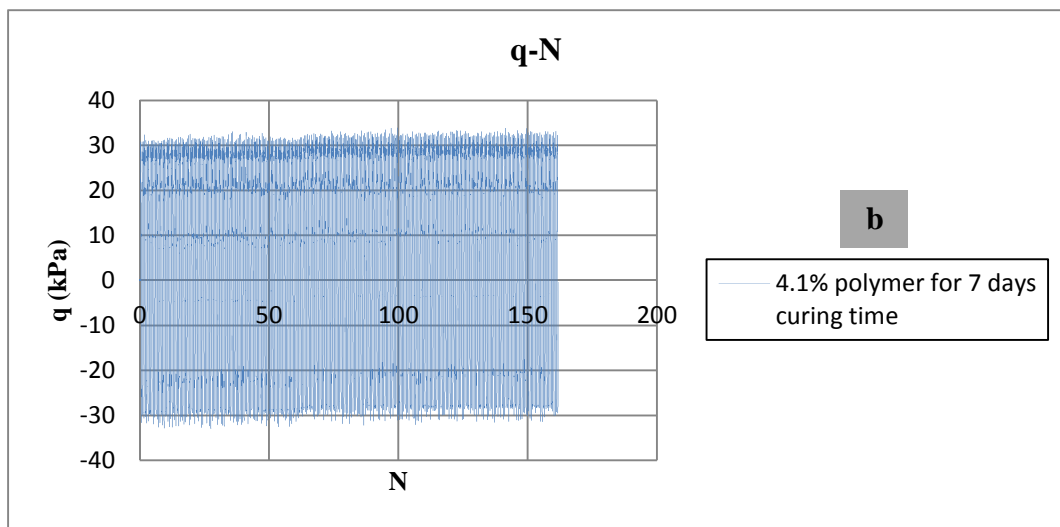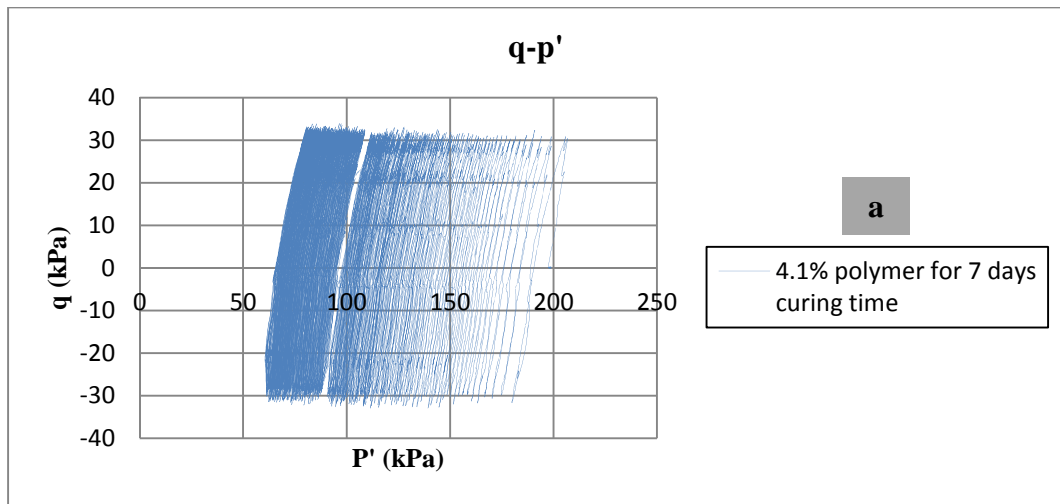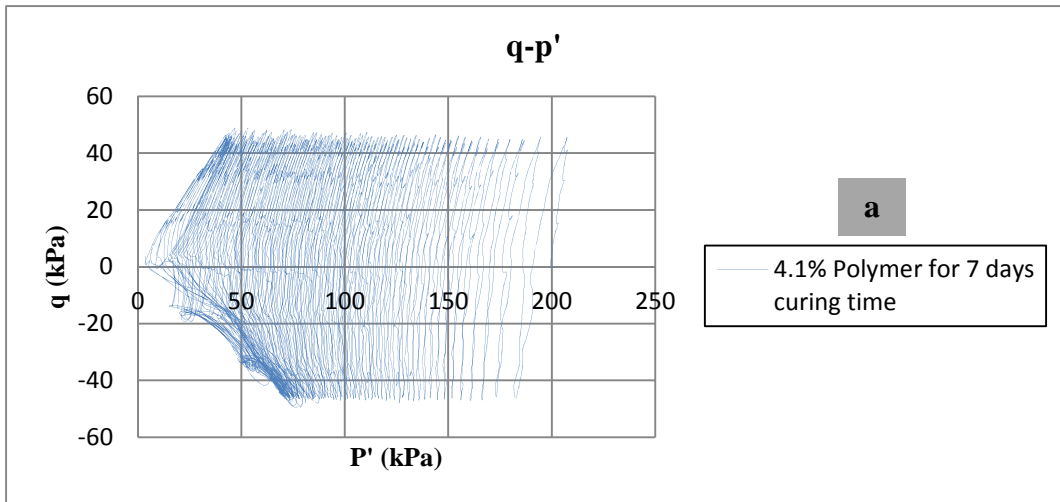
Figure 61: 4.1% Polymer to sand with 0.3 CSR & 0.02 frequency

q-p'

q (kPa) vs P' (kPa)

a

4.1% Polymer for 7 days curing time

q-N

q (kPa) vs N

b

4.1% polymer for 7 days curing time

-N

(%) vs N

c

4.1% polymer for 7 days curing time

u-N
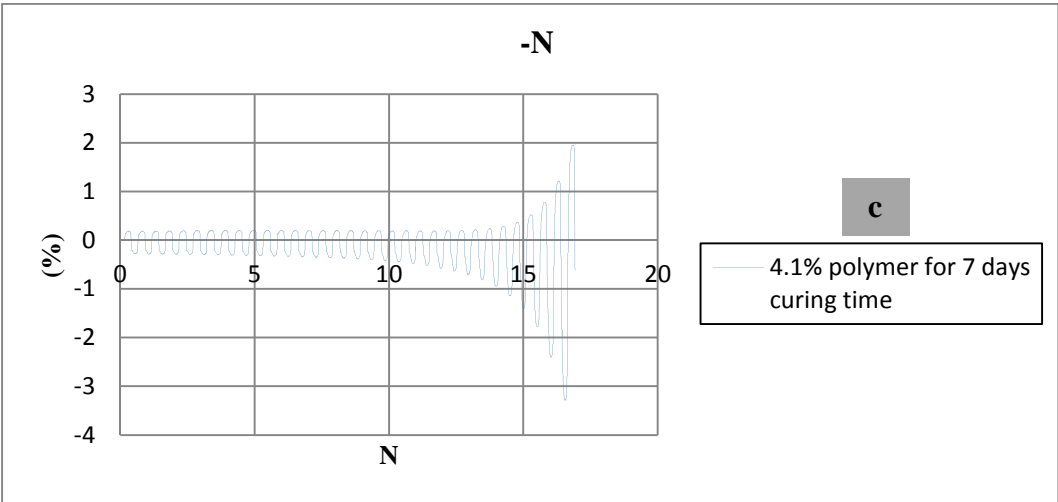
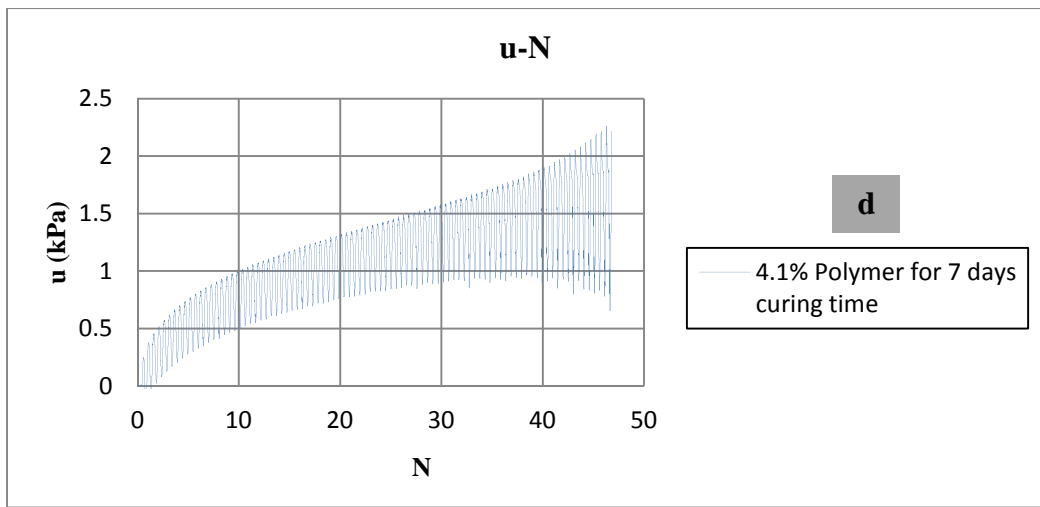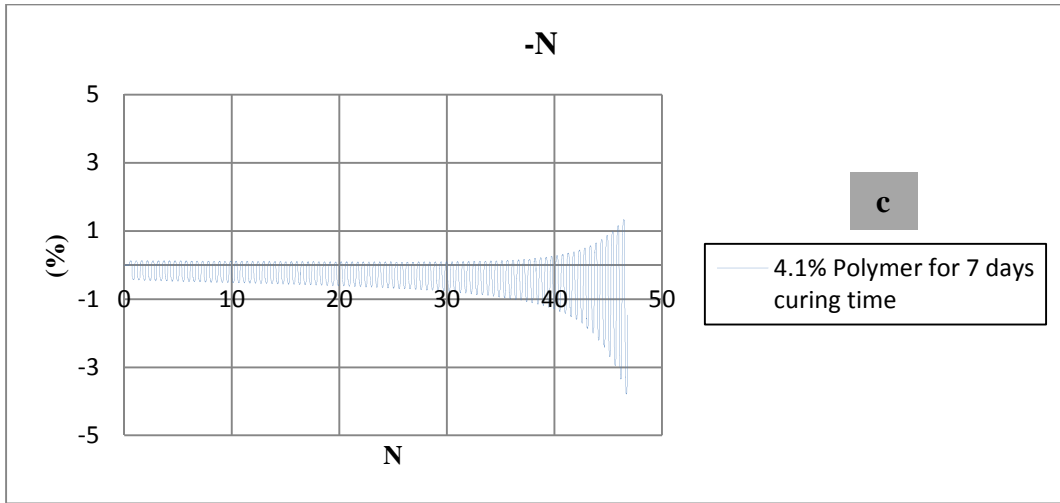Figure 62: 4.1% Polymer to sand with 0.37 CSR & 0.02 frequency

q-p'

q-N

Figure 63: 4.1% Polymer to sand with 0.45 CSR & 0.02 frequency

Appendix B

The software used in the cyclic tests was LabVIEW program that had different tabs corresponding to stages of testing as shown in Figure 64-67.

1. Startup menu presented the program.

Figure 64: Startup menu of LabVIEW software

2. Saturation stage as illustrated in Figure 65.

The initial step in cyclic triaxial loading test after confinement of samples was saturation of samples. At this stage the samples were saturated gradually by giving the samples confining and pore-water pressure at a time in order to reach 95% B-value at last. The values of cell and pore-water pressure at the beginning of saturation step were chosen 30 & 10 kPa respectively.
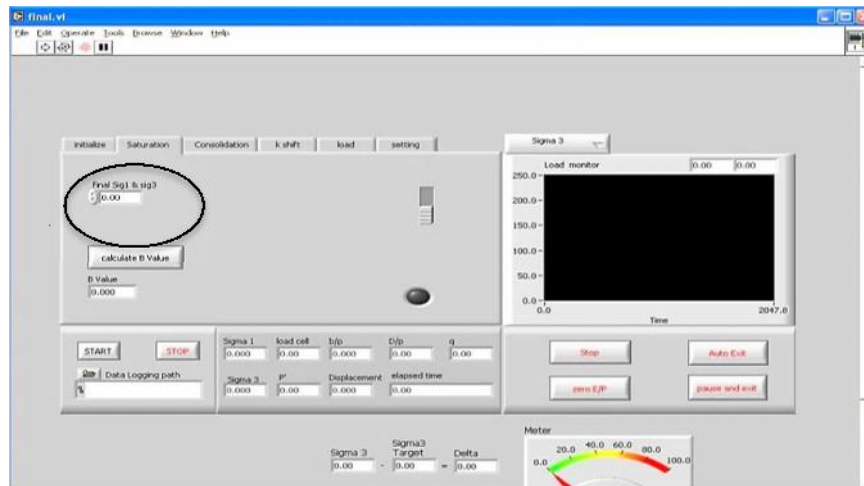
Figure 65: Saturation tab, LabVIEW program

3. Consolidation stage as shown in Figure 66.

Subsequent stage after saturation of samples was consolidation step that the samples were consolidated with 200kPa in P' box inside the oval as illustrated in Figure 66. Also the confining pressure changes were controlled through the monitor of LabVIEW program inside the double brackets.
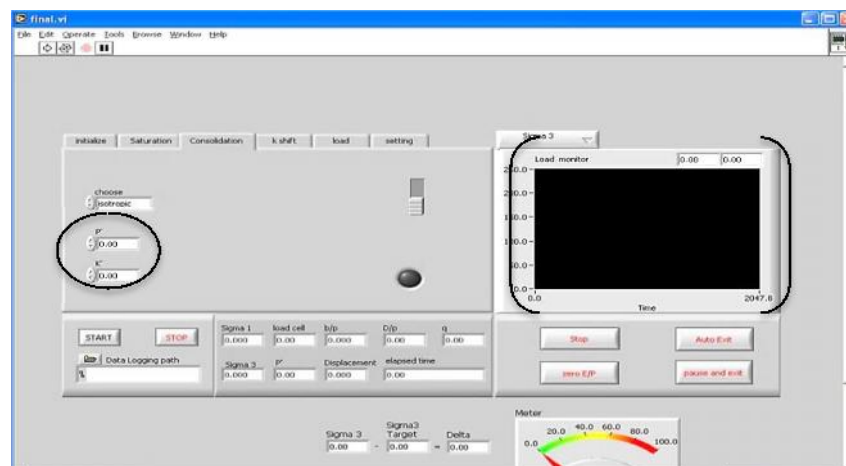

Figure 66: Consolidation tab, LabVIEW program

4. Cyclic loading as depicted in Figure 67.

Finally, the samples were cyclic loaded. The cyclic triaxial device used in this research was stress controlled. As a result stress selection switch activated when two boxes of amplitude and frequency filled with required values as shown by oval shape in Figure 67.
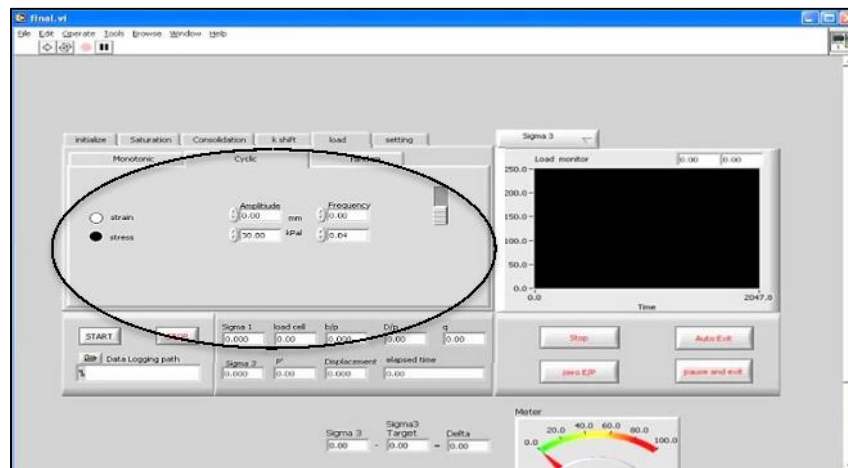

Figure 67: Cyclic section in consolidation tab, LabVIEW program